Title
Regulation and transcriptional role of CRTC1 during activity in neurons

Author
DeSalvo, Martina

Publication Date
2016

Peer reviewed|Thesis/dissertation

UNIVERSITY OF CALIFORNIA

Los Angeles

Regulation and transcriptional role of CRTC1 during activity in neurons.

A dissertation submitted in partial satisfaction

of the requirements for the degree Doctor of Philosophy

in Neuroscience

by

Martina DeSalvo

2016

ABSTRACT OF THE DISSERTATION

Regulation and transcriptional role of CRTC1 during activity in neurons.

by

Martina DeSalvo

Doctor of Philosophy in Neuroscience

University of California, Los Angeles, 2016

Professor Kelsey C. Martin, Chair

Long term memory is mediated by long-lasting forms of synaptic plasticity that require new gene transcription for their persistence. Previous work has shown that neuronal CREB-regulated transcriptional coactivator 1 (CRTC1) plays a crucial role during learning and memory by regulating activity-dependent gene expression. We have shown that CRTC1 undergoes synapse-to-nucleus translocation to regulate transcription of CREB target genes in response to neuronal activity. In this thesis, we investigate the regulation and retrograde transport of CRTC1 in neurons and examine the nuclear role of CRTC1 in activity-dependent gene transcription. Our first goal was to identify the mechanisms by which CRTC1 responds to activity. We describe key synaptic processes necessary to trigger dephosphorylation of three serine residues that are required for dynein-mediated transport of CRTC1 to the nucleus. Our second goal was to understand the role of CRCT1 as a transcriptional coactivator. We use a combination of ChIP-Seq, ATAC-Seq and RNA-Seq to understand how CRTC1

binding to CREB and other transcription factors correlates with changes in chromatin accessibility and transcription of activity-induced genes. Finally, we summarize a series of projects that attempt to elucidate how regulation of CRTC1's phosphorylation code may influence its function in neurons. These studies highlight the complexities of CRTC1 as an intrinsically disordered protein with 50 phosphorylated residues and a variety of potential interacting partners.

The dissertation of Martina DeSalvo is approved.

Thomas J. O'Dell

Alvaro Sagasti

James A. Wohlschlegel

S. Lawrence Zipursky

Kelsey C. Martin, Committee Chair

University of California, Los Angeles

2016

This dissertation is dedicated to my family and friends,

for their unwavering support, steadfast love and encouragement.

TABLE OF CONTENTS

LIST OF FIGURES

Chapter 1

Chapter 2

LIST OF TABLES

ACKNOWLEDGMENTS

I am truly grateful for all of my mentors, colleagues, collaborators, friends and family who contributed to this incredible journey through graduate school. First of all, I would like to thank my thesis advisor, Kelsey Martin. She has guided me through the last six years by providing a strong scientific foundation and allowing me to freely explore new questions at the boundaries of our knowledge. I have enjoyed every interaction with her, not only as my mentor, but also as a thoughtful and caring guide, who has valued my personal development as much as my scientific growth. It has been inspiring to learn from such a graceful and respected leader and I feel especially lucky to have such a wonderful role model.

I would like to thank all of the past and present members of the Martin lab. I cannot imagine the last six years without your help and support with experiments, brainstorming, and of course, lunch-time Tsujita excursions. In particular, I would like to thank Toh Hean Ch'ng who taught me countless techniques, helped me troubleshoot dozens of experiments and was always available to discuss and develop ideas. A very special thank you goes to Sylvia Neumann, who successfully replaced the irreplaceable Klara Olofsdotter. Sylvia has been a pleasure to work with on the last experiments needed for Chapter 3 and I hope that this work opens up a path to exciting future experiments for the lab. Constantinos Chronis, honorary member of the Martin lab, has also been a wonderful collaborator and mentor. His contributions to Chapter 3 have been invaluable.

Thank you, Patrick Chen and Shivan Bonanno for sharing bench space, desk space and, of course, lots of laughter and deep thoughts. My lab experience would not have been the same without Mariana Fontes and Elliott Meer. We've shared so many adventures both inside and outside the lab and I'm incredibly grateful for your friendship, support and cat videos. I would also like to thank Klara Olofdotter, Saadia Hasan, Nai Saeteurn, Jennifer Achiro, Wendy Herbst, Yang Tao, Ji-Ann Lee and Sarah Van Driesche for making our lab such a special place. Over the years, our lab has completely merged with the

neighboring Plath lab. They were always willing to share reagents, ideas and fun times, especially Nadia Sellami, Anna Sahakyan, Amy Pandya-Jones, Alissa Minkovsky, Martina Roos, Jarrett Miller and Robin Mckee. Thank you for all being part of such an exciting science family!

I would like to acknowledge the members of my committee for their guidance, advice and support during my PhD. Thank you for all of the helpful suggestions throughout the years and for pushing me to complete this project. I would also like to thank the NSIDP, for giving me a cohort of awesome scientists to discuss science and enjoy life with outside of lab. I will always cherish our hiking, camping and ski trips! Some of the best times of my graduate experience were shared after work, with my neuroscience roommates: Emily Dennis, Matt Schreiner and Maite Lazaro. Coming home to them after a long day in lab was always a treat! A huge thank you for the love and support of my friends Neel Parikshak, Kostya Bakhurin, Anthony Linares, Anthony Daggett, Nic Novak, Sarah Hersman, David DiTullio, Ryan Guglietta, Kathy Myers, Eric Gschweng, Micky Einstein and Camille Hommeyer.

Outside of lab, I would like to thank my passionate, dedicated colleagues in AWiSE, especially Kate Fehlhaber, Mariana Fontes, Jennifer Tribble, Kendra Nyberg, Wenting Tsai, Wendy Herbst, Julia Chin and Kathleen Wang. It has been wonderful to work with you and create so many profoundly impactful programs together.

I would not be who I am today without the constant love and support of my parents. You have instilled a deep curiosity about the world in each of your children, to produce not one, but three ever-questioning PhDs! Thank you for all of the sacrifices you have made for us over the years and for teaching us to always follow our passion. To my brother and sister, I am so grateful that we went through this crazy graduate school experience together. Gilberto, we will always have our differences, but thank you for forging the path, in life and in science. Giulia, even as my little sister, your dedication and hard work has always been inspiring. I can't wait to see what comes next for all of us!

Finally, I'd like to thank Nick Hardy, for being an incredible partner. The last four years have been amazing and full of unbelievable adventures. Thank you for always being there for all of the highs and lows, not just through the emotional rollercoaster of graduate school, but also literally, from skydiving to scuba diving! I am so excited about sharing many more exciting experiences with you and I am truly grateful to have such a supportive and loving partner.

Toh Hean Ch'ng is the first author of Chapter 2. The mass spectrometry experiments described in this chapter were done in collaboration with Ajay Vashisht in the Wohlschlegel lab at UCLA.

The ChIP-Seq, ATAC-Seq and RNA-Seq experiments and bioinformatic analysis in Chapter 3 were done in collaboration with Constantinos Chronis in the Plath lab at UCLA. Sylvia Neumann helped prepare samples for these experiments. Initial planning for this project was done in collaboration with Toh Hean Ch'ng.

Many of the experiments in Chapter 4 were done in collaboration with other Martin lab members, including Toh Hean Ch'ng, Sylvia Neumann and Shivan Bonanno. Mass spectrometry and SILAC experiments were done in collaboration with Ajay Vashisht in the Wohlschlegel lab.

The experiments in this dissertation were funded by the Philip Whitcome Pre-doctoral Training Program and by an NIH grant (R01 MH077022-06)

VITA

2005-2009	B.A., Molecular and Cellular Biology, Department honors in Neuroscience, B.A., Italian Studies University of California, Berkeley Berkeley, California
2010-2016	Ph.D. candidate Neuroscience Interdepartmental Program University of California, Los Angeles Los Angeles, California
2013	Society for Neuroscience Chapter Award Southern California Chapter Presented in New Orleans, Louisiana
2011-2014	Whitcome Pre-doctoral Training Grant University of California, Los Angeles Los Angeles, California
2011-2012	Project Brainstorm Teaching Assistant Neuroscience Interdepartmental Program University of California, Los Angeles Los Angeles, California

PUBLICATIONS AND PRESENTATIONS

Publications:

Ch'ng, T. H., DeSalvo, M., Lin, P., Vashisht, A., Wohlschlegel, J. A., & Martin, K. C. (2015). Cell biological mechanisms of activity-dependent synapse to nucleus translocation of CRTC1 in neurons. *Frontiers in Molecular Neuroscience*, *8*, 48. http://doi.org/10.3389/fnmol.2015.00048

Presentations:

DeSalvo, M.*, Chronis, K., Ch'ng T.H., Vashisht, A., Wohlschlegel, J., Martin, K.C. *Role and regulation of CRTC1 phosphorylation during activity-dependent synaptic plasticity.* Oct 20th 2015, Society for Neuroscience, Chicago

DeSalvo, M.*, Ch'ng T.H., Vashisht, A., Wohlschlegel, J., Martin, K.C. *Dynamic activity-dependent dephosphorylation of CRTC1 regulates synapse to nuclear transport.* Nov 10th 2013, Society for Neuroscience, San Diego

Chapter 1

Introduction

The molecular and cellular mechanisms underlying learning and memory have fascinated scientists for over a century. Since Ramon y Cajal first suggested that memories may be stored in the change in strength of connections between neurons (Ramon y Cajal 1894), scientists have explored this hypothesis and elucidated many aspects of this model. His idea was later renamed "synaptic plasticity" (Konorski & Jerzy, 1948), to describe the experience-dependent modulation of synaptic connections between neurons (Kandel 2001).

Long Term Potentiation and the role of CREB

Many studies have focused on a form of synaptic plasticity called long-term potentiation (LTP) that occurs in the hippocampus, a region of the brain important for memory formation (Squire, Stark, & Clark, 2004). LTP can be induced by brief trains of high-frequency stimulation of pre-synaptic neurons, which leads to a sustained increase in response from post-synaptic neurons (Bear & Malenka, 1994; Bliss & Collingridge, 1993). Long-term potentiation can be further dissected into two distinct phases, early phase (E-LTP) and late phase (L-LTP). E-LTP describes the initial increase in potentiation driven by calcium-dependent phosphorylation of synaptic proteins as well as the insertion of new AMPA receptors at the synapse (Figure 1.1). Crucially, these changes are independent of protein synthesis and only last about an hour. Long-lasting forms of long-term potentiation (L-LTP), which are thought to underlie long-term memories, require new gene transcription and protein translation (Figure 1.1; Abraham & Williams 2003). In particular, L-LTP requires activation of the transcription factor cAMP response element binding protein (CREB; Lonze & Ginty 2002).

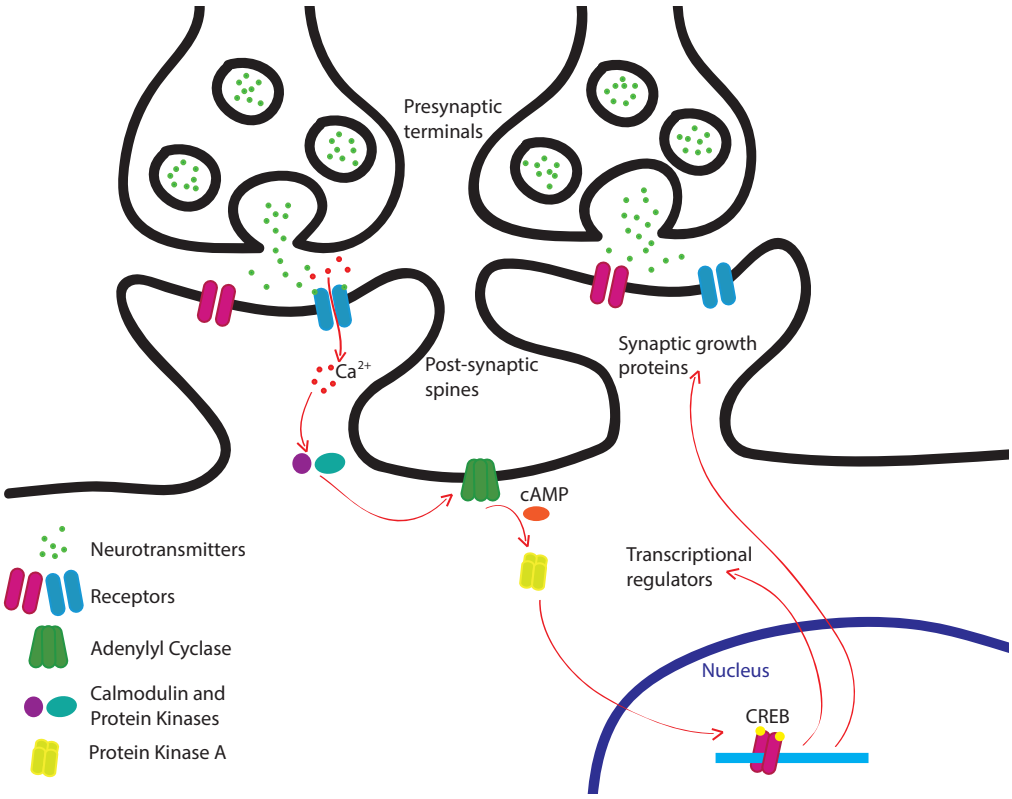

Figure 1.1: Diagram of the early and late phase of LTP. Adapted from Squire's Fundamental Neuroscience (2013).

During the early phase of LTP (E-LTP), postsynaptic NMDA receptor activation leads to calcium influx, which in turn triggers kinase activity and AMPA receptor insertion at the synapse. The late phase of LTP (L-LTP) is characterized by a cascade of events that lead to increases in CREB-dependent gene transcription in the nucleus. The protein products encoded by these new transcripts are necessary for maintenance of L-LTP. Blocking either transcription or translation eliminates the late phase of LTP even after prolonged stimulation.

CREB binds cAMP Response Elements (CREs) via a basic-region leucine zipper (bZIP) DNA binding and dimerization domain located on its carboxy-terminus. CREB's glutamine rich Q1 and Q2 domains and its kinase inducible domain (KID) make up its transactivation domains and interacting partners play an important role in its transcriptional regulation. The KID of CREB interacts with co-activator histone acetyltransferases CREB Binding Protein (CBP) and p300, while the Q2 domain is crucial for $hTAF_{II}130/135$ recruitment (Mayr & Montminy, 2001; Shaywitz & Greenberg, 1999). CREB-regulated genes are crucial for memory formation and many experiments have shown that L-LTP can be eliminated by preventing transcription and more specifically by blocking CREB function (Silva et al., 1998).

Synapse to nucleus signaling in neurons

Since the stimuli that trigger CREB-mediated gene expression in neurons are often received at synapses that are very far from the cell body and nucleus, it is important to understand how those signals are relayed to the nucleus to elicit new gene transcription. Neurons are unique in their morphology and often extend projections that measure many times the width of the soma. These projections are crucial for creating connections to other neurons, but long-range neuronal communication would not be possible without mechanisms to quickly and reliably transmit information over long distances. Neurons have evolved a variety of mechanisms to do so, depending on the type of information received and on the intended response to such a stimulus. One mechanism involves rapid electrochemical signaling to couple neuronal activity at the synapse to changes in gene expression in the nucleus. Other methods involve regenerative calcium waves in the ER that can quickly propagate towards the nucleus, transport of signaling endosomes, active transport of soluble molecules along actin filaments and microtubules, or the much slower and more localized effects of passive diffusion (Ch'ng &

Martin 2012). In concert with nuclear import and export pathways, these signaling routes act as crucial steps in the regulation and coordination of cell-wide responses to distal, localized events.

CREB-regulated transcriptional co-activator (CRTC1)

One method to couple synaptic events with transcriptional changes in the nucleus is the regulated nuclear import of synaptically-localized regulators of gene expression. Our lab and others have recently described the role of the synapse-to-nucleus translocation of CREB-regulated transcriptional coactivator 1 (CRTC1) in regulating transcription during LTP of rodent hippocampal synapses (Toh Hean Ch'ng & Martin, 2012; Kovács et al., 2007; Zhou et al., 2006).

CRTC (previously known as TORC, Transducers of Regulated CREB) was originally identified in non-neuronal cells in an *in vitro* screen to identify proteins that increase transcriptional activity of CREB (Conkright, Guzma, et al., 2003; Iourgenko et al., 2003; Screaton et al., 2004). Three conserved isoforms of CRTC are differentially expressed in mammalian tissues. CRTC1 is most abundant in the brain, specifically cortex, hippocampus and striatum (Watts, Sanchez-Watts, Liu, & Aguilera, 2011), CRTC2 is enriched in the liver and insulin-secreting B-islet cells (Wang, Vera, Fischer, & Montminy, 2009), while CRTC3 is expressed at high levels in white adipose tissue (Song et al., 2010).

Several labs have shown that CRTC1 plays diverse functions in the brain. These include modulation of memory in flies and rodents (Hirano et al., 2013; Nonaka et al., 2014; Sekeres et al., 2012; Zhou et al., 2006), entrainment of circadian rhythms (Jagannath et al., 2013), neuroprotection during ischemic stress (Sasaki et al., 2011), regulation of cocaine-induced plasticity (Hollander et al., 2010) and longevity and metabolism (Burkewitz et al., 2015; Riera et al., 2014). Moreover, two neurodegenerative diseases, Huntington's and Alzheimer's diseases, have been linked with CRTC1 activity (España et al., 2010; Jeong et al., 2011; Saura, 2012).

We have previously shown that CRCT1 is heavily phosphorylated and that its phosphorylation state changes upon neuronal stimulation (Ch'ng et al. 2012). As summarized in Figure 1.2, CRTC1 is phosphorylated at rest, which allows it to interact with 14-3-3 proteins that anchor CRTC1 at synapses. Following neuronal activation, increases in intracellular calcium activate calcineurin (CN), which dephosphorylates CRTC1. Calcineurin is required for CRTC1's nuclear translocation as dephosphorylation of CRTC1 releases it from 14-3-3 proteins. CRTC1 undergoes activity-dependent nuclear accumulation in excitatory neurons in culture and intracellular increases in cAMP are required to keep CRTC1 in the nucleus (Ch'ng et al., 2012). In the nucleus, CRTC1 binds CREB and other bZIP transcription factors (Conkright, Canettieri, et al., 2003 and Canettieri et al., 2009) and seems to play a crucial role in the induction of genes important for L-LTP.

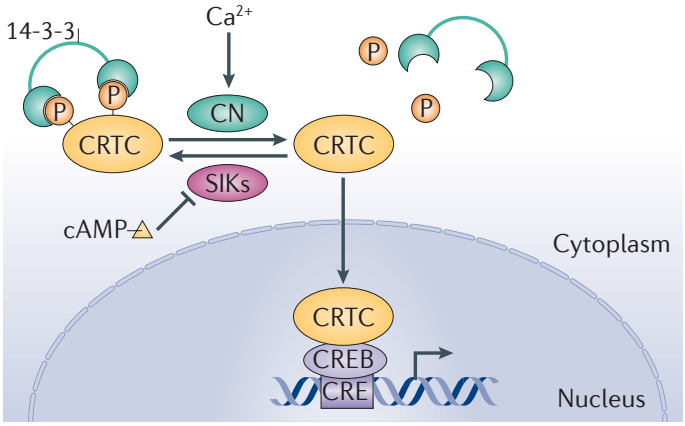

Figure 1.2: A model of CRTC nuclear translocation. (Altarejos & Montminy, 2011).

In unstimulated cells, CRTC1 is phosphorylated, which allows it to interact with 14-3-3 proteins that anchor it in the cytoplasm. Following activity, influx of calcium triggers calcineurin (CN) activity, which dephosphorylates CRTC, releasing it from 14-3-3. CRTC1 is transported to the nucleus where it potently activates CREB-dependent new gene transcription. Increases in cAMP prevent CRTC1 from being re-phophorylated, which keeps CRTC in the nucleus for longer periods of time.

Other groups have studied the role of CRTC1 in L-LTP and have shown that the transcription-dependent late phase, but not the transcription-independent early phase of LTP, is blocked by expression of dominant-negative CRTC1 in CA1 neurons (Kovács et al., 2007; Zhou et al., 2006). In parallel experiments, Zhou et al. (2006) demonstrated that overexpression of CRTC1 in CA1 neurons was found to lower the threshold for induction of late-phase LTP. These experiments suggest that CRTC1 plays a critical role in transcription during neuronal plasticity.

My research focuses on understanding CRTC1's role in neurons during transcription-dependent neuronal plasticity, and specifically how CRTC1's activity-dependent synapto-nuclear translocation triggers activity-dependent changes in gene transcription in the nucleus. We hypothesize that different types of stimulation lead to distinct patterns of CRTC1 phosphorylation, which regulate the nucleocytoplasmic trafficking of CRTC1 as well as its transcriptional activity in the nucleus.

Structural and biochemical considerations for CRTC1

Analysis of CRTC1 using protein structure prediction software (PyMOL) indicates that CRTC1 is a highly disordered protein. The only apparent structure is a N-terminal alpha helix that comprises the basic leucine zipper (bZip)-binding domain of CRTC1 (Figure 1.3). As such, CRTC1 can be categorized as an intrinsically disordered protein (IDP). Up to 35% of human proteins are predicted to possess intrinsically disordered regions of at least 30 consecutive disordered residues (Guharoy, Pauwels, & Tompa, 2015). IDPs contain disorder-promoting amino acids, such as polar serine, glutamine, lysine, arginine, aspartic acid and glutamic acid as well as structure-breaking prolines and glycines, which contribute to high rigidity and high flexibility, respectively (Radivojac et al., 2007). Analysis of CRTC1's amino acid composition reveals that 56% of its residues are disorder-promoting (351 out of 630 aa: 83 S, 30 D, 14 K, 73 P, 53 Q, 23 E, 26 R, 49 G).

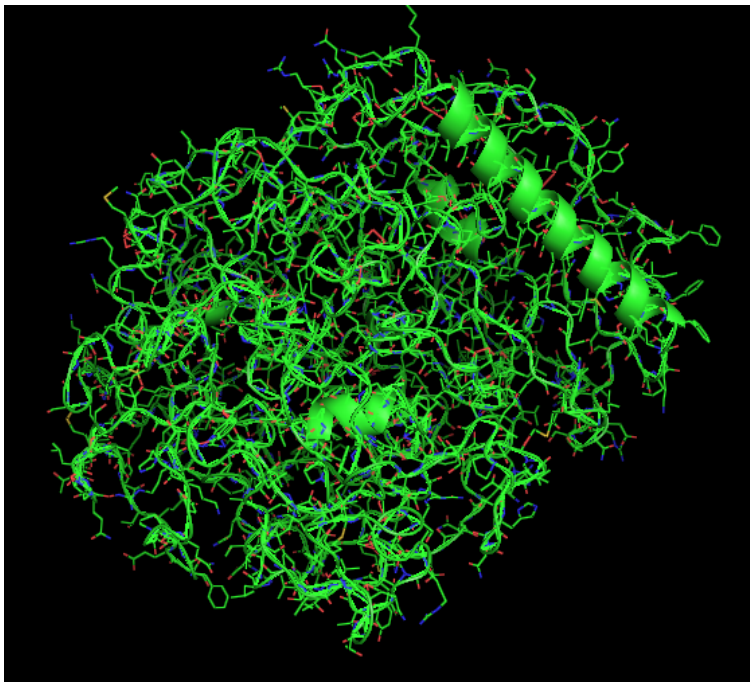

Figure 1.3: PyMOL prediction of CRTC1 structure.

This visualization of the predicted 3D structure of CRTC1 highlights the lack of tertiary structures.

IDPs are characterized by a lack of 3-dimentional structure and are more prevalent with increasing organismal complexity, since the same protein may need to be re-purposed for different functions. IDPs can dynamically fluctuate between conformations, depending on binding partners or post-translational modification and thus often act as switches or nodes in signaling networks (Babu, et al., 2011; Dyson & Wright, 2005; Uversky, 2015).

This ability to undergo binding-induced folding means that the same protein can mediate a variety of responses depending on what other proteins it interacts with. This is especially interesting for CRTC1 since we have shown that it undergoes activity-dependent translocation from synapse to nucleus. CRTC1 could play different roles depending on the subcellular environment it is exposed to (synapse vs nucleus), the proteins it can interact with locally (14-3-3 at the synapse vs CREB or other transcriptional

machinery in the nucleus) and/or the post-translational modifications that we have observed in these distinct subcellular compartments (phosphorylated at the synapse vs de-phosphorylated in the nucleus).

Another important consideration for IDPs is that regulation of these proteins is very sensitive to changes in stoichiometry (Babu et al., 2011). For instance, introducing exogenous IDPs could lead to non-functional interactions or promiscuous signaling. Changing the availability of these proteins (via up/down regulation) could lead to altered cellular response through loss or gain of protein function (Figure 1.4).

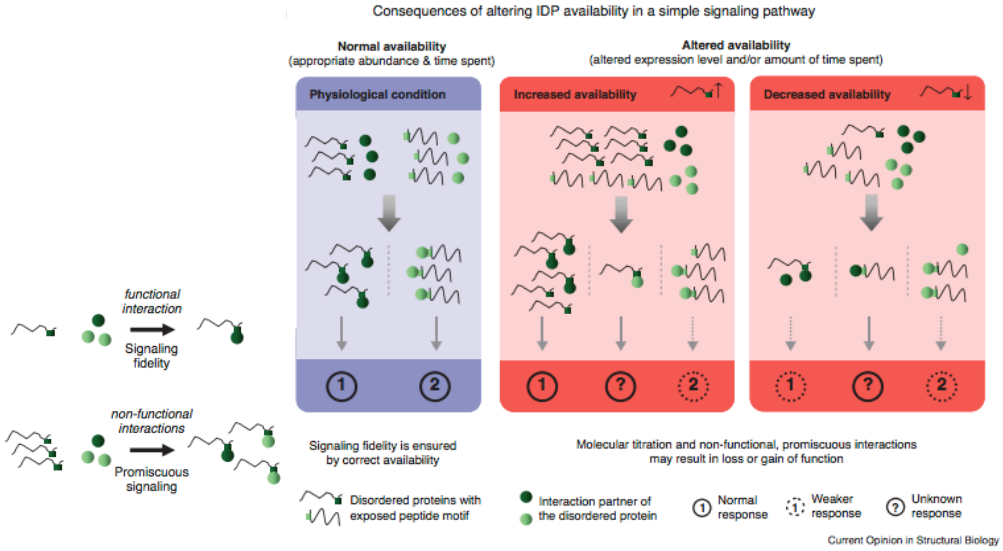

Figure 1.4: Molecular titration of IDPs affects their function. Adapted from (Babu et al., 2011). Altering IDP availability could lead to non-functional interactions or promiscuous signaling. Increased or decreasing availability of IDPs could lead to unintended consequences such as loss or gain of function.

Possibly because of its disordered, malleable structure, no CRTC1 antibody we have tested thus far has worked efficiently for immunoprecipitations. We also observed that highly overexpressed CRTC1 does not translocate in an activity-dependent manner (data not shown) which suggests that, like other IDPs, the molecular titration of CRTC1 is crucial for its normal regulation and function. The perfect tool to study CRTC1 would be a tagged-CRTC1 knock in mouse, but since we have as yet been unable to generate this transgenic animal, we have created a variety of tools to study CRTC1. In order to get around the issues described above, we designed an adeno-associated virus (AAV) that expresses a FLAG-tagged version of CRTC1 under a CaMKIIα promoter. This promoter expresses CRTC1 at near endogenous levels, only in excitatory neurons. This tool allows us to immunoprecipitate CRTC1 using the FLAG tag while minimizing the effects of overexpression.

Outline

The next chapters will summarize several avenues that I have explored during my PhD.

Chapter 2 delves into the molecular cell biology of CRTC1 regulation by neuronal activity. This work was published in a 2015 paper: "Cell biological mechanisms of activity-dependent synapse to nucleus translocation of CRTC1 in neurons" in Frontiers in Molecular Neuroscience.

Chapter 3 explores the transcriptional activity of CRTC1 following neuronal stimulation. It has been previously shown that CRTC mediates a drastic increase in CREB-mediated gene transcription, but its specific role in neurons is still unknown. This manuscript is currently being finalized, with plans for submission in December 2016.

Chapter 4 reviews a variety of different projects that did not lead to publications, but that could be of significant importance to future studies in the Martin lab.

The conclusions in *Chapter 5* offer a comprehensive view of my PhD research.

References:

Abraham, W. C., & Williams, J. M. (2003). Properties and mechanisms of LTP maintenance. *The Neuroscientist : A Review Journal Bringing Neurobiology, Neurology and Psychiatry*, *9*(6), 463–74. http://doi.org/10.1177/1073858403259119

Altarejos, J. Y., & Montminy, M. (2011). CREB and the CRTC co-activators: sensors for hormonal and metabolic signals. *Nature Reviews. Molecular Cell Biology*, *12*(3), 141–51. http://doi.org/10.1038/nrm3072

Babu, M. M., van der Lee, R., de Groot, N. S., & Gsponer, J. (2011). Intrinsically disordered proteins: regulation and disease. *Current Opinion in Structural Biology*, *21*(3), 432–440. http://doi.org/10.1016/j.sbi.2011.03.011

Bear, M. F., & Malenka, R. C. (1994). Synaptic plasticity: LTP and LTD. *Current Opinion in Neurobiology*, *4*(3), 389–399. http://doi.org/10.1016/0959-4388(94)90101-5

Bliss, T. V. P., & Collingridge, G. L. (1993). A synaptic model of memory: long-term potentiation in the hippocampus. *Nature*, *361*, 31–39.

Burkewitz, K., Morantte, I., Weir, H. J. M., Yeo, R., Zhang, Y., Huynh, F. K., … Mair, W. B. (2015). Neuronal CRTC-1 Governs Systemic Mitochondrial Metabolism and Lifespan via a Catecholamine Signal. *Cell*, *160*(5), 842–855. http://doi.org/10.1016/j.cell.2015.02.004

Canettieri, G., Coni, S., Della Guardia, M., Nocerino, V., Antonucci, L., Di Magno, L., … Gulino, A. (2009). The coactivator CRTC1 promotes cell proliferation and transformation via AP-1. *Proceedings of the National Academy of Sciences of the United States of America*, *106*(5), 1445–50. http://doi.org/10.1073/pnas.0808749106

Ch'ng, T. H., & Martin, K. C. (2012). Synapse to nucleus signaling. *Current Opinion in Neurobiology*, *21*(2), 345–352. http://doi.org/10.1016/j.conb.2011.01.011.Synapse

Ch'ng, T. H., Uzgil, B., Lin, P., Avliyakulov, N. K., O'Dell, T. J., & Martin, K. C. (2012). Activity-dependent

transport of the transcriptional coactivator CRTC1 from synapse to nucleus. *Cell*, *150*(1), 207–221. http://doi.org/10.1016/j.cell.2012.05.027

Conkright, M. D., Canettieri, G., Screaton, R., Guzman, E., Miraglia, L., Hogenesch, J. B., … Jolla, L. (2003). TORCs : Transducers of Regulated CREB Activity The Salk Institute for Biological Studies. *Molecular Cell*, *12*, 413–423.

Conkright, M. D., Guzma, E., Flechner, L., Su, A. I., Hogenesch, J. B., & Montminy, M. (2003). Genome-Wide Analysis of CREB Target Genes Reveals A Core Promoter Requirement for cAMP Responsiveness Salk Institute for Biological Studies. *Molecular Cell*, *11*(1), 1101–1108.

Dyson, H. J., & Wright, P. E. (2005). Intrinsically unstructured proteins and their functions. *Nature Reviews Molecular Cell Biology*, *6*, 197–208. http://doi.org/10.1038/nrm1589

España, J., Valero, J., Miñano-Molina, A. J., Masgrau, R., Martín, E., Guardia-Laguarta, C., … Saura, C. a. (2010). beta-Amyloid disrupts activity-dependent gene transcription required for memory through the CREB coactivator CRTC1. *The Journal of Neuroscience : The Official Journal of the Society for Neuroscience*, *30*(28), 9402–10. http://doi.org/10.1523/JNEUROSCI.2154-10.2010

Guharoy, M., Pauwels, K., & Tompa, P. (2015). SnapShot: Intrinsic Structural Disorder. *Cell*, *161*(5), 1230–1230.e1. http://doi.org/10.1016/j.cell.2015.05.024

Hirano, Y., Masuda, T., Naganos, S., Matsuno, M., Ueno, K., Miyashita, T., … Saitoe, M. (2013). Fasting Launches CRTC to Facilitate Long-Term Memory Formation in Drosophila. *Science*, *339*, 443–446.

Hollander, J. A., Im, H.-I., Amelio, A. L., Kocerha, J., Bali, P., Lu, Q., … Kenny, P. J. (2010). Striatal microRNA controls cocaine intake through CREB signalling. *Nature*, *466*. http://doi.org/10.1038/nature09202

Iourgenko, V., Zhang, W., Mickanin, C., Daly, I., Jiang, C., Hexham, J. M., … Labow, M. a. (2003). Identification of a family of cAMP response element-binding protein coactivators by genome-scale functional analysis in mammalian cells. *Proceedings of the National Academy of Sciences of the*

United States of America, *100*(21), 12147–52. http://doi.org/10.1073/pnas.1932773100

Jagannath, A., Butler, R., Godinho, S. I. H., Couch, Y., Brown, L. A., Vasudevan, S. R., … Peirson, S. N. (2013). The CRTC1-SIK1 Pathway Regulates Entrainment of the Circadian Clock. *Cell*, *154*(5), 1100–1111. http://doi.org/10.1016/j.cell.2013.08.004

Jeong, H., Cohen, D. E., Cui, L., Supinski, A., Savas, J. N., Mazzulli, J. R., … Krainc, D. (2011). Sirt1 mediates neuroprotection from mutant huntingtin by activation of the TORC1 and CREB transcriptional pathway. *Nature Medicine*, *18*(1), 159–165. http://doi.org/10.1038/nm.2559

Kandel, E. R. (2001). The molecular biology of memory storage: a dialogue between genes and synapses. *Science (New York, N.Y.)*, *294*(5544), 1030–8. http://doi.org/10.1126/science.1067020

Konorski, & Jerzy. (1948). Conditioned reflexes and neuron organization. Cambridge University Press.

Kovács, K. a, Steullet, P., Steinmann, M., Do, K. Q., Magistretti, P. J., Halfon, O., & Cardinaux, J.-R. (2007). TORC1 is a calcium- and cAMP-sensitive coincidence detector involved in hippocampal long-term synaptic plasticity. *Proceedings of the National Academy of Sciences of the United States of America*, *104*(11), 4700–5. http://doi.org/10.1073/pnas.0607524104

Lonze, B. E., & Ginty, D. D. (2002). Function and Regulation of CREB Family Transcription Factors in the Nervous System. *Neuron*, *35*, 605–623.

Mayr, B., & Montminy, M. (2001). Transcriptional regulation by the phosphorylation-dependent factor CREB. *Nature Reviews Molecular Cell Biology*, *2*(8), 599–609. http://doi.org/10.1038/35085068

Nonaka, M., Kim, R., Fukushima, H., Sasaki, K., Suzuki, K., Okamura, M., … Bito, H. (2014). Region-Specific Activation of CRTC1-CREB Signaling Mediates Long-Term Fear Memory. *Neuron*, *84*(1), 92–106. http://doi.org/10.1016/j.neuron.2014.08.049

Radivojac, P., Iakoucheva, L. M., Oldfield, C. J., Obradovic, Z., Uversky, V. N., & Dunker, A. K. (2007). Intrinsic Disorder and Functional Proteomics. *Biophysical Journal*, *92*(5), 1439–1456. http://doi.org/10.1529/biophysj.106.094045

Ramon, S., & Cajal, Y. (1894). Structure des Centres Nerveux The Croonian Lecture: La Fine Email alerting service. *Proc. R. Soc. Lond*, *1*(55), 444–468. Retrieved from http://rspl.royalsocietypublishing.org/

Riera, C. E., Huising, M. O., Follett, P., Leblanc, M., Halloran, J., Van Andel, R., … Dillin, A. (2014). TRPV1 Pain Receptors Regulate Longevity and Metabolism by Neuropeptide Signaling. *Cell*, *157*(5), 1023–1036. http://doi.org/10.1016/j.cell.2014.03.051

Sasaki, T., Takemori, H., Yagita, Y., Terasaki, Y., Uebi, T., Horike, N., … Kitagawa, K. (2011). SIK2 is a key regulator for neuronal survival after ischemia via TORC1-CREB. *Neuron*, *69*(1), 106–19. http://doi.org/10.1016/j.neuron.2010.12.004

Saura, C. A. (2012). CREB-regulated transcription coactivator 1-dependent transcription in Alzheimer's disease mice. *Neuro-Degenerative Diseases*, *10*(1–4), 250–2. http://doi.org/10.1159/000333341

Screaton, R. a, Conkright, M. D., Katoh, Y., Best, J. L., Canettieri, G., Jeffries, S., … Montminy, M. (2004). The CREB coactivator TORC2 functions as a calcium- and cAMP-sensitive coincidence detector. *Cell*, *119*(1), 61–74. http://doi.org/10.1016/j.cell.2004.09.015

Sekeres, M. J., Mercaldo, V., Richards, B., Sargin, D., Mahadevan, V., Woodin, M. A., … Josselyn, S. A. (2012). Increasing CRTC1 Function in the Dentate Gyrus during Memory Formation or Reactivation Increases Memory Strength without Compromising Memory Quality. *The Journal of Neuroscience*, *32*(49), 17857–17868. http://doi.org/10.1523/JNEUROSCI.1419-12.2012

Shaywitz, A. J., & Greenberg, M. E. (1999). CREB: a stimulus-induced transcription factor activated by a diverse array of extracellular signals. *Annual Review of Biochemistry*, *68*, 821–61. http://doi.org/10.1146/annurev.biochem.68.1.821

Silva, A. J., Kogan, J. H., Frankland, P. W., & Kida, S. (1998). CREB AND MEMORY. *Annual Review of Neuroscience*, *21*(1), 127–148. http://doi.org/10.1146/annurev.neuro.21.1.127

Song, Y., Altarejos, J., Goodarzi, M. O., Inoue, H., Guo, X., Berdeaux, R., … Montminy, M. (2010). CRTC3 links catecholamine signalling to energy balance. *Nature*, *468*. http://doi.org/10.1038/nature09564

Squire, Larry R. (2013). *Fundamental neuroscience*. Amsterdam: Elsevier/Academic Press.

Squire, L. R., Stark, C. E. L., & Clark, R. E. (2004). The medial temporal lobe. *Annual Review of Neuroscience*, *27*, 279–306. http://doi.org/10.1146/annurev.neuro.27.070203.144130

The PyMOL Molecular Graphics System, Version 1.8 Schrödinger, LLC.

Uversky, V. N. (2015). The multifaceted roles of intrinsic disorder in protein complexes. *FEBS Letters*, *589*(19), 2498–2506. http://doi.org/10.1016/j.febslet.2015.06.004

Wang, Y., Vera, L., Fischer, W. H., & Montminy, M. (2009). The CREB coactivator CRTC2 links hepatic ER stress and fasting gluconeogenesis. *Nature*, *460*(7254), 534–7. http://doi.org/10.1038/nature08111

Watts, A. G., Sanchez-Watts, G., Liu, Y., & Aguilera, G. (2011). The distribution of messenger RNAs encoding the three isoforms of the transducer of regulated cAMP responsive element binding protein activity in the rat forebrain. *Journal of Neuroendocrinology*, *23*(8), 754–66. http://doi.org/10.1111/j.1365-2826.2011.02178.x

Zhou, Y., Wu, H., Li, S., Chen, Q., Cheng, X.-W., Zheng, J., … Xiong, Z.-Q. (2006). Requirement of TORC1 for late-phase long-term potentiation in the hippocampus. *PloS One*, *1*(1), e16. http://doi.org/10.1371/journal.pone.0000016

Chapter 2

Cell Biological Mechanisms of Activity-Dependent Synapse to Nucleus Translocation of CRTC1 in Neurons

This Chapter was originally published in Ch'ng, T.H., DeSalvo, M., Lin, P. Vashisht, A., Wohlschlegel, A. J., and Martin, K.C. (2015). *Frontiers in Molecular Neuroscience* 8. Frontiers Media SA: 48. doi:10.3389/fnmol.2015.00048.

Abstract

Previous studies have revealed a critical role for CREB-regulated transcriptional coactivator (CRTC1) in regulating neuronal gene expression during learning and memory. CRTC1 localizes to synapses but undergoes activity-dependent nuclear translocation to regulate the transcription of CREB target genes. Here we investigate the long-distance retrograde transport of CRTC1 in hippocampal neurons. We show that local elevations in calcium, triggered by activation of synaptic glutamate receptors and L-type voltage-gated calcium channels, initiate active, dynein-mediated retrograde transport of CRTC1 along microtubules. We identify a nuclear localization signal within CRTC1, and characterize three conserved serine residues whose dephosphorylation is required for nuclear import. Domain analysis reveals that the amino-terminal third of CRTC1 contains all of the signals required for regulated nucleocytoplasmic trafficking. We fuse this region to Dendra2 to generate a reporter construct and perform live-cell imaging coupled with local uncaging of glutamate and photoconversion to characterize the dynamics of stimulus-induced retrograde transport and nuclear accumulation.

Introduction

Long-lasting forms of synaptic plasticity, including those underlying long-term memory, require new transcription for their persistence (Alberini, 2009; Kandel, 2001; Leslie & Nedivi, 2011). While neurons are specialized for rapid communication between compartments via electrochemical signaling, activity-dependent transcription is also regulated by the transport of soluble signaling molecules from stimulated synapses to the nucleus (Ch'ng et al, 2012; Karpova et al, 2013). Neurons are highly polarized cells that elaborate processes whose lengths can exceed that of the soma by orders of magnitude. The long-distance transport of signals from stimulated synapses to the nucleus thus requires active, regulated transport mechanisms to couple synaptic stimulation with transcription.

The regulated nuclear import of dendritically and/or synaptically localized transcriptional regulators serves as one means of directly coupling synaptic events with gene expression in the nucleus. Recent studies describe a role for the synapse to nucleus translocation of CREB-regulated transcriptional coactivator 1 (CRTC1) in regulating gene expression during long-term potentiation (LTP) of rodent hippocampal synapses (Ch'ng et al, 2012; Kovacs et al, 2007; Nonaka et al, 2014; Zhou et al, 2006). CRTC1 was originally identified in an *in vitro* screen aimed at identifying proteins that enhance the transcriptional activity of CREB in non-neuronal cells (Iourgenko et al, 2003; Screaton et al, 2004). It has diverse functions in the brain including modulation of memory in rodents and flies (Hirano et al, 2013; Nonaka et al, 2014; Sekeres et al, 2012; Zhou et al, 2006), entrainment of circadian rhythms (Jagannath et al, 2013), neuroprotection during ischemia (Sasaki et al, 2011), and regulation of cocaine-induced plasticity (Hollander et al, 2010). Both Huntington's and Alzheimer's diseases have also been linked with CRTC1-mediated activation of CREB transcription of specific target genes (Jeong et al, 2012; Saura, 2012).

We previously reported that CRTC1 undergoes activity-dependent rapid translocation from distal dendrites to the nucleus during long-term plasticity of hippocampal neurons (Ch'ng et al, 2012).

We showed that CRTC1 translocation required glutamate receptor activation, involved calcineurin-dependent dephosphorylation of CRTC1, and was critical to the activity-dependent expression of several CREB target genes (Ch'ng et al, 2012). These findings raised many questions about the mechanisms mediating the long-distance retrograde transport of CRTC1 from synapse to nucleus. The experiments described in this study are aimed at addressing these questions. Of note, while previous studies have examined the transport of vesicles and organelles in axons and dendrites (Maeder et al, 2014; van den Berg & Hoogenraad, 2012), much less is known about the cell biological mechanisms mediating the long-distance retrograde transport of soluble molecules in neurons. As such, our study provides insights into not only the transport of CRTC1, but also more broadly the retrograde transport of soluble molecules within dendrites.

We first examine the specific types of stimuli that trigger synapse to nuclear import of CRTC1 and find that it requires synaptic but not extrasynaptic glutamate receptors, calcium influx though L-type but not P/Q or N-type calcium channels, and local rather than bulk elevations in intracellular calcium. We then show that CRTC1 is actively transported along microtubules by the dynein motor protein. Using protein domain analysis, we show that the N-terminal 270 amino acids of CRTC1 are sufficient for regulated nucleocytoplasmic localization, and within this region identify a non-canonical nuclear localization signal that is necessary and sufficient for CRTC1 nuclear import. We generate Ser to Ala mutations at three highly conserved Ser residues within the N-terminal third of CRTC1, and show that dephosphorylation of all three residues is necessary and sufficient for dissociation from 14-3-3e at the synapse and for nuclear accumulation. Finally, we create a viral reporter construct consisting of the N-terminal third of CRTC1 fused to the photoconvertible fluorescent protein dendra2, and perform live cell imaging to visualize and characterize the dynamics of synapse-specific activation of CRTC1 nuclear import.

Results

Glutamatergic receptor and L-type calcium channel activation promote nuclear translocation of CRTC1

We previously reported that activation of synaptic NMDA receptors was required for CRTC1 synapse to nucleus transport (Ch'ng et al, 2012) but did not rule out a role for extrasynaptic NMDA receptors. This distinction is important since NMDA receptors are located both synaptically and extrasynaptically (Papouin & Oliet, 2014) and activation of each triggers distinct signaling pathways, with the former eliciting synaptic plasticity and the latter leading to cell death (Hardingham et al, 2002). To determine whether activation of extrasynaptic NMDA receptors also triggers CRTC1 nuclear import, we bath applied NMDA to cultured neurons to activate NMDA receptors while blocking distinct subpopulations of NMDA receptors with APV, which blocks both synaptic and extrasynaptic NMDA receptors; MK801, an open channel, usage-dependent antagonist that only blocks activated NMDA receptors (Thompson et al, 1990); or ifenprodil, an antagonist of GluN2B subunit containing NMDA receptors, which are enriched at extrasynaptic sites (Hardingham et al, 2002). Immunocytochemical analysis revealed that MK801 blocked NMDA-induced nuclear accumulation of CRTC1 and phosphorylation of CREB at serine 133, but that ifenprodil did not. In fact, stimulation with NMDA in the presence of ifenprodil triggered significantly more nuclear accumulation of CRTC1 than did NMDA alone, suggesting that activation of extrasynaptic NMDARs functions to repress CRTC1 synapse to nucleus import (Fig 2.1A and Appendix fig S2.1A).

Next, we focused on the AMPA receptor, which plays a crucial function in various forms of learning-related neuronal plasticity (Kessels & Malinow, 2009). Inhibition of NMDA receptors with APV greatly reduces but does not completely abolish bicuculline (BIC) -induced CRTC1 translocation (Ch'ng et al, 2012), indicating that other synaptic glutamatergic receptors contribute to CRTC1 nuclear localization. Selective activation of AMPA receptors with AMPA triggered robust CRTC1 nuclear accumulation, which was significantly reduced by the AMPA receptor blocker NBQX (Fig 2.1B). The L-

type VGCC antagonist nimodipine also reduced AMPA receptor-mediated CRTC1 nuclear accumulation, suggesting that activation of AMPA receptors at the synapse produces sufficient local depolarization to activate VGCCs and to relieve the Mg^{2+} block in NMDA receptors (Higley & Sabatini, 2012; Macias et al, 2001). We tested this hypothesis by selectively activating synaptic NMDA receptors in the presence of AMPA receptor antagonists by preincubating neurons with TTX (to block action potentials) and ifenprodil (to block extrasynaptic NMDA receptors) and then incubating neurons with NMDA in the presence of the AMPA receptor blocker NBQX. Under these conditions, NMDA-induced CRTC1 nuclear accumulation was significantly diminished, consistent with a role for AMPA receptors in NMDA receptor-mediated regulation of CRTC1. To confirm that AMPA receptor activation functions by relieving the Mg^{2+} block in NMDA receptors, we reduced the Mg^{2+} ions in the Tyrode's solution by 10 fold during NMDA stimulation and showed that CRTC1 translocation no longer required AMPA receptor function (Fig 2.1C).

In addition to inhibiting CRTC1 nuclear import induced by incubation with AMPA, we previously showed that the L-type VGCC antagonist nimodopine also blocked CRTC1 nuclear import induced by incubation with the $GABA_A$ receptor antagonist bicuculline (Ch'ng et al, 2012). To test whether the N-type or P/Q type VGCCs were also required for CRTC1 synapse to nucleus import, we depolarized neurons with KCl in the presence of conotoxin to block N-type VGCCs, agatoxin to block P/Q-type VGCCs, or nimodipine to block L-type VGCCs. As shown in figure 2.1D, only inhibition of L-type VGCCs with nimodipine blocked KCl-induced CRTC1 translocation. Consistent with previously published reports, we also found that only L-type VGCCs were required to trigger depolarization-induced increase in pCREB S133 immunoreactivity (Appendix fig S2.1C; Wheeler et al, 2012).

To further characterize the source of calcium entry required for stimulus-induced CRTC1 nuclear import, we assayed the effect of both high affinity, fast-acting (BAPTA) and low affinity and slower-acting (EGTA) calcium chelators. BAPTA rapidly suppresses local elevations in calcium near their source of entry at the plasma membrane while EGTA has a 100 fold slower on rate and thus blocks bulk

cytosolic elevations in calcium (Deisseroth et al, 1996; Neher & Almers, 1986). We found that BAPTA, but not EGTA completely blocked the nuclear accumulation of CRTC1 and phosphorylation of CREB at Serine 133 induced by KCl depolarization (Fig 2.1E and Appendix fig S2.1D). Together, these findings indicate that the local influx of calcium produced by activation of synaptic NMDA receptors lies directly upstream of CRTC1 nuclear translocation. We also found that the function of AMPA receptors and L-type VGCCs in promoting CRTC1 nuclear import is primarily to relieve the Mg^{2+} block in the NMDA receptors.

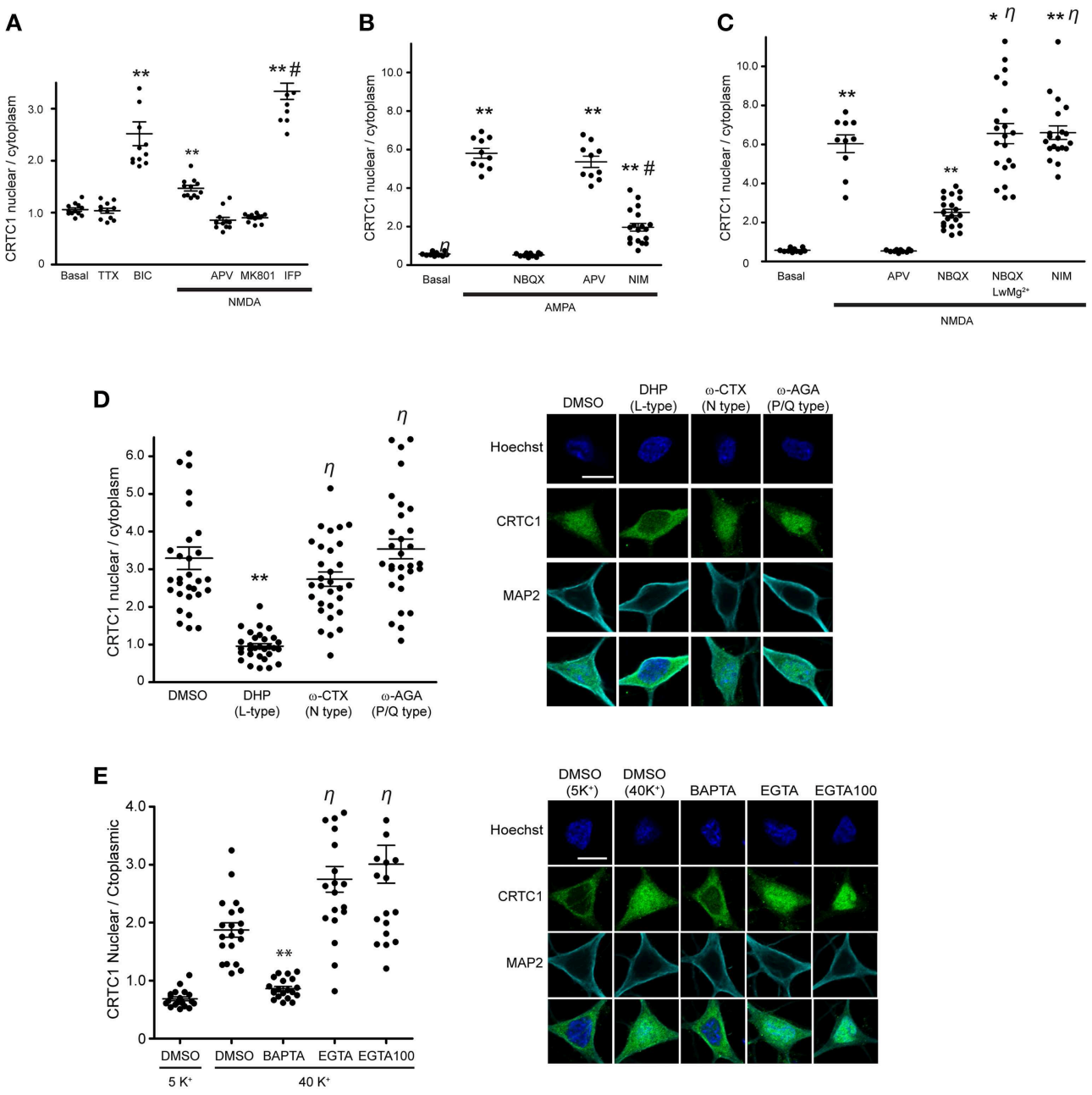

Figure 2.1: CRTC1 nuclear translocation requires local calcium influx via glutamate receptors and L-type VGCCs

(A) Nuclear to cytoplasmic ratio of CRTC1 in cultured neurons after stimulation with NMDA in the presence of different NMDA receptor antagonists, APV, MK801 or Ifenprodil (IFP) (**p<0.001 relative to basal).

(B and C) Nuclear to cytoplasmic ratio of CRTC1 in cultured neurons pre-incubated with TTX and IFP, in conjunction with either NBQX, APV or nimodipine (NIM) before being stimulated with either AMPA or NMDA. Experiments were performed in either Tyrode's with regular $MgCl_2$ (1 mM) or low $MgCl_2$ (0.1 mM) (** p<0.001 relative to basal; *p<0.001 relative to NBQX).

(D) Confocal micrographs and nuclear to cytoplasmic ratio quantification of CRTC1 in neurons depolarized with KCl in the presence of NIM, conotoxin (ω-CTX), agatoxin (ω-AGA) or mock treated with DMSO (** p<0.001 relative to DMSO).

(E) Membrane permeable calcium chelators BAPTA and EGTA (25 µM/100µM) were incubated in neurons prior to depolarization with KCl ($5K^+$ 5 mM; $40K^+$ 40 mM). Nuclear to cytoplasmic ratio of CRTC1 was quantified (** p<0.001 relative to DMSO $40K^+$). All scale bars = 10 µm.

CRTC1 synapse to nuclear transport involves active, dynein-dependent movement along microtubules

In our previous experiments, the rapid nuclear accumulation of CRTC1 following synaptic stimulation suggested that soluble CRTC1 must be actively transported to the nucleus. To determine how CRTC1 is transported from distal stimulated synapses to the nucleus, we asked whether it required active transport, which, unlike passive diffusion, can be blocked at 10 ºC (Talcott & Moore, 1999; Wiegert et al, 2007). Stimulation of neurons with BIC at 10 ºC or 37 ºC revealed that CRTC1 nuclear accumulation was blocked at lower temperatures (Fig 2.2A), consistent with an active transport process. We then asked whether microtubules are required for the transport by depolymerizing microtubules with low concentrations of nocodazole and found that this significantly inhibited the nuclear accumulation of CRTC1 in response to BIC (Fig 2.2B) without compromising the viability, morphology or synapse density of the neurons (Appendix fig S2.2A).

We next asked whether CRTC1 nuclear import was mediated by the microtubule-based retrograde motor protein dynein. In initial experiments, we incubated cultures with EHNA, a chemical inhibitor that blocks dynein ATPase activity (Penningroth et al, 1982; Tsai et al, 2009), and found that it inhibited BIC-induced CRTC1 nuclear translocation (Fig 2.2C). As EHNA is a broad spectrum inhibitor, we also specifically disrupted cytoplasmic dynein function by overexpressing dynamitin, which functions as a dominant negative by triggering the disassembly of dynactin, a multiprotein complex required for dynein-based movement (Melkonian et al, 2007; Shrum et al, 2009). Dynamitin overexpression in neurons significantly decreased nuclear CRTC1 accumulation following BIC stimulation (Fig 2.2D). To complement these experiments, we used siRNA to knockdown the expression of dynein heavy chain (Appendix fig S2.2B), and found that this also significantly decreased BIC-induced CRTC1 nuclear accumulation as compared to BIC-stimulated control neurons incubated with non-targeted siRNA (Fig 2.2E). Together, these data indicate that dynein mediates the long-distance retrograde transport of CRTC1 along microtubules.

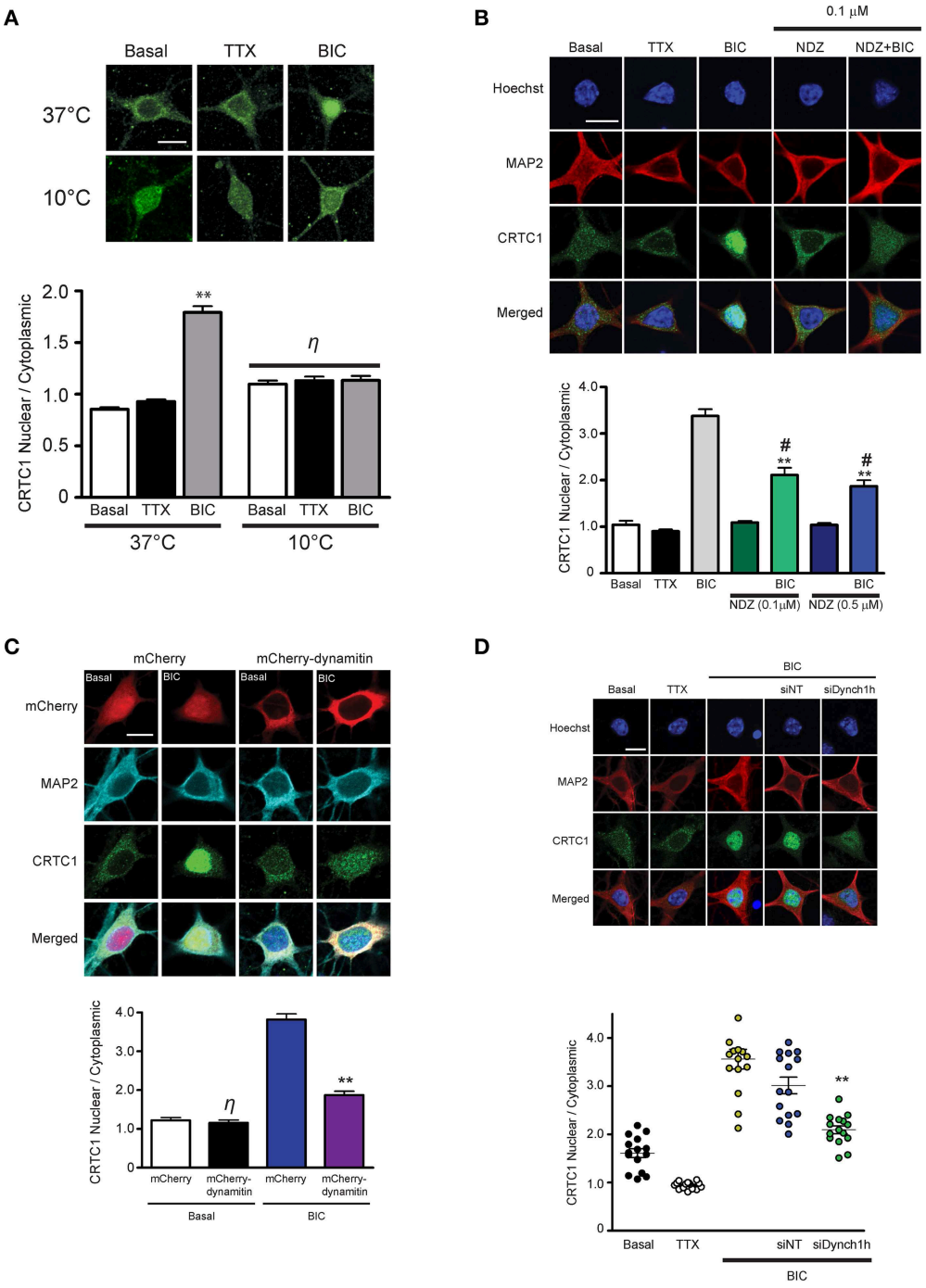

Figure 2.2: Nuclear accumulation of CRTC1 involves active, dynein-mediated transport along microtubules

(A) Neurons were stimulated with either TTX or BIC in incubators at 37°C or 10°C. CRTC1 nuclear to cytoplasmic ratio was quantified (**p<0.001 relative to basal; n.s. not significant).

(B) Neurons were incubated with nocodazole (NDZ, 0.1 μM or 0.5 μM) to depolymerize microtubules prior to BIC stimulation (**p<0.001 relative to non-BIC samples).

(C) Neurons were treated with EHNA to inhibit retrograde dynein movement prior to stimulation with BIC (** p<0.001 relative to BIC stimulated samples).

(D) Neurons expressing either mCherry or mCherry-dynamitin were stimulated with BIC. Endogenous expression of CRTC1 in the nucleus and cytoplasm of mCherry expressing neurons were quantified (** p<0.001 relative to mCherry only samples; n.s. not significant).

(E) Mouse hippocampal neurons (21-28 DIV) were incubated with dynein heavy chain siRNA (siDynch1h) or non-targeted control (siNT) followed by stimulation with TTX or BIC (**p<0.001 CRTC1 nuclear to cytoplasmic ratio relative to siNT and BIC). All scale bars = 10 μm.

CRTC1 encodes an arginine-rich nuclear localization signal

Having determined the source of calcium entry at the synapse that triggers CRTC1 synapse to nuclear import, and shown that CRTC1 retrograde transport is active and occurs along microtubules in a dynein-dependent manner, we next focused on the signals which regulate CRTC1 transport into the nucleus. Nuclear import of proteins larger than 40-60kD is typically facilitated by transport proteins that recognize nuclear localization signals (NLSs), which are often comprised of short stretches of basic amino acids (Lange et al, 2007). Analysis of the CRTC1 primary amino acid sequence revealed three highly conserved clusters of basic residues near the amino-terminus of the protein (Fig 2.3A). To determine whether these amino acid clusters comprised an NLS, we fused a 57 amino-acid sequence (aa 92 to 148) from CRTC1 that contained all three arginine-rich clusters (CRTC1-AR) to four tandem copies of GFP (4xGFP, Fig 3B). While 4xGFP localized exclusively to the cytoplasm of neurons, fusion to CRTC1-AR promoted robust nuclear accumulation of 4xGFP (Fig 2.3B). The amount of nuclear accumulation was greater than the nuclear accumulation observed when 4xGFP was fused to the canonical SV40 NLS. To identify the minimal region required for nuclear translocation, we further divided CRTC1-AR into two sub-fragments, CRTC1-N1 (amino acids 103-135), which contained two clusters of arginine residues, and CRTC1-C1 (amino acids 135-147). As shown in figure 2.3B, only CRTC1-N1 fragment was able to confer accumulation in the nucleus of neurons, although to a lesser extent than full length CRTC1-AR, while the CRTC1-C1 fragment remained cytoplasmically localized. We also tested these sequences in HEK293T cells, and found that the full length CRTC1-AR and the CRTC1-N1 fragment both promoted nuclear import of CRTC1 (Appendix fig S2.3A).

To probe the necessity of the NLS in mediating the nuclear import of CRTC1, we generated two HA epitope-tagged full-length CRTC1 alanine mutants. In the first (HA-mNLS1), we mutated four highly conserved arginines to alanines (R103A, R106A, R108A and R110A). In the second mutant (HA-mNLS2), we mutated one proline and two arginine residues to alanine (P114A, R116A and R117A). Neither of

these mutants disrupted phosphorylation of CRTC1 at serine residue 151, a site that has been shown to regulate nucleocytoplasmic trafficking in non-neuronal cells (Appendix fig S2.3B; (Screaton et al, 2004)). However, neither of these mutants were efficiently imported into the nucleus upon BIC stimulation, indicating that these particular conserved residues constitute essential components of the NLS (Fig 2.3C).

To determine if the classical nuclear import pathway was involved in CRTC1 nuclear entry (Jeffrey et al, 2009; Thompson et al, 2004), we used siRNA to knock down importin β1 (KPNB1) expression to 45% of baseline values (using GAPDH siRNA knockdown as controls) in HEK293T cells (Fig 2.3D and Appendix fig S2.3C). While the knockdown blocked the nuclear import of a canonical NLS (4xGFP-SV40), it did not inhibit the nuclear translocation of 4xGFP-tagged CRTC1-AR (Fig 2.3D). We also inhibited the classical nuclear import pathway using cell-permeable inhibitor peptides that mimic the NLS of NFκB SN50 (Lai et al, 2008) and did not detect any effect on BIC-induced CRTC1 nuclear translocation (Supplementary fig. S2.3D). Finally, we overexpressed 4xGFP-tagged CRTC1-AR and SV40 NLS in neurons (Appendix fig S2.3E) and showed that at high expression levels, only the CRTC1 arginine-rich NLS but not the SV40 NLS was able to inhibit nuclear translocation of endogenous CRTC1. Taken together, our experiments indicate that CRTC1 undergoes active transport into the nucleus in a manner that is independent of the classical importin α / β1-mediated pathway.

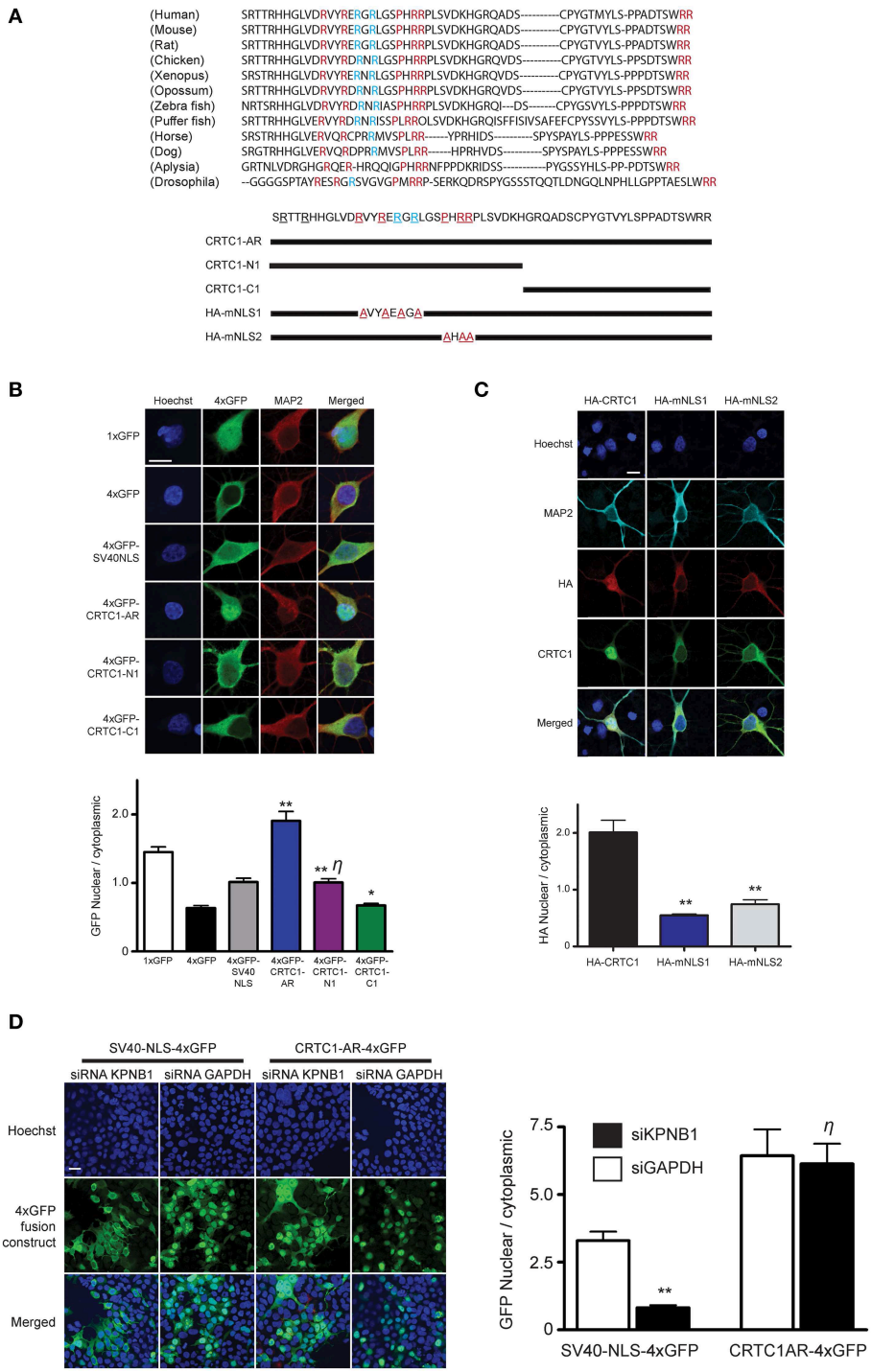

Figure 2.3: Characterization of CRTC1's arginine-rich NLS

(A) A 57 amino acid fragment (S92-R148) in CRTC1 with sequence identity (red) and similarity (blue) across species. Expression constructs described below.

(B) As diagramed in (A), the full length arginine-rich fragment (CRTC1-AR) as well as CRTC1-N1, CRTC1-C1 and SV40NLS control fragment fused to 4xGFP were expressed in neurons. GFP signal in the nucleus and cytoplasm were quantified (** $p<0.001$ relative to 4xGFP; * ns relative to SV40NLS).

(C) Neurons expressing full length HA-tagged CRTC1 and alanine mutations in two arginine-rich clusters (HA-mNLS1 and HA-mNLS2, as diagramed in A) were stimulated with BIC and immunostained with antibodies against HA epitope (** $p<0.001$ relative to HA-CRTC1).

(D) HEK293T cells were treated with siRNA against KPNB1 (Importin β1) or GAPDH before being transiently transfected with SV40NLS-4xGFP or CRTC1-AR-4xGFP. The nuclear to cytoplasmic ratio of GFP was quantified (**$p<0.001$ relative to siGAPDH). Scale bars = 10 μm.

The first 270 amino acids of CRTC1 are sufficient for stimulus-induced nucleocytoplasmic shuttling

In the course of analyzing the different domains to identify the NLS in CRTC1, we observed that a fragment containing amino acids 1-270 of CRTC1 localized strongly to the nucleus of CHO cells. In contrast, the carboxy terminal fragment of CRTC1, from amino acids 271-630, localized exclusively to the cytoplasm (Appendix fig S2.4A). Further analysis in neurons show that fragment 1-270 localizes to dendrites and synapses in silenced neurons but underwent stimulus-induced translocation in a manner that was indistinguishable from full-length CRTC1 (Fig 2.4B and Appendix fig S2.4A). These findings indicated that the N-terminal 270 amino acids contained all of the signals required for regulated synaptic and nuclear localization.

We took advantage of this finding to develop a fluorescent reporter to monitor synapse to nucleus CRTC1 signaling by fusing the amino terminal fragment (aa 1-270) of CRTC1 to Dendra2, a photoconvertible fluorescent protein that switches from green (507 nm) to red (573 nm) emission following brief UV illumination. Unlike the full-length CRTC1, this fusion protein was small enough to package in a lentivirus using a *Camk2α* promoter to achieve modest levels of expression exclusively in excitatory neurons. Using this reporter, henceforth identified as $CRTC1^{270}$, we were able to photoconvert a subpopulation of CRTC1 in dendrites of cultured hippocampal neurons (21 to 28 DIV) and track its stimulus-induced movement and nuclear accumulation (Chudakov et al, 2010). Long-term expression (> 1 wk) of the fusion protein in cultured neurons did not have any visible effect on neuronal viability.

To ensure that overexpression of $CRTC1^{270}$ did not function as a dominant negative and thereby interfere with CREB-mediated activity-dependent transcription, we transfected neurons with $CRTC1^{270}$ and used qPCR to test the induction of CREB target genes following TTX withdrawal (Saha et al, 2011). As shown in figure 2.4A, overexpression of $CRTC1^{270}$ did not alter the basal or the activity-induced expression of any CREB target genes, indicating that it did not have any dominant-negative activity.

We next set out to determine whether the dynamics of stimulus-induced synapse to nuclear import of $CRTC1^{270}$ showed any differences from that of endogenous, full-length CRTC1. Towards this end, we cultured neurons and transduced them with lentivirus to express $CRTC1^{270}$. We then stimulated with BIC, and performed immunocytochemistry with anti-dendra2 antibodies to visualize the localization of $CRTC1^{270}$. In parallel, we performed immunocytochemistry with anti-CRTC1 antibodies to visualize CRTC1 localization in neurons that were not transduced with $CRTC1^{270}$. As shown in figure 2.4B, similar to endogenous full length CRTC1, BIC stimulated robust $CRTC1^{270}$ nuclear translocation that required calcineurin, NMDA and L-type VGCC activation. Moreover, the kinetics of nuclear export of $CRTC1^{270}$ following BIC stimulation was indistinguishable from that of full-length, endogenous CRTC1 (Fig 2.4C).

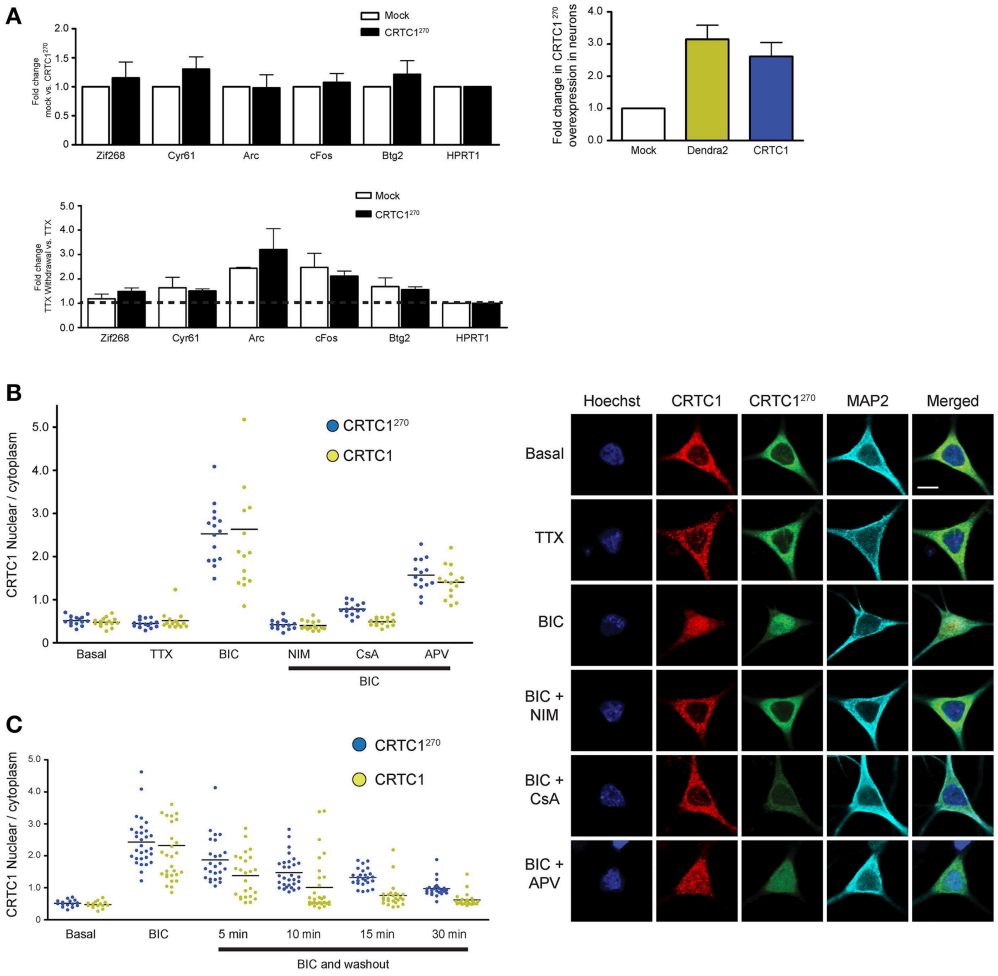

Figure 2.4: The nuclear translocation of CRTC1^{270} is identical to endogenous full length CRTC1 and does not inhibit transcription of CREB target genes

(A) Rat neurons expressing CRTC1^{270} or mock transduced were incubated with TTX. In half the samples, TTX was withdrawn to stimulate neuronal activity while the other half of the sample remained incubated in TTX. Total RNA was extracted after treatment and CREB target genes were analyzed via qPCR (n=5 basal TTX; n=3 stimulation by TTX withdrawal). The expression of CRTC1^{270} in neurons was also measured via qPCR using primers against Dendra2 or mouse CRTC1.

(B and C) Neurons transduced with CRTC1^{270} were pretreated with APV, NIM, TTX and cyclosporinA (CsA), stimulated with BIC, and fixed immediately or at the indicated time points after BIC washout. The amount of endogenous CRTC1 and CRTC1^{270} in the nucleus and cytoplasm were quantified. Scale bars = 10 μm.

Local uncaging of glutamate at synapses drives distally-localized CRTC1 into the nucleus

These findings encouraged us to undertake live-cell imaging of neurons expressing CRTC1^{270} (Fig 2.5). We previously showed that bath applied stimuli triggered nuclear accumulation of overexpressed CRTC1-Dendra2 (Ch'ng et al, 2012). Here we used CRTC1^{270} to label and visualize in real time the nuclear accumulation of CRTC1^{270} that is derived specifically from stimulated synapses. To do this, we transduced neurons with CRTC1^{270}, incubated neurons in low Mg^{2+} Tyrode's solution in the presence of TTX and used UV illumination to simultaneously uncage glutamate and photoconvert CRTC1^{270} in a 10 µm dendritic region of activation (ROA) located approximately 100 µm away from the soma (Fig 2.5 and Appendix figure S2.4D). Calcium imaging using Fluo4AM revealed that local uncaging of glutamate triggered local elevations of intracellular calcium around the region of activation, which rapidly dissipated and did not reach the soma (Appendix fig S2.4E). We first photoconverted CRTC1^{270} and uncaged glutamate in a single dendritic branch, and failed to detect nuclear accumulation of photoconverted CRTC1 (Appendix fig S2.4F). We then photoconverted CRTC1^{270} and uncaged glutamate in two ROAs located on adjacent dendritic branches and observed robust nuclear accumulation of photoconverted CRTC1 (Fig 2.5). We also optimized parameters for UV illumination to ensure maximal green to red photoconversion while minimizing photobleaching. This optimized protocol was used in all subsequent live imaging experiments.

Photoconverted (red) CRTC1^{270} was initially detected in the nucleus approximately 100-120s (t=10) after uncaging (Fig 2.5A), consistent with the speed of motor-driven active transport of vesicular structures in neuronal processes (0.8-1.2 µm/s; (van den Berg & Hoogenraad, 2012). The nuclear accumulation of native (green) CRTC1^{270} signal is not surprising given that the UV stimulation at the ROA did not completely convert all the native green Dendra2 protein to red. Following that, we performed additional experiments to ensure that the cell biological mechanisms underlying CRTC1^{270} were identical to those mediating the nuclear import of endogenous full-length CRTC1. As shown in figure 2.5, we

found that, like full-length CRTC1, BIC-induced nuclear import of $CRTC1^{270}$ required both NMDA and AMPA receptors (Fig 2.5B), was temperature-sensitive (Fig 2.5C) and involved microtubule-dependent transport (Fig 2.5D). We also found that, like endogenous full-length CRTC1, $CRTC1^{270}$ translocation from stimulated synapses to the nucleus was blocked by BAPTA but not EGTA, indicating that, like endogenous CRTC1, its nuclear translocation was triggered by local and not bulk elevations in Ca^{2+} at the plasma membrane (Fig 2.5E). Together, these findings indicate that $CRTC1^{270}$ serves as a faithful reporter of stimulus-induced CRTC1 synapse to nuclear transport.

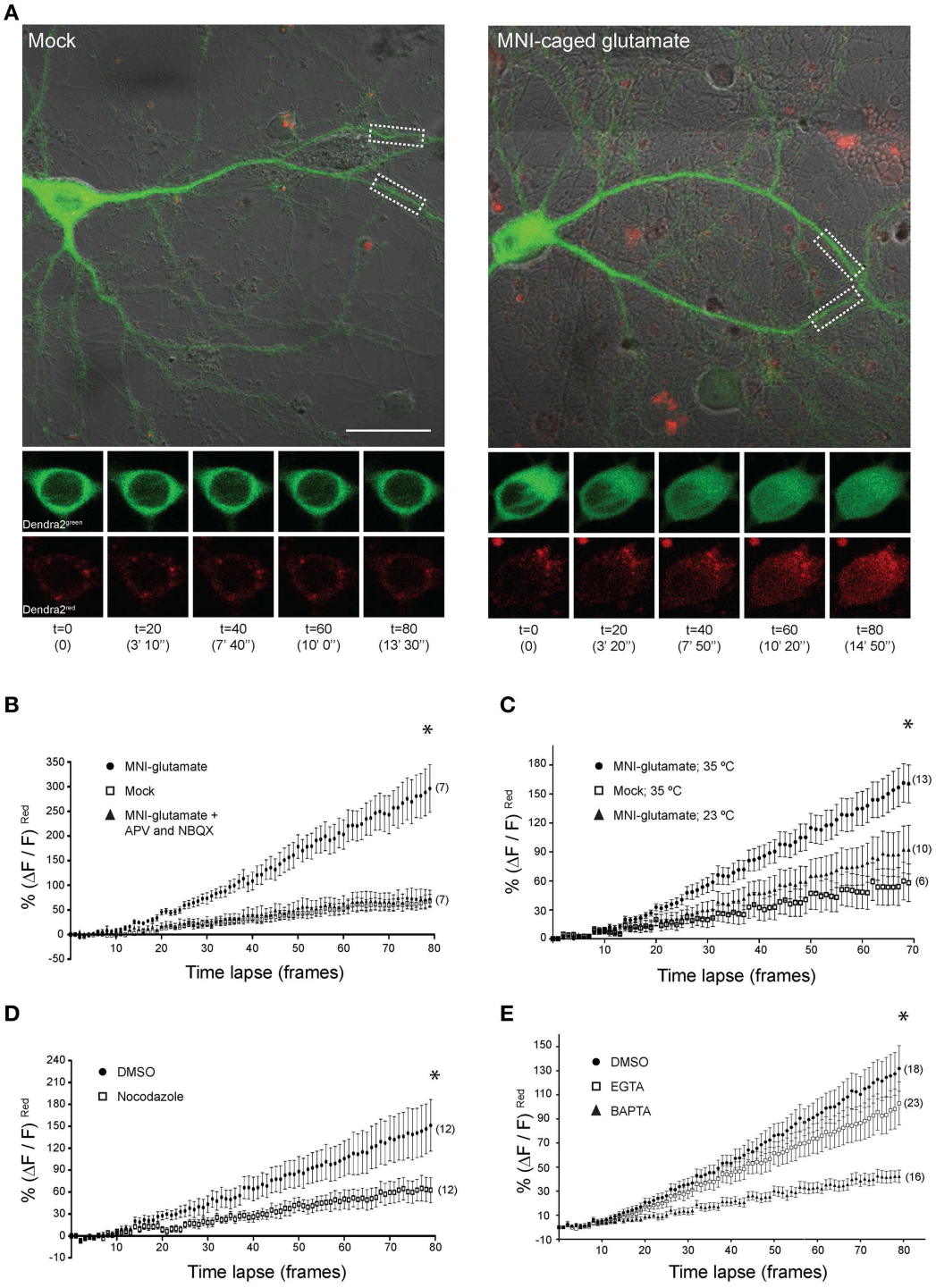

Figure 2.5: Local uncaging of glutamate at synapses can drive distally-localized CRTC1^{270} into the nucleus

(A) Neurons expressing CRTC1^{270} were illuminated with a UV laser in the presence or absence (mock) of MNI-caged glutamate. The white dashed boxes indicate the region of activation (~ 10 um; ROA). Time-lapse images of the soma at every 20th frame (time stamp in parenthesis) are shown for CRTC1^{270} in both native green and photoconverted red channels. Scale bar = 20 mm. (B-E) Neurons expressing CRTC1^{270} were stimulated with (B) mock or MNI-glutamate in the presence or absence of APV and NBQX (*p=0.49 mock vs. APV/NBQX; p<0.0001 MNI vs. mock and APV/NBQX), (C) MNI-glutamate at 35 ºC or 23 ºC (*p<0.0001 Mock 35 ºC vs. MNI 35 ºC, Mock 35 ºC vs. MNI 23 ºC and MNI 35 ºC vs. MNI 23 ºC), (D) MNI-glutamate after incubation with NDZ (*p<0.0001 DMSO vs. NDZ), or (E) pretreated with either BAPTA-AM or EGTA-AM prior to glutamate uncaging (*p<0.0001 DMSO vs. EGTA vs. BAPTA and EGTA vs. BAPTA). Statistics were performed with linear regression analysis of the slopes for comparison of fit between data sets.

CRTC1^{270} movement is biased toward the nucleus following neuronal stimulation

As previous live-imaging studies of transport within dendrites have focused more on the movement of vesicles and organelles (Maeder et al, 2014), we set out to use the CRTC1^{270} reporter to visualize the retrograde transport of soluble molecules within dendrites. Towards this end, we visualized the transport of CRTC1 within a single dendritic branch, using spinning disc microscopy for rapid image acquisition (~100 ms/frame). The signal we detected within the dendrite from local uncaging of glutamate was too weak to monitor by time lapse microscopy, and we thus combined local photoconversion of CRTC1^{270} with bath stimulation with BIC and forskolin (which promotes persistence of CRTC1 in the nucleus) to visualize the dynamics of a local population of photoconverted CRTC1, or, as a control, photoconverted Dendra2, within the dendrites of unstimulated and stimulated neurons. We tested multiple photoconversion parameters to optimize image acquisition and minimize photobleaching without compromising neuronal viability (Appendix fig S2.4G-H) . In unstimulated conditions, photoconverted CRTC1^{270} underwent rapid bidirectional movement from the ROA, as did the control Dendra2 protein (Fig 2.6A). When neurons were stimulated, the movement of CRTC1^{270} became biased toward the soma (proximal), as detected by an increase in the average normalized intensity across the length of the dendrite proximal to the stimulation site over time (Fig 2.6B). We quantified the difference in normalized pixel intensity for pairwise length measurements (1.5 µm segments) along the distal and proximal lengths of the dendrite originating from the ROA and plotted a bias index. The majority of data points for stimulated CRTC1^{270} had a positive bias index, indicating a bias in movement toward the soma. Conversely, the non-stimulated CRTC1^{270} control had averages closer to zero, indicating a bidirectional distribution of the photoconverted signal across the length of the dendrite (Figs 2.6B and C). To better illustrate the shift in fluorescence intensity over time, we graphed the cumulative bias of CRTC1^{270} moving toward the soma during the length of the experiment (Fig. 2.6C). A

positive cumulative slope indicates that activated CRTC1^{270} concentrations are much higher on the proximal branch of the dendrite throughout image acquisition.

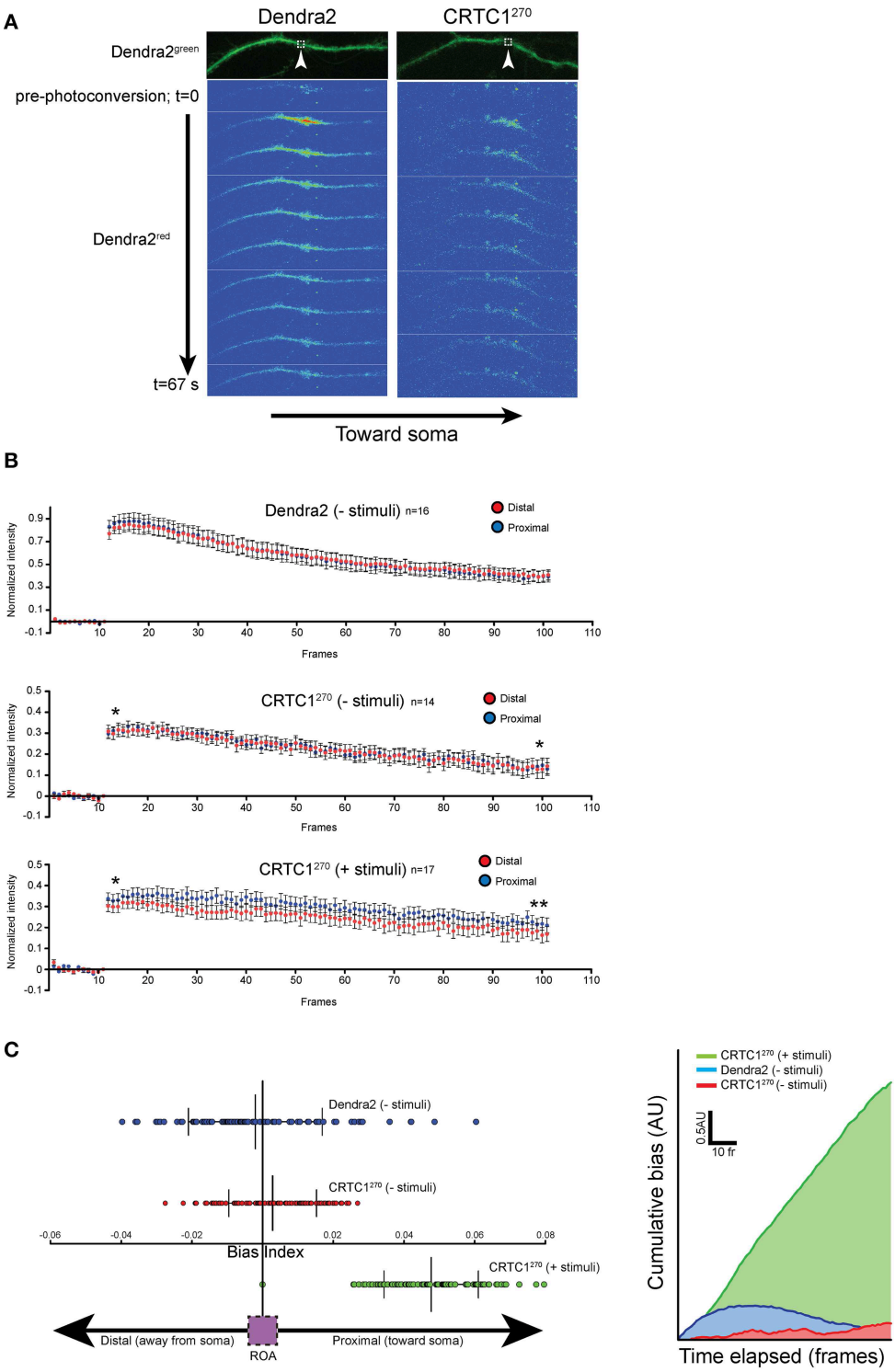

Figure 2.6: Local CRTC1^{270} transport from dendrites is biased toward the nucleus during glutamatergic stimulation

(A, B) Neurons expressing either Dendra2 alone or CRTC1^{270} were mock treated (-stimuli) or bath stimulated (+stimuli) followed by UV activation in a (1.5 um^2) region (white box) of dendrite. The rapid movement of Dendra2^{red} was captured by spinning disc microscopy. The normalized intensity (over baseline levels) over time of Dendra2^{red} was quantified for a 40µm segment of the dendrite either proximal (closer to the soma) or distal to the area of the photoconversion (upaired t-test, two-tailed ** $p<0.05$ at t=95-100; *$p>0.05$, not significant at t=11-15).

(C) The difference in pairwise spatial measurements of normalized Dendra2^{red} along the dendrite from the ROA was quantified as a bias index. A positive bias indicates a higher signal intensity in proximal dendrites. Data points were then plotted as a cumulative bias index over time elapsed for each stimulation paradigm (AU= arbitrary units).

Dephosphorylation at three conserved serine residues in CRTC1 triggers release of CRTC1 from 14-3-3ε and synapse to nucleus translocation

The phosphorylation state of CRTC1 undergoes complex changes after synaptic activity in rodent hippocampal neurons (Ch'ng et al, 2012; Nonaka et al, 2014). We hypothesized that the nuclear translocation of CRTC1 involved dephosphorylation of specific residues. Analysis of the mouse CRTC1 primary amino acid sequence revealed a significant enrichment of serine and threonine residues (Fig 2.7A and Appendix fig 2.5A). To identify the residues that are phosphorylated in CRTC1, we transiently transfected mouse Neuro-2A cell lines with full-length HA epitope-tagged CRTC1 protein, purified the protein using HA antibodies and analyzed the samples by mass spectometry. We identified candidate phosphopeptides containing 50 putative phosphoresidues (33 Ser, 14 Thr and 3 Tyr residues; Fig. 2.7A; labeled in color). This is likely an underestimate of the total number of phosphorylated residues in CRTC1 since we omitted phosphopeptide hits identified with less than 90% confidence levels. Sequence homology of CRTC1 indicated that 11 of the phosphorylated residues are 100% conserved across ten species (Fig. 2.7A; labeled in red). Nine of these are located within the N-terminal 270 amino acids. To begin to dissect the role of regulated dephosphorylation in the synapse to nucleus transport of CRTC1, we generated phosphoincompetent (serine to alanine) mutations at three of these sites, S64, S151 and S245, as single, double and triple mutants within $CRTC1^{270}$. Dephosphorylation of S151 has been shown to be sufficient for nuclear import in non-neuronal cells (Altarejos et al, 2008; Kovacs et al, 2007), while dephosphorylation of both S151 and S245 has been reported to be sufficient for significant CRTC1 nuclear accumulation in neurons (Nonaka et al, 2014). We also included S64 in our studies because, as shown in Fig. 2.8, like S245, S64 shares 100% similarity across 13 species (with S64 being a T in *C. elegans*) and S64 and S245 have identical flanking amino acids (GGSLP), which are also highly conserved across species.

To elucidate the function of S64 and the conserved amino acids flanking S64, we made several substitution mutations at and surrounding S64 in CRTC1^{270}, including a double tyrosine to alanine (Y60A/Y61A) mutant and a glutamine to alanine substitution mutant (Q70A; Appendix fig S2.5B) and expressed these mutant proteins in neurons. As shown in figure 2.7B and Appendix figure S2.5B, the S64A mutant was cytoplasmically localized in TTX-silenced neurons, but exhibited enhanced nuclear accumulation compared to wildtype CRTC1^{270} in BIC-stimulated neurons and in control, unsilenced neurons (which have basal levels of action potential firing). Mutations at Y60, Y61, Q70 or at the conserved serine at 245 did not alter the localization of CRTC1^{270} as compared to wild type CRTC1^{270} in either silenced, basal or stimulated neurons.

We previously reported that unlike in non-neuronal cells (Altarejos et al, 2008), CRTC1 bearing a S151A mutation did not result in constitutive CRTC1 nuclear accumulation. We generated the S151A mutation for CRTC1^{270}, and again found that when expressed in neurons, the mutant localized to the cytoplasm in TTX-silenced neurons. Although we observed significantly more S151A-CRTC1^{270} in the nucleus in unsilenced neuronal cultures, we did not detect any enhancement of nuclear accumulation in BIC-stimulated neurons (Fig 2.7). Similarly, a single serine to alanine mutation at S245 also did not result in constitutive accumulation of CRTC1^{270} in the nucleus. These results indicate that dephosphorylation of S151 alone, similar to S64 and S245 is not sufficient to promote robust nuclear import of CRTC1.

Since none of the single serine to alanine mutations generated a constitutive nuclear localization of CRTC1^{270} in TTX-silenced neurons, we tested the possibility that dephosphorylation at combinations of the three sites was required for nuclear accumulation. To test this idea, we generated double and triple serine to alanine substitution mutants (S64A/S151A; S64A/S245A; S151A/S245A; and S64A/S151A/S245A) in CRTC1^{270}. We found that all three double mutants exhibited increased nuclear accumulation of CRTC1^{270} in TTX-silenced neurons, and enhanced nuclear accumulation in basal and BIC-stimulated neurons. The amount of CRTC1^{270} nuclear accumulation in the double mutants was less than

in the triple S64A/S151A/S245A mutant under all conditions. Thus, when all three serine residues were simultaneously mutated to alanine, CRTC1^{270} was constitutively localized in the nucleus (Fig 2.7 and Appendix figure 2.5B). We also constructed serine to aspartic acid or glutamic acid phosphomimetic mutations at S64, S151 and S245 individually but found that none of these mutations constitutively localized CRTC1 to the cytoplasm (Appendix figure S2.5B-C).

A

```
1    MATSNNPRKF SEKIALHNQK QAEETAAFEE VMKDLSLTRA ARLQLQKSQY
51   LQLGPSRGQY YGGSLPNVNQ IGSSSVDLAF QTPFQSSGLD TSRTTRHHGL
101  VDRVYRERGR LGSPHRRPLS VDKHGRQADS CPYGTVYLSP PADTSWRRTN
151  SDSALHQSTM TPSQAESFTG GSQDAHQKRV LLLTVPGMED TGAETDKTLS
201  KQSWDSKKAG SRPKSCEVPG INIFPSADQE NTTALIPATH NTGGSLPDLT
251  NIHFPSPLPT PLDPEEPPFP ALTSSSSTGS LAHLGVGGAG QGMNTPSSSP
301  QHRPAVVSPL SLSTEARRQQ AQQVSPTLSP LSPITQAVAM DALSLEQQLP
351  YAFFTQTGSQ QPPPQPQPPP PPPPVSQQQP PPPQVSVGLP QGGPLLPSAS
401  LTRGPQLPPL SVTVPSTLPQ SPTENPGQSP MGIDATSAPA LQYRTSAGSP
451  ATQSPTSPVS NQGFSPGSSP QHTSTLGSVF GDAYYEQQMT ARQANALSRQ
501  LEQFNMMENA ISSSSLYNPG STLNYSQAAM MGLSGSHGGL QDPQQLGYTG
551  HGGIPNIILT VTGESPPSLS KELSSTLAGV SDVSFDSDHQ FPLDELKIDP
601  LTLDGLHMLN DPDMVLADPA TEDTFRMDRL
```

B

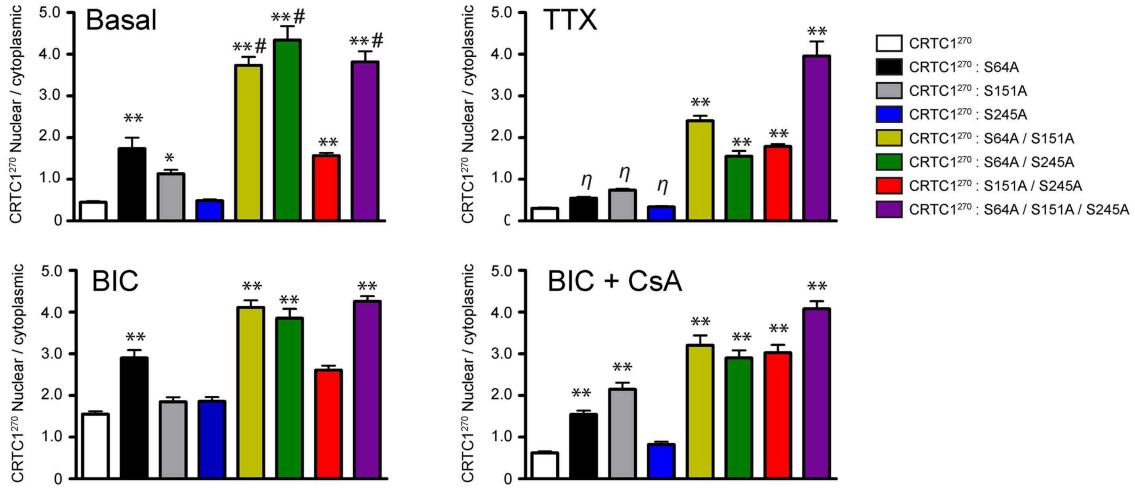

Figure 2.7: Phosphorylation state of CRTC1

(A) HA-tagged CRTC1 was immunoprecipitated from Neuro-2A cells and analyzed by mass spectrometry. Residues in both blue and red (50/643) were identified as phosphorylation sites. Phosphorylated sites labeled in red (13/50) share 100 % conservation across 10 different species. All serine, threonine and tyrosines are underlined.

(B) Single, double or triple CRTC1^{270} serine to alanine mutations were generated (S64A, S151A and S245A) and expressed in neurons that were silenced with TTX, stimulated with BIC or BIC and CsA (** $p<0.001$ relative to CRTC1^{270}; * $p<0.05$ relative to CRTC1^{270}).

We used a combination of conventional and PhosTag immunoblotting to monitor the effect of these mutations on the mobility of CRTC1^{270}. The mobility of CRTC1^{270} was higher in TTX silenced than in BIC-stimulated neurons, with phosphatase treatment of the lysates dropping the molecular weight (MW) of CRTC1^{270} similar to the MW observed in BIC-stimulated neurons (Fig 2.8A). Of the three single mutations, only the S245A mutation showed significant amounts of the lowest MW band in TTX stimulated neurons, though PhosTag gel analysis indicated that the S245 protein was not completely dephosphorylated (Fig 2.8A). One possible explanation is that S245A mutation resulted in subsequent dephosphorylation at multiple sites on CRTC1, resulting in a lower molecular weight band. All three serine to alanine mutants were responsive to BIC stimulation, as BIC increased the concentration of the lowest MW species. In contrast, the triple mutant S64A/S151A/S245A looked like the phosphatase-treated sample, with only the lowest MW band in both TTX-silenced and BIC-stimulated neurons (Fig 2.8A). As our earlier 2-D gel analyses revealed a large number of CRTC1 species, each with differential patterns of phosphorylation (Ch'ng et al, 2012), the results shown in Fig 2.8A suggest that dephosphorylation of S64, S151 and S245 may function to trigger subsequent differential dephosphorylation throughout CRTC1.

We previously demonstrated that CRTC1 binds to 14-3-3ε in an activity-dependent manner (Ch'ng et al, 2012). When neurons were silenced with TTX, phosphorylated CRTC1 bound 14-3-3e and was sequestered in the cytoplasm; BIC triggered CRTC1 dephosphorylation and dissociation from 14-3-3e. To assess whether S64, S151 or S245 play roles in anchoring CRTC1 to 14-3-3e, we transduced cultured cortical neurons with lentiviral vectors expressing CRTC1^{270} harboring substitution mutations (S64A, S151A, S245A or S64A/S151A/S245A), collected neuronal lysates and incubated with 14-3-3e-GST. As shown in Fig 2.8B, single point mutations at S64, S151 and S245 diminished but did not abolish the interaction between CRTC1 and 14-3-3e. Notably, the degree of interaction between the mutants and 14-3-3e correlated inversely with their nuclear accumulation (i.e. S64A had the highest nuclear

accumulation but lowest interaction with 14-3-3e ; Fig 2.8). The triple S64A/S151A/S245A mutant did not bind 14-3-3e, similar to 14-3-3e by phosphatase-treated $CRTC1^{270}$ (Fig 2.8B).

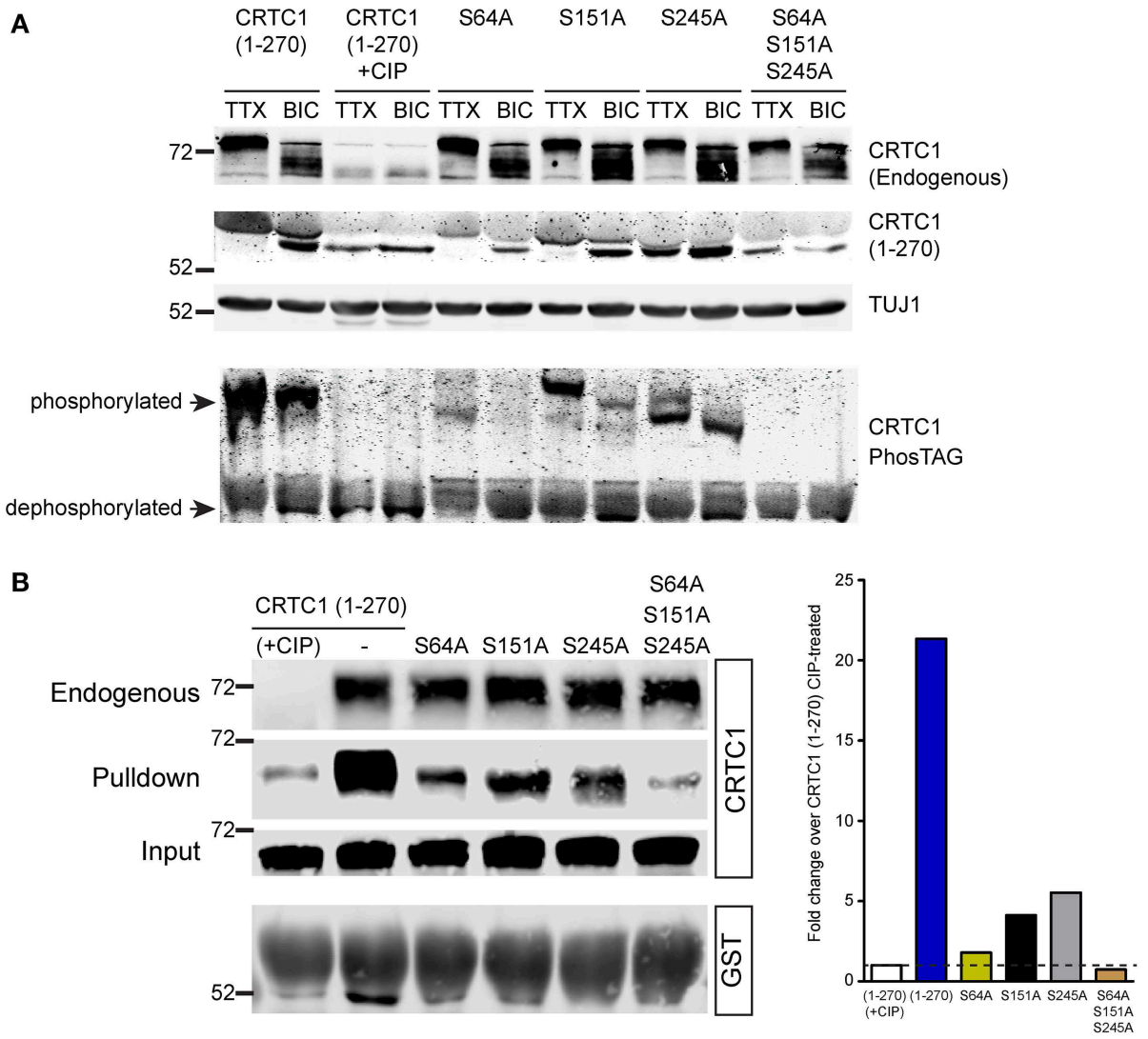

Figure 2.8: Dephosphorylation of S64, S151 and S245 regulates interaction of CRTC1 with 14-3-3e

(A) The single and triple alanine CRTC1^{270} mutations described in figure 2.7 were expressed in cortical neurons (21-28 DIV) and incubated with TTX or BIC. Neuronal lysates were analyzed via traditional or PhosTAG acrylamide gels and immunoblotted with antibodies against CRTC1 and TUJ1.

(B) Cortical neuron expressing CRTC1^{270} point mutants were lysed and incubated with GST-purified 14-3-3ε and pulldowns were analyzed by immunoblotting with antibodies against GST or CRTC1. Endogenous CRTC1 binds to GST 14-3-3 ε comparably across all samples while input controls indicate equivalent expression of all CRTC1^{270} proteins is neurons.

Discussion

CRTC1 undergoes robust nuclear translocation during learning-related synaptic plasticity (Ch'ng et al, 2012; Kovacs et al, 2007; Nonaka et al, 2014; Zhou et al, 2006) but the mechanism for this activity-dependent translocation remains elusive. Our goal was to further characterize the cell biology of activity-dependent CRTC1 synapse to nucleus transport. Our studies revealed that local activation of synaptic glutamatergic receptors generate the source of calcium required for the regulated nuclear import of CRTC1. We also showed that CRTC1 undergoes dynein-mediated and NLS-dependent transport along microtubules to reach the nucleus. Next, we identified the regions of CRTC1 that are critical for regulated trafficking of CRTC1, including three serine residues that undergo dephosphorylation to be released from 14-3-3e at the synapse. Finally, we developed a reporter containing the minimal regions of CRTC1 required for regulated nuclear import fused to the photoconvertible fluorescent protein Dendra2, and used this to monitor in real time, stimulus-induced synapse to nucleus transport of CRTC1 in neurons.

CRTC1 nuclear translocation has been shown to depend on elevations in intracellular calcium resulting from synaptic activation (Ch'ng et al, 2012; Kovacs et al, 2007; Nonaka et al, 2014; Zhou et al, 2006). In this report, we dissected the contributions of specific channels and receptors in generating the elevations in calcium required for CRTC1 nuclear translocation. We found that inhibition of AMPA-type receptors blocks CRTC1 synapse to nucleus translocation, but that calcium entry through AMPA receptors itself was not sufficient to promote CRTC1 nuclear import. Rather, our data support the model that AMPA receptor activation, and L-type VGCC activation, provides local depolarization to relieve the Mg^{2+} block in NMDA receptors (Macias et al, 2001), and that local calcium influx predominantly through NMDA receptors provides the essential trigger for CRTC1 nuclear import (Fig 2.1). Recent studies indicate that depolarization activates L-type VGCC to couple local calcium influx with transcription in the nucleus (Wheeler et al, 2012) in a manner that involves calcineurin-mediated dephosphorylation of

gCamKII, which in turn transports calcium-calmodulin to the nucleus where it activates CamKIV, leading to the phosphorylation of CREB (Ma et al, 2014). In contrast, we find that activation of NMDA receptors in the absence of L-type VGCC activation is sufficient to promote CRTC1 synapse to nucleus translocation, suggesting that CRTC1-mediated transcription, like that of NFkB (Meffert et al, 2003) and Jacob (Karpova et al, 2013), tracks synaptic stimulation rather than cell-wide neuronal depolarization. While local activation of L-type VGCCs and AMPA receptors contribute significantly to CRTC1 nuclear import, our data indicates that the proximal trigger is calcium influx through the NMDA receptor. We also show that activation of extrasynaptic NMDA receptors does not trigger nuclear import of CRTC1, and that blocking extrasynaptic NMDA receptors with antagonists enhances CRTC1 nuclear translocation (Fig 2.1). Since activation of extrasynaptic NMDA receptors promotes cell death (Hardingham et al, 2001; Hardingham et al, 2002), our data support a role for CRTC1 in regulating transcription associated with neuronal plasticity rather than cell death.

A paucity of cell biological studies address the long-distance retrograde transport of soluble proteins in dendrites. Theoretical evidence suggest that fast local signaling can be mediated by diffusion only under short distances (<200 nm); (Howe, 2005; Kholodenko, 2003). In this paper, we show that CRTC1 is actively transported to the nucleus in an energy-dependent manner that requires microtubules and is mediated by the motor protein dynein (Fig 2.2). While dynein is a major microtubule-based molecular motor for cargo transport from soma to dendrites (Kapitein et al, 2010), its role in synapse to nucleus signaling is not well characterized. Since microtubules have mixed polarity in dendrites (Silverman et al, 2010), our studies support a critical role for the minus-end directed motor dynein in mediating the retrograde transport of CRTC1 from synapse to nucleus.

Unlike movement of large organelles or vesicular trafficking, studying the transport of soluble proteins such as CRTC1 in dendrites poses a greater challenge since the protein moves diffusely throughout the dendrite rather than as a punctate vesicular structure that can be tracked. By

fluorescently labeling a subpopulation of CRTC1 in dendrites via photoconversion of Dendra2, we were able to track and quantify the movement of the soluble protein as a fluorescent "plume" as it propagated along dendrites and to monitor the accumulation of photoconverted Dendra2 signal in the nucleus. We detected a small but significant bias of retrograde movement of CRTC1 toward the soma following stimulation. It is likely that the small ROA coupled with the relative abundance of fluorescent CRTC1 in dendrites decreases signal to noise and thus reduced our ability to detect a larger magnitude bias in retrograde movement toward the soma. At present, it is unclear if soluble proteins in dendrites are transported as a single protein or as a macromolecular signaling complex associated with motor proteins. In axons, the hypothesis that bulk movement of soluble proteins is mainly transported as "slow" axoplasmic flow has been recently challenged by observations that soluble proteins can assemble into higher order structures that engage the active transport machinery for axonal transport (Scott et al, 2011).

We chose to study CRTC1^{270} instead of the full length protein because our goal was to identify the minimal region and the signals contained within this region that drives activity-dependent nuclear translocation and for the practical reason that tagged full-length CRTC1 was too large to package in neurotrophic viral vectors. By excluding the carboxy-terminal transcriptional activation domain of the protein, we also avoided any aberrant transcription that might occur due to overexpression of CRTC1^{270}. We systematically tested CRTC1^{270} and found it responds to stimuli and translocates to the nucleus similar to wild type protein, that it does not act as a dominant negative inhibitor of CREB-mediated transcription, and that lentiviral-mediated expression under control of the *Camk2α* promoter does not affect the long term viability of mature neurons. Our results suggest that CRTC1^{270} is a faithful reporter of neuronal activity and can be used as a tool for studying synapse to nuclear signaling in *in vivo* preparations, where its nuclear translocation may be used to rapidly identify neurons that are activated in response to specific stimuli. Moreover, our results suggest that CRTC1^{270} has the potential to serve as

a useful tool for activity-dependent delivery of molecules to the nucleus. Thus, one could couple $CRTC1^{270}$ to a chimeric transcriptional regulator, and deliver it to the nucleus only following glutamatergic activity.

CRTC1 is one of several post-synaptically localized proteins that undergo nucleocytoplasmic shuttling during various forms of neuronal plasticity (Ch'ng & Martin, 2011; Karpova et al, 2013; Lai et al, 2008; Lee et al, 2007; Marcora & Kennedy, 2010) . Many of these proteins contain strong NLSs that engages the heterodimeric importin α/β1 classical nuclear adaptor protein complex that couples to dynein-mediated microtubule transport to enter the nucleus (Ben-Yaakov et al, 2012; Mikenberg et al, 2007; Perlson et al, 2005; Shrum et al, 2009). We have identified a highly conserved and potent NLS in CRTC1 that is both necessary and sufficient to trigger nuclear entry. However, while CRTC1 is actively transported to the nucleus, its entry is not mediated by the classical nuclear import pathway. CRTC1 may enter the nucleus by binding to other NLS-bearing proteins or by other non-conventional nuclear import pathways such as via a member of the importin β superfamily (Chook and Suel, 2010), direct binding to nuclear pore complex (Koike et al, 2004) or it may be escorted by other nuclear chaperone proteins (Fagotto et al, 1998).

We discovered three residues, S64, S151 and S245 that play crucial and synergistic roles in nuclear accumulation of CRTC1. While individual point mutations at these serine residues did not significantly alter the localization of CRTC1 in silenced neurons, a triple phospho-incompetent mutation resulted in constitutive nuclear localization in the absence of neuronal activity (Fig 2.8). Since the nuclear accumulation of the phosphorylation-incompetent mutants inversely correlated with the association with 14-3-3ε cytoplasmic anchoring protein, it is likely that the constitutive transport of CRTC1 into the nucleus, as opposed to defects in nuclear export, underlies the robust nuclear accumulation of the phospho-incompetent mutants.

Nonaka and colleagues recently reported that alanine scanning mutations in S151 and S245 resulted in constitutive nuclear localization of CRTC1 in cortical neurons (Nonaka et al, 2014). However, we found that a S151 and S245 double mutation showed only a slight enhancement of nuclear accumulation over the wild type protein in silenced neurons. In contrast, we provide evidence that phosphorylation at S64 is a potent regulator of CRTC1 nuclear translocation. In unstimulated neurons, a single point mutation at S64 alone led to a 2 fold increase in the nuclear to cytoplasmic ratio of CRTC1 while a double mutation of S64 paired with either S151 or S245 resulted in a 4-5 fold increase in the nuclear accumulation of CRTC1. Taken together, our results indicate that the phosphorylation state of S64 is a major contributor, together with S151 and S245, in regulating CRTC1 nucleocytoplasmic shuttling in neurons.

The fact that dephosphorylation of only 3 amino acids is sufficient to trigger nuclear import of CRTC1 raises questions about the function of the large number of remaining, highly conserved phosphorylated residues. It is unclear if dephosphorylation of any of these 3 amino acids also results in a coordinated dephosphorylation at other phosphorylation sites. Given that CRTC1 exists in multiple phosphorylated forms as assessed by two dimensional gel analysis (Ch'ng et al, 2012), it is plausible that the activation of distinct signaling pathways within dendrites and spines following specific types of stimulation can differentially alter the pattern of CRTC1 phosphorylation which may serve as a code that couples patterns of stimulation with specific programs of gene expression.

Materials and Methods

Plasmids and antibodies. The CMV-mCherry-dynamitin expression vector was kindly shared by M. Meffert (Johns Hopkins, MD; (Shrum et al, 2009) while the mCherry plasmid was a gift from R.Y. Tsien (UC San Diego, CA). The 4xGFP construct was a gift from W. Hampe (UMC Hamburg-Eppendorf, Hambug; (Seibel et al, 2007). Commercial plasmids include Dendra2 (Evrogen) and CRTC1 (Open Biosystems, Huntsville, AL). Antibodies used in all these experiments include: rabbit polyclonal antibodies against CRTC1 (Bethyl, Montgomery, TX), pCRTC1(S151; Bethyl) Dendra2 (Evrogen, Moscow, Russia), TUJ1 (Covance, Princeton, NJ), Dynein heavy chain (Santa Cruz, Dallas, TX), and phosphoCREB-S133 (Cell Signaling); mouse monoclonal antibodies against PSD95 (Thermoscientific, Rockford, IL), synapsin1 (Millipore, Billerica, MA), CamKIIα (Millipore), HA-epitope (Sigma), GAPDH (Fitzgerald, Acton, MA), GFP (Clontech, Mt. View, CA), GAD67 (Millipore) and KPNB1 (ABR, Golden, CO); polyclonal chicken antibody against MAP2 (Phosphosolutions, Aurora, CO) and synaptotagmin (Chemicon, Temecula, CA). All secondary antibodies are conjugated to Alexa dyes (488, 546, 555, 568 and 633; Invitrogen).

Viruses and expression constructs. Lentiviral packaging constructs bearing the L22 (*Camk2α*) promoter were kind gifts from Pavel Osten's lab (Dittgen et al, 2004). All production of lentiviral particles is as described in Dittgen et al. 2004. Lentiviral transduction of neurons was carried out in a reduced volume (250 µl / 1 ml) for 24 h before replacement with conditioned medium. The integrated constructs were allowed to express for at least 6 d prior to experiments.

Dissociated neuron cultures protocols and pharmacological treatments. Unless otherwise stated, all experiments in this report uses mature hippocampal neurons (DIV 21-28) dissected from newborn (P0) rats and plated on poly-DL-lysine (0.5 mg/ml) coated cover slips (Carolina Biologicals, Burlington, NC). Only the siRNA knockdown of dynein heavy chain experiment utilizes cultured mouse neurons. A

defined serum-free media was used to culture the neurons: Neurobasal media, (Invitrogen, Carlsbad, CA); β-mercaptoethanol (Sigma, St. Louis, MO); monosodium glutamate (Sigma); B27 (Invitrogen); GlutaMAXI (Invitrogen). For most of the experiments, unless otherwise indicated, neurons were incubated with various pharmacological agents in conditioned neuronal media, in a 37 ºC, 5% CO_2 incubator for the appropriate amount of time before cells were either fixed for immunocytochemistry or lysates were collected for immunoblots. For temperature-dependence experiment, neurons were maintained in parallel incubator kept at a constant 10 ºC. For neuronal transfection of plasmids, we employ a calcium chloride transfection protocol modified as previous described (Jiang & Chen, 2006). For receptor antagonist treatments (APV, NBQX, ifenprodil, etc.), unless otherwise stated, the cultured neurons were usually pre-treated with the antagonist for 30-60 min prior to stimulation. Unless otherwise stated, BIC stimulation of neurons lasts for 15 min while AMPA or NMDA treatments lasts for 10 min followed by a washout and recovery for 5 min prior to processing for immunocytochemistry. The following pharmacological agents were used: bicuculline (BIC, 40 μM; Sigma), forskolin (FSK, 25 μM; Calbiochem, San Diego, CA), tetrodotoxin (TTX, 1 μM; Tocris, Ellisville, MO), APV (100 μM; Tocris), cyclosporin A (CsA, 5 μM; Sigma), nocodazole (NDZ, 0.1 μM or 20 μM; Tocris), EHNA (0.1 μM; Tocris), BAPTA-AM (25 μM, Tocris), EGTA-AM (25 mM or 100 mM; Invitrogen), nimodipine (NIM, 10 μM; Tocris), ω-conotoxin (2 μM; Tocris) and ω-agatoxin (0.1 μM; Tocris), MNI-caged glutamate (0.2 mM; Tocris), NBQX (100 μM; Tocris); Trolox (10 nM; Tokyo Chemical Industry, Tokyo, Japan), ifenprodil (IFP, 50 μM; Tocris), MK801 (50 μM; Tocris), NMDA (20 μM; Tocris), AMPA (25 μM; Tocris), SN50 and SN50M (Enzo Lifesciences).

Immunocytochemistry. All cells were fixed at room temperature with parafomalydehyde (3.2%) for 10 min, permeabilized with 0.1% Triton-X 100 (Calbiochem) for 5 min and blocked in 10% goat-serum for 30 min. Neurons were then incubated in primary antibodies either for 4 h at room temperature or

overnight at 4 ºC. Secondary antibodies and Hoechst nuclear dye (Invitrogen) were incubated at room temperature at 1:2000 (2 μg/ml) dilution for 2 h. All antibodies were diluted in 10% goat serum and coverslips were mounted with aqua/polymount (Polysciences, Warrington, PA).

Calcium chelators (BAPTA-AM and EGTA-AM) and calcium channel antagonists. Hippocampal neurons were pre-treated with TTX (1 μM) in the presence of DMSO, BAPTA-AM (25 mM), EGTA-AM (25 mM or 100 mM) in conditioned media. After 30 min of pretreatment, neurons were was washed with conditioned media and allowed to recover for 10 min before being stimulated in Tyrode's solution with varying concentrations of KCl (5 mM [$5K^+$] or 40 mM [$40K^+$]) for 5-7 min. Neurons were then washed and allow to recover in regular Tyrode's solution (5 mM) for another 5 min before being fixed and stained for immunocytochemistry. TTX (1 μM) was present in all media and solutions throughout pre-treatment, stimulation and recovery periods. Similarly, for calcium channel antagonists nimodipine (10 μM; NIM), ω-conotoxin (2 μM; CTX) and ω-agatoxin (0.1 μM; AGA), neurons were pre-treated for 30 min before being stimulated in Tyrode's solution containing elevated levels of KCl (40 mM) briefly for 5-7 min, washed and recovered in regular Tyrode's solution (5 mM) for another 5 min prior to fixation. TTX was present throughout the entire treatment protocol. Tyrode's solution (140 mM NaCl; 10 mM HEPES pH 7.3; 5 mM KCl; 3 mM $CaCl_2$; 1 mM $MgCl_2$; 10 mM glucose pH 7.35).

Photomanipulation and analysis of CRTC1^{270} in neurons. Hippocampal neurons were transduced with virus expressing either Dendra2 or CRTC1^{270}. After 1 wk of expression, neurons were transferred on to a glass bottom live imaging setup containing a low Mg^{2+} Tyrode's solution (140 mM NaCl; 10 mM HEPES pH 7.3; 5 mM KCl; 3 mM $CaCl_2$; 0.1 mM $MgCl_2$; 10 mM glucose; 10 nM Trolox pH 7.35) with the appropriate reagents added as indicated for each experiment (TTX,1 μM; MNI-caged glutamate, 200 μM; DMSO). Neurons were allowed to recover on a heated stage assembly on a Zeiss LSM 700 scanning

confocal microscope for approx. 10-15 min prior to the first imaging session. Once target neurons are selected based on comparable expression of fusion protein, two regions of interest, each on separate branches of dendrites located roughly 100 µm away from the soma were selected and exposed briefly to UV (405 nm) laser (pixel dwell time: 51.2 msec). A total of 80 frames were captured per neuron. However, since the dimensions of each image capture varies slightly between neurons, the time it takes to capture 80 frames for each neuron will also have minor differences, with the average total time of image capture per neuron averaging between 13-15 min. To maintain consistency across the different time-lapse plots, we have chosen to plot the time elapsed in frames. Pharmacological reagents used during the experiments include APV (100 µM); NBQX (100 µM); EGTA-AM (25 µM); BAPTA-AM (25 µM); Nocodazole (0.1 µM 6 h pre-treatment prior to imaging). To analyze the data, the amount of Dendra2^{red} signal was quantified in the nucleus and the change in signal intensity over baseline was plotted over the total amount of frames acquired.

Zeiss Scanning Confocal Microscope LSM 700

Objectives: Plan Apochromat 63X 1.40 Oil DIC

Temperature: 25 or 35 ºC (Zeiss Temp-control 37-2)

Media: Tyrode's solution for live imaging

Lasers: 405 nm, 488 nm, 555 nm and 639 nm solid state lasers

Data acquisition: Zen 2009

Local photoconversion and analysis of CRTC1^{270} in distal dendrites. Neurons were transduced and prepared for imaging as described in the previous section "photomanipulation of CRTC1^{270} in neurons". However, we employed a Marianas spinning disc confocal system that is coupled to a Photometrics Evolve camera (Intelligent Imaging Innovations, Denver, CO) for high speed image acquisition. The entire

unit is enclosed within a humidified environmental chamber for regulated temperature control. A 2.25 cm^2 ROA was selected on a dendritic branch that is approximately 50-70 µm away from the soma. Using a Vector scan module attached to the system, the selected ROA was briefly exposed to UV laser (50% intensity; 2 ms dwell; Appendix fig S2.4). A total of 100 frames (alternating 473 nm and 523 nm beam excitation) were acquired per imaging session (approx. 660 ms/frame). Pharmacological reagents used in the experiment include BIC (40 µM) and forskolin (25 µM). To analyze the data, Prism Graph pad was used to quantify the total change of $Dendra2^{red}$ fluorescence over each 10 µm segment of the dendrite either proximal (toward soma) or distal (away from soma) at the point of photoconversion (ROA).

3i Marianas spinning disc confocal system (CSU22 Yokugawa Scanner).

Objectives: Plan Apochromat 63X 1.40 Oil DIC

Temperature: 35 ºC (Okolab temperature control chamber)

Media: Tyrode's solution for live imaging (methods and materials)

Lasers: 405 nm, 488 nm and 561 nm solid state lasers

Camera: Photometric Evolve EMCCD camera

Data acquisition: Slidebook 5.0

Cell cultures, transfections and siRNA treatment. All cell lines (HEK293T) were grown on Dulbecco's Modified Eagle Media (DMEM; Invitrogen) supplemented with 10% fetal bovine serum (HyClone, Logan, UT), and 1% Penicillin/Streptomycin (Invitrogen). Transfection of plasmids in cell lines was carried out with Lipofectamine 2000 (Invitrogen) using protocols recommended by the manufacturer. For siRNA treatment of human CRTC1 or GAPDH in HEK293T cells, we purchased custom designed siGENOME SMARTpool siRNA from Dharmacon (Lafeyette, CO). The SMARTpool siRNA (50 nM) was delivered into cells using Lipofectamine RNAiMAX (Invitrogen) reagent over the course of 72 h with refeeding of siRNA

every 24 h and the replating and reseeding of cell after 48 h. For siRNA treatment of human importin β1 (50 nM; KPNB1; SMARTpool siRNA; Dharmacon) and GAPDH, HEK293T cells were incubated with KPNB1 siRNA for 48 h before expression plasmids bearing different 4xGFP fusion constructs were transfected into cells for another 12 h prior to immunocytochemistry or immunoblotting. For siRNA treatment of mouse neurons with Dynch1h, we purchased custom designed siGENOME SMARTpool Accell siRNA from Dharmacon. The Accell siRNA (1 μM) was delivered into neurons directly and allowed to incubate for 48 h-96 h. After the incubation period, cells were either fixed for immunocytochemistry or harvested in lysis buffer for analysis via Western blots.

Image analysis and synapse quantification. All nuclear to cytoplasmic quantification was performed with Slidebook v4.2-v5.5 (Intelligent Imaging Innovations). Unless otherwise stated, all data sets are presented as mean ± SEM either as bar graphs or scatter plots. Unless otherwise stated, all p-values were determined using one-way analysis of variance (ANOVA) with Bonferroni's Correction post-hoc test. To analyze synaptic integrity, hippocampal neurons were transduced with an AAV expressing GFP being driven under the neuron-specific synapsin promoter. After 1 wk of expression, neurons were incubated in NDZ (0.1 μM) for 6 h before being stimulated and processed for immunocytochemistry using antibodies against PSD95, Synapsin and MAP2. To quantify for the number of synapses, Slidebook was used to isolate only PSD95-positive and synapsin-positive puncta based on signal intensity, size exclusion and overlapping fluorescence intensities. The stringent selection criteria to increase signal to noise for each puncta likely resulted in undersampling. To identify synapses, only PSD95 and synapsin masks that overlapped were considered as a positive score. Student's t-test (two-tailed, unpaired) was used as a statistical analysis.

Gene expression in CRTC1^{270} transduced hippocampal neuronal cultures. Hippocampal cultures were transduced with lentivirus expressing CRTC1^{270} and 1 wk post-transduction, neurons were pre-treated with TTX (1 μM) for another 3 h before either being continuously maintained in TTX or the TTX was withdrawn, washed and replaced with regular conditioned media. The neurons were allowed to recover for 30 min before RNA was extracted with TRIzol (Invitrogen), column purified with RNeasy kit (Qiagen, Valencia, CA) and the concentration determined via the Nanodrop (Thermo Scientific). For RT-PCR, we generated cDNA using reverse transcriptase and poly dT primers (Invtirogen). We then conducted quantitative real time PCR experiments (Stratagene Mx3000P), with SYBR Green Master Mix (Invitrogen) and specific primer pairs (Operon, Huntsville, AL) listed below. DD Ct values were calculated for all raw qPCR results by normalizing against mock, untreated controls and corrections for loading error we made against DCt values for HPRT1, a non-activity-dependent gene. Primer pairs used include crtc1 (5-tggacagagtatatcgtgagcg; 5-catgcttgtctactgacaggg), arc (5-ccgtcccctcctctcttga; 5-aaggcacctcctctttgtaatcctat), hprt1 (5-agtcccagcgtcgtgattag; 5-ccatctccttcatgacatctcg), btg2 (5-tcctgaggactcggggctgc; 5-gcgatagccggagcccttgg), cfos (5-tcccagctgcactacctatacgt; 5-tgcgcagctagggaagga), cyr61 (5-aactcggagtgccgcctggt; 5-gccgcagtatttgggccgg), zif268 (5-attgatgtctccgctgcagat; 5-gtagttgtccatggtgggtga) and Dendra2 (5-ggaattaacctgatcaagga; 5-tggaagaagcagtcgccctc).

GST-14-3-3ε pulldowns of CRTC1^{270} fusion proteins. Cortical neuron cultures (DIV 21-28) were transduced with lentiviruses expressing either full length or serine to alanine CRTC1^{270} mutants. After 1 wk. post-transduction, neuronal lysates were collected (25 mM Tris, pH7.4; 137 mM NaCl; 1% NP40; 10% glycerol; protease and phosphatase inhibitors; (Ballif et al, 2006) and subjected to pulldowns using purified GST-14-3-3 ε bound on glutathione beads. The beads were then washed extensively, resuspended in sample buffer and analyzed via immunoblots using either conventional or PhosTAG acrylamide gels.

Mass Spectrometry. Four confluent 10 cm dishes of Neuro-2A cells were transfected with HA-CRTC1 plasmid using Lipofectamine-2000. After 16 h, cells were washed twice in ice cold PBS and lysed cells in lysis buffer (150 mM NaCl, 50 mM Tris (pH 8.0), 1% NP40) supplemented with protease and phosphatase inhibitors (Roche). The lysates were incubated on ice for 20 min with benzonase DNase (Millipore) to reduce viscosity, then centrifuged to clarify insoluble proteins. HA-CRTC1 was immunoprecipitated using pre-equilibrated EZview Red Anti-HA Affinity Gel (Sigma) for 2 h at 4°C with constant rotation. Beads were washed 3X in ice-cold lysis buffer, and eluted using 100 µl 8M urea. Samples were mixed with loading buffer, boiled and loaded onto NuPAGE Novex 4-12% Bis-Tris gradient gel. To purify HA-CRTC1 for mass spec, the gel was stained with Simply Blue SafeStain (Invitrogen) and CRTC1 was excised from gel slices, digested with either trypsin or chymotrypsin before fractionated online using a C18 reversed phase column, and analyzed by MS/MS on a Thermofisher LTQ- Orbitrap XL as previously described (1,2). MS/MS spectra were subsequently analyzed using the ProLuCID and DTASelect algorithms (3,4). Phosphopeptides were identified using a differential modification search that considered a mass shift of +79.9663 on serines, threonines and tyrosines. All phosphorylated sites reported in Fig 2.8 exhibit an AScore of at least 90% confidence levels.

Supplementary Figures

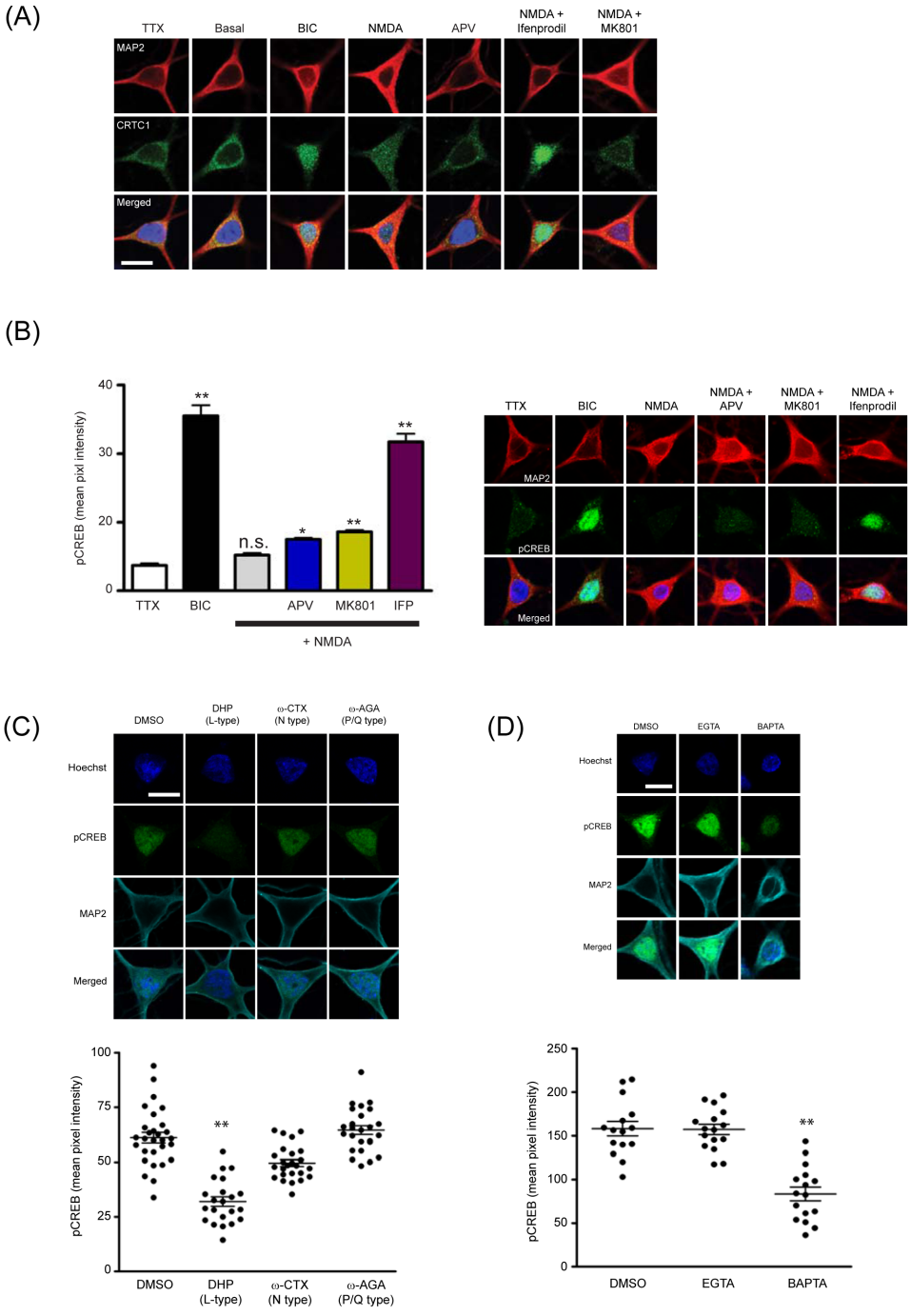

Supplementary Figure S2.1: CREB phosphorylation (S133) requires activation of synaptic NMDA receptors and L-type VGCC

(A) Neurons were treated as described in figure 2.1A and immunostained with antibodies against CRTC1, MAP2 and Hoechst nuclear dye (blue).

(B) Neurons were incubated with TTX, IFP or MK801 before being stimulated with NMDA in the presence of the receptor antagonists. Neurons were immunolabeled with antibodies against pCREBS133, MAP2, and Hoechst nuclear dye (blue). The mean pixel intensity of pCREB in the nucleus was quantified and graphed (**$p<0.001$, *$p<0.05$ relative to TTX-silenced).

(C) Mean nuclear intensity of pCREB133 in neurons were quantified after depolarization with KCl in the presence of NIM, conotoxin (ω-CTX), agatoxin (ω-AGA) or mock treated with DMSO (** $p<0.001$ relative to DMSO).

(D) Membrane permeable calcium chelators BAPTA and EGTA were incubated in neurons prior to depolarization with KCl. Mean nuclear intensity of pCREB133 in neurons were quantified (** $p<0.001$ relative to DMSO). All scale bars = 10 μm.

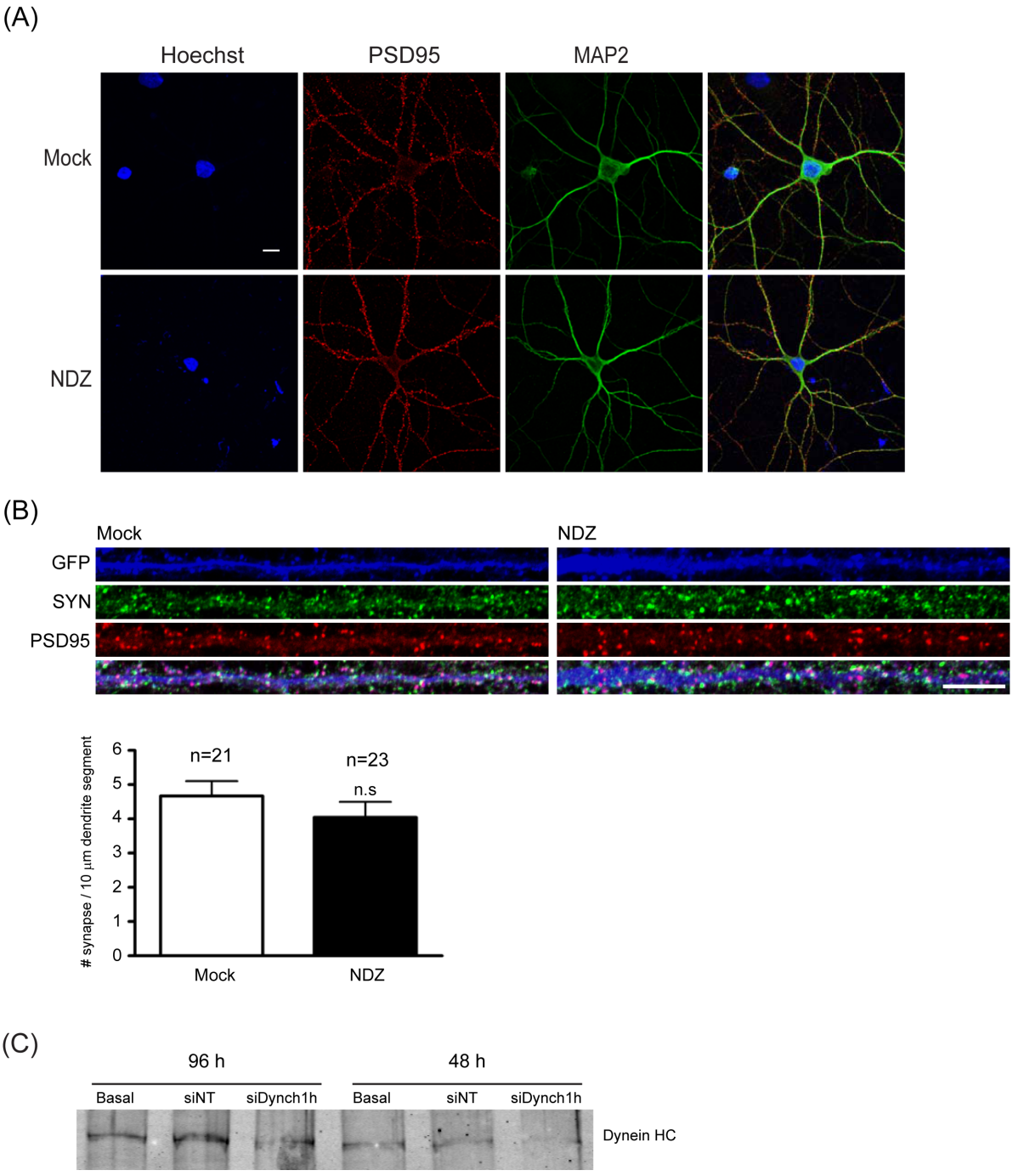

Supplementary Figure S2.2: CRTC1 is actively transported to the nucleus

(A) Neurons were incubated with either DMSO or NDZ before being immunolabeled with antibodies against MAP2 (green), PSD95 (red) and Hoechst nuclear dye (blue).

(B) Neurons were transduced with AAV expressing GFP (blue) driven under the neuron-specific synapsin promoter and treated with DMSO (mock) or NDZ. Neurons were then immunostained with synapsin (SYN) and PSD95 antibodies. The number of synapses per 10 µm segment of dendrites was quantified (refer to methods and materials).

(C) Mouse hippocampal neurons were incubated with siRNA targeted against dynein heavy chain (siDynch1h) or non-targeted control (siNT). Neurons lysates were immunoblotted with antibodies against the dynein heavy chain.

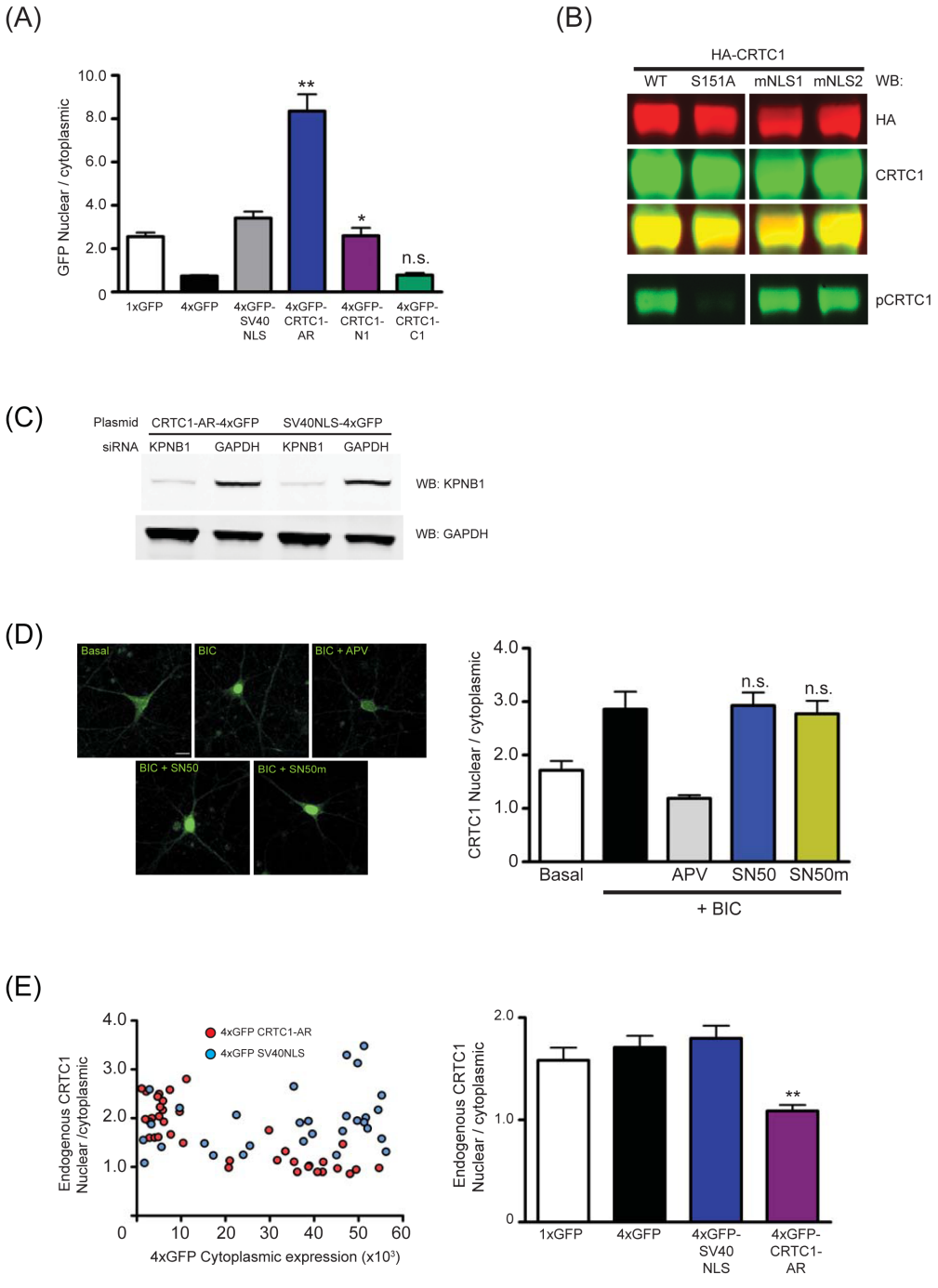

Supplementary figure S2.3: CRTC1 encodes an arginine-rich NLS that does not engage the classical nuclear import pathway

(A) HEK293T cells were transfected with 4xGFP fusion constructs as described in Figure 2.3. The GFP signal in the nucleus and cytoplasm was quantified (** p<0.001 relative to 4xGFP; * not

significant relative to SV40NLS but $p<0.001$ relative to 4xGFP; n.s. not significant relative to 4xGFP).

(B) HEK293T cells were individually transfected with plasmids expressing i) HA-tagged wildtype CRTC1 (WT), ii) HA-tagged S151A CRTC1 mutant (S151A) or iii) HA-tagged CRTC1 nuclear localization mutants (mNLS1) and (mNLS2). Immunoblotting with antibodies specific for the HA-epitope, CRTC1 or phosphorylated CRTC1 at residue 151 (pCRTC1) was performed.

(C) HEK293T cells were transfected with CRTC1-AR-4xGFP or SV40NLS-4xGFP after incubation with siRNA against KPNB1 or GAPDH. Lysates were immunoblotted for KPNB1 or GAPDH and quantified. KPNB1 siRNA decreased importin β1 protein concentration by 45% compared to cells incubated with GAPDH siRNA.

(D) Neurons were incubated with membrane-permeable NLS peptide (SN50) or a mutant NLS peptide (SN50m) and stimulated with BIC (n.s. not significant relative to BIC only).

(E) Neurons expressing 4xGFP-CRTC1-AR or 4xGFP-SV40NLS were stimulated with BIC and the endogenous CRTC1 with the corresponding total intensity of 4xGFP in the nucleus and cytoplasm of each neuron were quantified. Neurons where 4xGFP signal is overexpressed (>20, 000 total fluorescence units) were selected and quantified for endogenous CRTC1 (** $p<0.001$ relative to 4xGFP-SV40NLS).

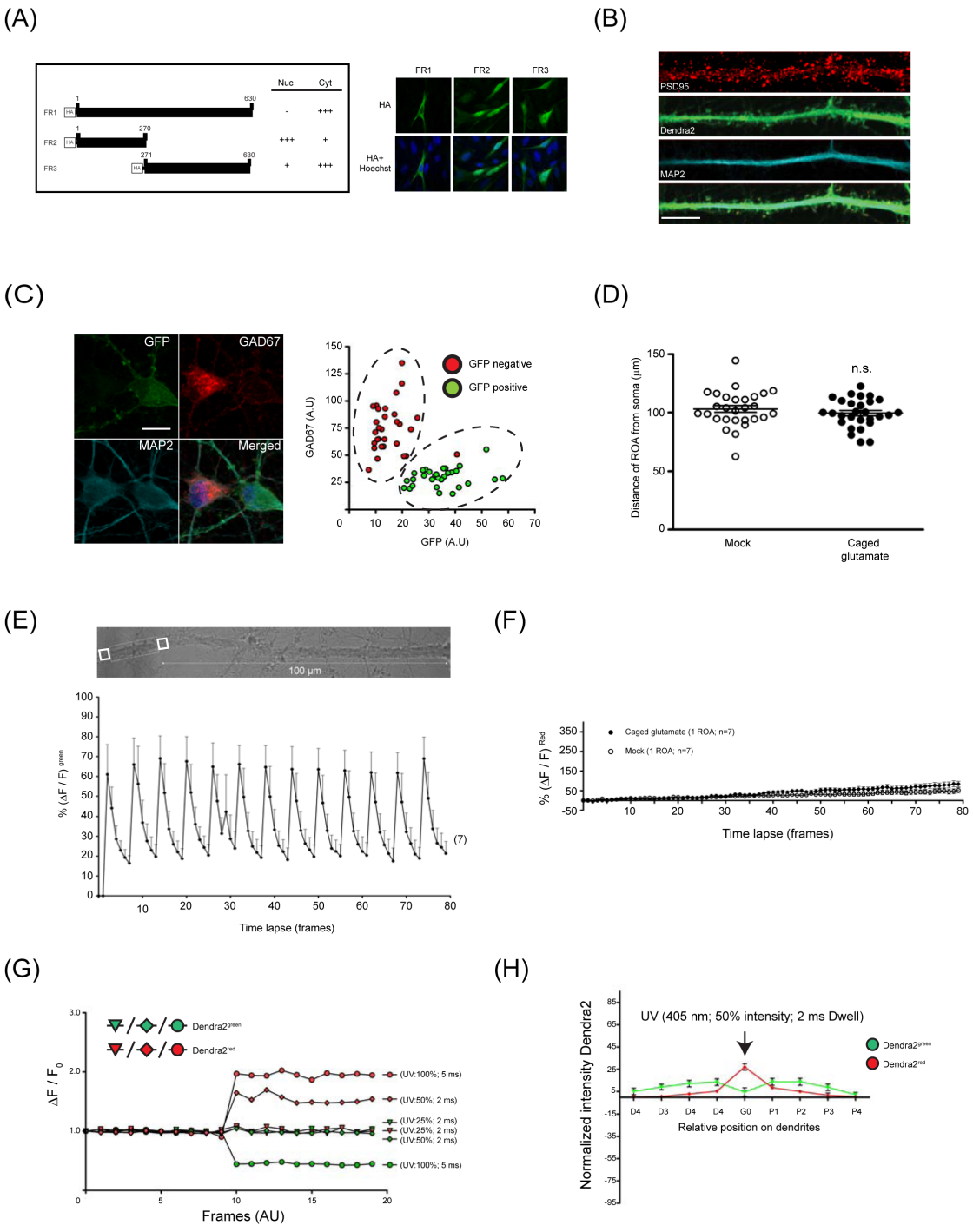

Supplementary Figure S2.4: Time-lapse imaging of CRTC1^{270} translocation in neurons

(A) The nuclear and cytoplasmic localization of HA-tagged full length CRTC1 (FR1), CRTC1 amino terminal fragment (FR1: 1-270) and carboxy-terminal fragment (FR3: 271-630) were qualitatively assessed in Chinese Hamster Ovary (CHO) cell culture.

(B) Neurons expressing $CRTC1^{270}$ were incubated with TTX and immunostained with antibodies for PSD95, MAP2 and Dendra2. A magnified image of a dendrite is shown.

(C) Neurons expressing farnesylated GFP driven under the expression of a *Camk2α* promoter were fixed and immunostained. The mean pixel intensity of GFP and GAD67 in randomly selected neuronal cell bodies was quantified. Two populations of neurons were identified and highlighted by dashed ellipses. One group with robust GFP expression has low levels of GAD67 signal. Conversely, neurons with robust GAD67 signal have little to no GFP expression.

(D) Neurons were transduced and treated as described in figure 2.5 for time-lapse imaging. Two regions of activation where the dendrites are exposed to UV illumination (ROA; white dashed box in figure 2.5) were selected approximately 100 µm away from the soma. The distance of the ROA from the soma was measured for each experimental condition and plotted on a bar graph (n.s. not significant).

(E) Neurons loaded with Fluo4AM and calcium transients were recorded upon glutamate uncaging (Video S1). The white box (dashed) indicates the ROA in dendrites (approx. 100 mm away from the cell body) subjected to UV excitation to uncage glutamate. To quantify the change of Fluo4AM fluorescence in dendrites, the average intensity of two regions (white box; solid) flanking the ROA was quantified and plotted as a line graph showing the change of fluorescence compared to baseline values over time.

(F) Neurons expressing CRTC1^{270} were imaged as described in figure 2.5 except that UV activation is targeted to only a single dendritic branch (1 ROA). The amount of nuclear Dendra2^{red} signal was quantified and plotted.

(G) To ensure optimal photoconversion without photobleaching, neurons were transduced with a lentivirus expressing Dendra2 for 1 wk before being fixed and placed in the same chamber setup used for time-lapse imaging of neurons. Using the same live-cell imaging methodologies, the neuronal soma was subjected to varying intensities of UV (405 nm) excitation as well as variable laser dwell times (2 ms-5 ms). The intensity of the native Dendra2 green emission as well as the photoconverted red emissions were imaged and quantified.

(H) To ensure that local photoconversion of Dendra2 in dendrites is localized precisely within the boundaries of the ROA (2.25 μm^2), fixed neurons were UV stimulated as described above (50% UV intensity; 2 ms dwell time). The normalized intensities of both the native green and photoconverted red Dendra2 intensities were calculated every 10 µm (up to 40 µm) from the point of photoconversion (G0) in the dendrites to either proximal (P1 to P4) or distal (D1-D4) to the site of photoconversion. Data reported as mean ± SEM.

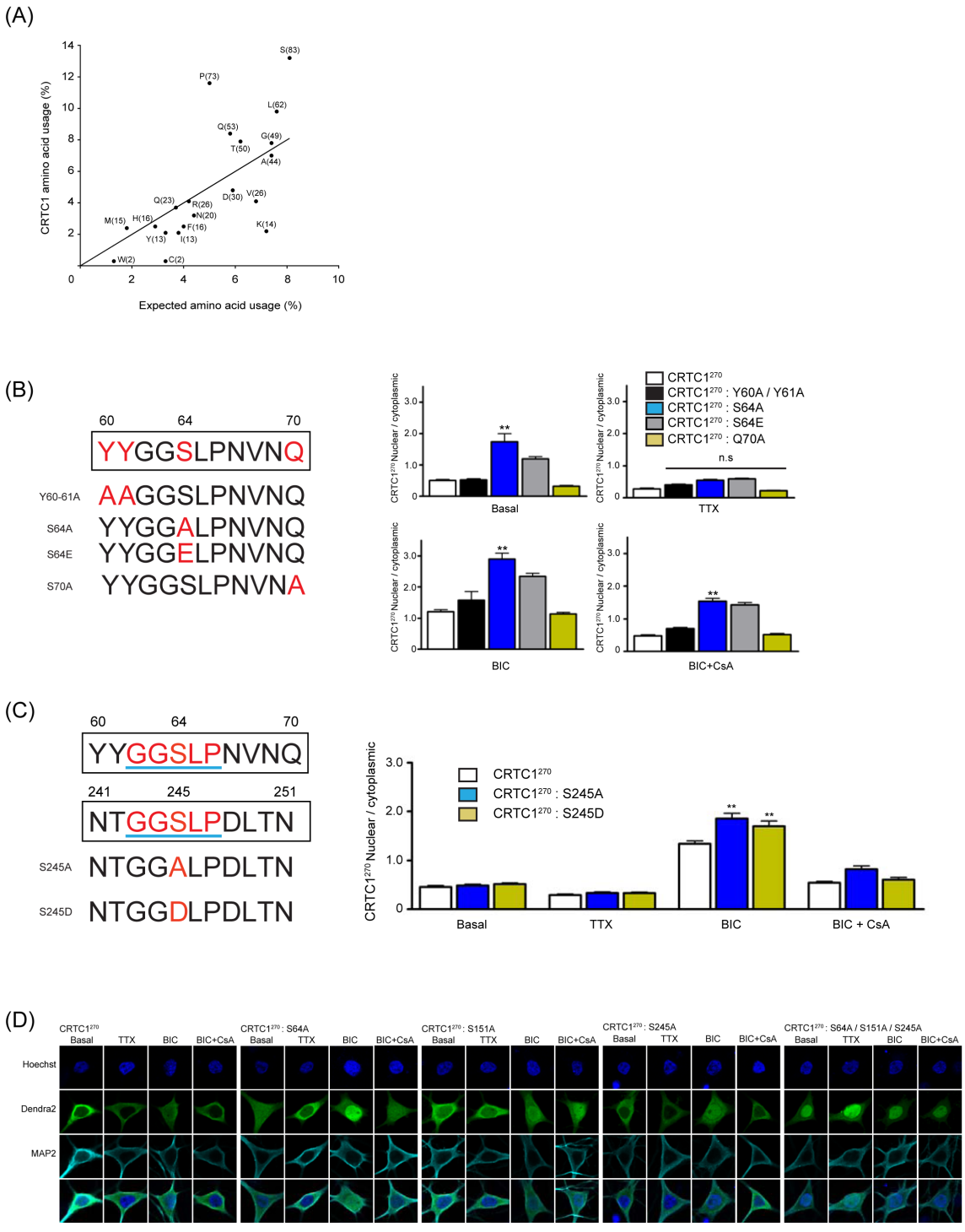

Supplementary Figure S2.5: Phosphorylation state of CRTC1

(A) Scatter plot showing expected and observed CRTC1 amino acid usage. Brackets after each single letter amino acid code indicates the number of that particular residue present in CRTC1.

Any amino acid that falls above the perfect correlation line indicates overrepresentation of that amino acid in CRTC1.

(B) $CRTC1^{270}$ serine to alanine mutations were created in the region flanking the conserved amino acid S64 which includes Y60A/Y61A, S64A, S64E and Q70A. These constructs were expressed in neurons stimulated with TTX, BIC or BIC in the presence of CsA (** $p<0.001$ relative to $CRTC1^{270}$ for each treatment condition).

(C) Neurons were transduced with lentivirus expressing a serine to aspartic acid phosphomimetic mutation at S245. The neurons were then stimulated and processed for immunocytochemistry as described in (A) (** $p<0.001$ relative to $CRTC1^{270}$).

(D) Confocal micrographs of neurons expressing either $CRTC1^{270}$ or the serine to alanine mutants (single and triple) and stimulated as described in figure 2.8.

References

Alberini CM (2009) Transcription factors in long-term memory and synaptic plasticity. *Physiol Rev* 89: 121-145

Altarejos JY, Goebel N, Conkright MD, Inoue H, Xie J, Arias CM, Sawchenko PE, Montminy M (2008) The Creb1 coactivator Crtc1 is required for energy balance and fertility. *Nat Med* 14: 1112-1117

Ballif BA, Cao Z, Schwartz D, Carraway KL, 3rd, Gygi SP (2006) Identification of 14-3-3epsilon substrates from embryonic murine brain. *J Proteome Res* 5: 2372-2379

Ben-Yaakov K, Dagan SY, Segal-Ruder Y, Shalem O, Vuppalanchi D, Willis DE, Yudin D, Rishal I, Rother F, Bader M, Blesch A, Pilpel Y, Twiss JL, Fainzilber M (2012) Axonal transcription factors signal retrogradely in lesioned peripheral nerve. *Embo J* 31: 1350-1363

Ch'ng TH, Martin KC (2011) Synapse-to-nucleus signaling. *Curr Opin Neurobiol* 21: 345-352

Ch'ng TH, Uzgil B, Lin P, Avliyakulov NK, O'Dell TJ, Martin KC (2012) Activity-dependent transport of the transcriptional coactivator CRTC1 from synapse to nucleus. *Cell* 150: 207-221

Chudakov DM, Matz MV, Lukyanov S, Lukyanov KA (2010) Fluorescent proteins and their applications in imaging living cells and tissues. *Physiol Rev* 90: 1103-1163

Deisseroth K, Bito H, Tsien RW (1996) Signaling from synapse to nucleus: postsynaptic CREB phosphorylation during multiple forms of hippocampal synaptic plasticity. *Neuron* 16: 89-101

Dittgen T, Nimmerjahn A, Komai S, Licznerski P, Waters J, Margrie TW, Helmchen F, Denk W, Brecht M, Osten P (2004) Lentivirus-based genetic manipulations of cortical neurons and their optical and electrophysiological monitoring in vivo. *Proc Natl Acad Sci U S A* 101: 18206-18211

Fagotto F, Gluck U, Gumbiner BM (1998) Nuclear localization signal-independent and importin/karyopherin-independent nuclear import of beta-catenin. *Curr Biol* 8: 181-190

Hardingham GE, Arnold FJ, Bading H (2001) Nuclear calcium signaling controls CREB-mediated gene expression triggered by synaptic activity. *Nat Neurosci* 4: 261-267

Hardingham GE, Fukunaga Y, Bading H (2002) Extrasynaptic NMDARs oppose synaptic NMDARs by triggering CREB shut-off and cell death pathways. *Nat Neurosci* 5: 405-414

Higley MJ, Sabatini BL (2012) Calcium signaling in dendritic spines. *Cold Spring Harb Perspect Biol* 4: a005686

Hirano Y, Masuda T, Naganos S, Matsuno M, Ueno K, Miyashita T, Horiuchi J, Saitoe M (2013) Fasting launches CRTC to facilitate long-term memory formation in Drosophila. *Science* 339: 443-446

Hollander JA, Im HI, Amelio AL, Kocerha J, Bali P, Lu Q, Willoughby D, Wahlestedt C, Conkright MD, Kenny PJ (2010) Striatal microRNA controls cocaine intake through CREB signalling. *Nature* 466: 197-202

Howe CL (2005) Modeling the signaling endosome hypothesis: why a drive to the nucleus is better than a (random) walk. *Theor Biol Med Model* 2: 43

Iourgenko V, Zhang W, Mickanin C, Daly I, Jiang C, Hexham JM, Orth AP, Miraglia L, Meltzer J, Garza D, Chirn GW, McWhinnie E, Cohen D, Skelton J, Terry R, Yu Y, Bodian D, Buxton FP, Zhu J, Song C, Labow MA (2003) Identification of a family of cAMP response element-binding protein coactivators by genome-scale functional analysis in mammalian cells. *Proc Natl Acad Sci U S A* 100: 12147-12152

Jagannath A, Butler R, Godinho SI, Couch Y, Brown LA, Vasudevan SR, Flanagan KC, Anthony D, Churchill GC, Wood MJ, Steiner G, Ebeling M, Hossbach M, Wettstein JG, Duffield GE, Gatti S, Hankins MW, Foster RG, Peirson SN (2013) The CRTC1-SIK1 pathway regulates entrainment of the circadian clock. *Cell* 154: 1100-1111

Jeffrey RA, Ch'ng TH, O'Dell TJ, Martin KC (2009) Activity-dependent anchoring of importin alpha at the synapse involves regulated binding to the cytoplasmic tail of the NR1-1a subunit of the NMDA receptor. *J Neurosci* 29: 15613-15620

Jeong H, Cohen DE, Cui L, Supinski A, Savas JN, Mazzulli JR, Yates JR, 3rd, Bordone L, Guarente L, Krainc D (2012) Sirt1 mediates neuroprotection from mutant huntingtin by activation of the TORC1 and CREB transcriptional pathway. *Nat Med* 18: 159-165

Jiang M, Chen G (2006) High Ca2+-phosphate transfection efficiency in low-density neuronal cultures. *Nat Protoc* 1: 695-700

Kandel ER (2001) The molecular biology of memory storage: a dialog between genes and synapses. *Biosci Rep* 21: 565-611

Kapitein LC, Schlager MA, Kuijpers M, Wulf PS, van Spronsen M, MacKintosh FC, Hoogenraad CC (2010) Mixed microtubules steer dynein-driven cargo transport into dendrites. *Curr Biol* 20: 290-299

Karpova A, Mikhaylova M, Bera S, Bar J, Reddy PP, Behnisch T, Rankovic V, Spilker C, Bethge P, Sahin J, Kaushik R, Zuschratter W, Kahne T, Naumann M, Gundelfinger ED, Kreutz MR (2013) Encoding and transducing the synaptic or extrasynaptic origin of NMDA receptor signals to the nucleus. *Cell* 152: 1119-1133

Kessels HW, Malinow R (2009) Synaptic AMPA receptor plasticity and behavior. *Neuron* 61: 340-350

Kholodenko BN (2003) Four-dimensional organization of protein kinase signaling cascades: the roles of diffusion, endocytosis and molecular motors. *J Exp Biol* 206: 2073-2082

Koike M, Kose S, Furuta M, Taniguchi N, Yokoya F, Yoneda Y, Imamoto N (2004) beta-Catenin shows an overlapping sequence requirement but distinct molecular interactions for its bidirectional passage through nuclear pores. *J Biol Chem* 279: 34038-34047

Kovacs KA, Steullet P, Steinmann M, Do KQ, Magistretti PJ, Halfon O, Cardinaux JR (2007) TORC1 is a calcium- and cAMP-sensitive coincidence detector involved in hippocampal long-term synaptic plasticity. *Proc Natl Acad Sci U S A* 104: 4700-4705

Lai KO, Zhao Y, Ch'ng TH, Martin KC (2008) Importin-mediated retrograde transport of CREB2 from distal processes to the nucleus in neurons. *Proc Natl Acad Sci U S A* 105: 17175-17180

Lange A, Mills RE, Lange CJ, Stewart M, Devine SE, Corbett AH (2007) Classical nuclear localization signals: definition, function, and interaction with importin alpha. *J Biol Chem* 282: 5101-5105

Lee SH, Lim CS, Park H, Lee JA, Han JH, Kim H, Cheang YH, Lee YS, Ko HG, Jang DH, Miniaci MC, Bartsch D, Kim E, Bailey CH, Kandel ER, Kaang BK (2007) Nuclear translocation of CAM-associated protein activates transcription for long-term facilitation in Aplysia. *Cell* 129: 801-812

Leslie JH, Nedivi E (2011) Activity-regulated genes as mediators of neural circuit plasticity. *Prog Neurobiol* 94: 223-237

Ma H, Groth RD, Cohen SM, Emery JF, Li B, Hoedt E, Zhang G, Neubert TA, Tsien RW (2014) gammaCaMKII shuttles Ca(2)(+)/CaM to the nucleus to trigger CREB phosphorylation and gene expression. *Cell* 159: 281-294

Macias W, Carlson R, Rajadhyaksha A, Barczak A, Konradi C (2001) Potassium chloride depolarization mediates CREB phosphorylation in striatal neurons in an NMDA receptor-dependent manner. *Brain Res* 890: 222-232

Maeder CI, Shen K, Hoogenraad CC (2014) Axon and dendritic trafficking. *Curr Opin Neurobiol* 27: 165-170

Marcora E, Kennedy MB (2010) The Huntington's disease mutation impairs Huntingtin's role in the transport of NF-kappaB from the synapse to the nucleus. *Hum Mol Genet* 19: 4373-4384

Meffert MK, Chang JM, Wiltgen BJ, Fanselow MS, Baltimore D (2003) NF-kappa B functions in synaptic signaling and behavior. *Nat Neurosci* 6: 1072-1078

Melkonian KA, Maier KC, Godfrey JE, Rodgers M, Schroer TA (2007) Mechanism of dynamitin-mediated disruption of dynactin. *J Biol Chem* 282: 19355-19364

Mikenberg I, Widera D, Kaus A, Kaltschmidt B, Kaltschmidt C (2007) Transcription factor NF-kappaB is transported to the nucleus via cytoplasmic dynein/dynactin motor complex in hippocampal neurons. *PLoS ONE* 2: e589

Neher E, Almers W (1986) Patch pipettes used for loading small cells with fluorescent indicator dyes. *Adv Exp Med Biol* 211: 1-5

Nonaka M, Kim R, Fukushima H, Sasaki K, Suzuki K, Okamura M, Ishii Y, Kawashima T, Kamijo S, Takemoto-Kimura S, Okuno H, Kida S, Bito H (2014) Region-specific activation of CRTC1-CREB signaling mediates long-term fear memory. *Neuron* 84: 92-106

Papouin T, Oliet SH (2014) Organization, control and function of extrasynaptic NMDA receptors. *Philos Trans R Soc Lond B Biol Sci* 369: 20130601

Penningroth SM, Cheung A, Bouchard P, Gagnon C, Bardin CW (1982) Dynein ATPase is inhibited selectively in vitro by erythro-9-[3-2-(hydroxynonyl)]adenine. *Biochem Biophys Res Commun* 104: 234-240

Perlson E, Hanz S, Ben-Yaakov K, Segal-Ruder Y, Seger R, Fainzilber M (2005) Vimentin-dependent spatial translocation of an activated MAP kinase in injured nerve. *Neuron* 45: 715-726

Saha RN, Wissink EM, Bailey ER, Zhao M, Fargo DC, Hwang JY, Daigle KR, Fenn JD, Adelman K, Dudek SM (2011) Rapid activity-induced transcription of Arc and other IEGs relies on poised RNA polymerase II. *Nat Neurosci* 14: 848-856

Sasaki T, Takemori H, Yagita Y, Terasaki Y, Uebi T, Horike N, Takagi H, Susumu T, Teraoka H, Kusano K, Hatano O, Oyama N, Sugiyama Y, Sakoda S, Kitagawa K (2011) SIK2 is a key regulator for neuronal survival after ischemia via TORC1-CREB. *Neuron* 69: 106-119

Saura CA (2012) CREB-regulated transcription coactivator 1-dependent transcription in Alzheimer's disease mice. *Neurodegener Dis* 10: 250-252

Scott DA, Das U, Tang Y, Roy S (2011) Mechanistic logic underlying the axonal transport of cytosolic proteins. *Neuron* 70: 441-454

Screaton RA, Conkright MD, Katoh Y, Best JL, Canettieri G, Jeffries S, Guzman E, Niessen S, Yates JR, 3rd, Takemori H, Okamoto M, Montminy M (2004) The CREB coactivator TORC2 functions as a calcium- and cAMP-sensitive coincidence detector. *Cell* 119: 61-74

Seibel NM, Eljouni J, Nalaskowski MM, Hampe W (2007) Nuclear localization of enhanced green fluorescent protein homomultimers. *Anal Biochem* 368: 95-99

Sekeres MJ, Mercaldo V, Richards B, Sargin D, Mahadevan V, Woodin MA, Frankland PW, Josselyn SA (2012) Increasing CRTC1 function in the dentate gyrus during memory formation or reactivation increases memory strength without compromising memory quality. *J Neurosci* 32: 17857-17868

Shrum CK, Defrancisco D, Meffert MK (2009) Stimulated nuclear translocation of NF-kappaB and shuttling differentially depend on dynein and the dynactin complex. *Proc Natl Acad Sci U S A* 106: 2647-2652

Silverman MA, Kaech S, Ramser EM, Lu X, Lasarev MR, Nagalla S, Banker G (2010) Expression of kinesin superfamily genes in cultured hippocampal neurons. *Cytoskeleton (Hoboken)* 67: 784-795

Talcott B, Moore MS (1999) Getting across the nuclear pore complex. *Trends Cell Biol* 9: 312-318

Thompson KR, Otis KO, Chen DY, Zhao Y, O'Dell TJ, Martin KC (2004) Synapse to nucleus signaling during long-term synaptic plasticity; a role for the classical active nuclear import pathway. *Neuron* 44: 997-1009

Thompson WJ, Anderson PS, Britcher SF, Lyle TA, Thies JE, Magill CA, Varga SL, Schwering JE, Lyle PA, Christy ME, et al. (1990) Synthesis and pharmacological evaluation of a series of dibenzo[a,d]cycloalkenimines as N-methyl-D-aspartate antagonists. *J Med Chem* 33: 789-808

Tsai NP, Tsui YC, Wei LN (2009) Dynein motor contributes to stress granule dynamics in primary neurons. *Neuroscience* 159: 647-656

van den Berg R, Hoogenraad CC (2012) Molecular motors in cargo trafficking and synapse assembly. *Adv Exp Med Biol* 970: 173-196

Wheeler DG, Groth RD, Ma H, Barrett CF, Owen SF, Safa P, Tsien RW (2012) Ca(V)1 and Ca(V)2 channels engage distinct modes of Ca(2+) signaling to control CREB-dependent gene expression. *Cell* 149: 1112-1124

Wiegert JS, Bengtson CP, Bading H (2007) Diffusion and not active transport underlies and limits ERK1/2 synapse-to-nucleus signaling in hippocampal neurons. *J Biol Chem* 282: 29621-29633

Zhou Y, Wu H, Li S, Chen Q, Cheng XW, Zheng J, Takemori H, Xiong ZQ (2006) Requirement of TORC1 for late-phase long-term potentiation in the hippocampus. *PLoS ONE* 1: e16

Chapter 3

Transcriptional role of CRTC1 during neuronal activity

Introduction

If we compare the number of genes in invertebrates to the number of genes present in humans, the relatively small difference in genetic make-up does not explain the remarkable structural and functional complexity of humans relative to invertebrates. This jump in complexity could be due to the same protein taking on different function in specific cell types or in response to specific stimuli. Underlying these cellular characteristics are differences in transcription and its regulation. Tightly regulated transcription can lead to spatial and temporal differences in gene expression that ultimately define specific cell types and organ tissues.

Our brains are spectacularly complex in this regard, making it difficult to characterize and understand every cell type and how they all connect and communicate with each other. Additionally, many neuron-specific characteristics rely on rapid transcription and translation to respond to multiple stimuli and to generate long lasting changes in neuronal function. For instance, communication between neurons relies on the strengthening or weakening of synapses in response to changes in activity, through a process called synaptic plasticity. The persistence of these changes is dependent on new gene transcription and new protein translation. Several families of transcription factors are known to play a role in synaptic plasticity and memory formation, including the CREB/ATF, AP-1, C/EBP, Egr and NF-kB families of transcription factors (Alberini 1999).

CREB is of particular interest in the field of learning and memory as one of the key transcription factors necessary to encode long-lasting changes in neurons. CREB binds cAMP Response Elements (CREs), a palindromic TGACGTCA sequence, via a basic leucine zipper (bZIP) domain. It has also been shown that CREB can bind CRE half-sites and TRE/AP-1 sequences (Mayr and Montminy 2001). CREB has a bipartite transactivation domain, composed of a constitutive Q2 domain, which mediates interactions with the TFIID complex and an inducible Kinase Induced Domain (KID), which is activated by phosphorylation of Ser133 and is responsible for recruiting the transcriptional coactivators CREB Binding

Protein (CBP) and p300. CBP and p300 acetylate histone tails near CREB target genes and directly recruit RNA polymerase II (Vo and Goodman 2001). Ser133 can be phosphorylated by a variety of different kinases, thus facilitating recruitment of transcriptional coactivators that enhance CRE-dependent gene transcription (Mayr and Montminy 2001).

The CREB/ATF family of transcription factors includes CREB, CREM (cAMP response element modulator) and ATF-1 (activating transcription factor-1), which are 70% homologous overall and more than 90% homologous within the bZIP and KID transactivation domains. CREB family members can either homodimerize or heterodimerize. Additionally, they can heterodimerize with other bZIP factors such as JUN, Fos and C/EBP, which effectively amplifies the possible combinations of these factors. Such different combinations may be crucial for the specificity and diversity of transcriptional responses (Dwarki, Montminy, and Verma 1990; Hai and Currant 1991; Millhouse et al. 1998; Rutberg et al. 1999). Additionally, the bZIP domain chiefly provides dimerization and DNA-binding activities, but more recently it has been shown to also bind coactivators (Conkright, Guzma, et al. 2003).

Early work with CREB knockout mice showed that CREB is required for the transcription-dependent late phase of long-term potentiation (L-LTP, Bourtchuladze et al. 1994). Many labs have since delved deeper into the finer details of CREB's regulation and role in a variety of different experimental paradigms, reiterating its crucial role in encoding memories. In 2003, two labs independently screened for and identified a novel type of CREB regulators. CREB Regulated Transcriptional Co-activators (CRTCs, originally know as TORCs) were found to potently increase CRE-dependent gene transcription (Conkright, Canettieri, et al. 2003).

CRTC's role was initially characterized in non-neuronal cell types and, because of CREB's role in memory, neuroscientists sought to investigate its role in learning and memory. Various experiments revealed that CRTC1 is crucial for the transcription dependent late-phase of LTP, suggesting that CRTC1 is a key coactivator in this process (Kovács et al. 2007; Zhou et al. 2006). Our lab investigated CRTC1's

dynamics in neurons and showed that, in un-stimulated neurons, CRTC1 is sequestered in the cytoplasm and partially localized at synapses. With synaptic activity and increases in local calcium concentrations, CRTC1 is dephosphorylated at three key serines (S64, S151 and S245), loses its interaction with 14-3-3 proteins and is rapidly shuttled to the nucleus in a dynein- and microtubule-dependent manner (Toh H. Ch'ng et al. 2012; Toh Hean Ch'ng et al. 2015).

Since CRTC1 rapidly translocates to the nucleus and binds CREB, we wanted to understand its role in the transcriptional response induced by synaptic activity in mature, synaptically connected neurons. Additionally, we were interested in determining whether CRTC1 binds CREB or if we could identify distinct programs of CRTC1-dependent and CRTC1-independent CREB transcription in the nucleus. Another possibility that we were interested in addressing was whether CRTC1 binding could occur independently of CREB. Since CRTC1 has such fast kinetics of activity-dependent nuclear import, we wanted to identify transcriptional changes that occur immediately after neuronal stimulation.

We used a variety of methods to address these questions, including assaying DNA binding for various transcription factors by Chromatin Immunoprecipitation coupled with sequencing (ChIP-seq), identifying open chromatin regions using an Assay for Transposase Accessible Chromatin sequencing (ATAC-seq), and monitoring global changes in gene transcription by RNA sequencing. These parallel approaches give us insight into transcriptional changes occurring immediately after synaptic activity, through the focal lens of CRTC1. One key aspect of our approach is to use ATAC-seq to identify chromatin conformational changes that occur within minutes of synaptic activity. Other groups have used this assay to look at open chromatin regions in different neuronal cell types (Mo et al. 2015), but, to our knowledge, this is the first time this method has been used in neurons to study synaptic activity-dependent chromatin remodeling on a genome wide scale.

Most studies assaying transcriptional changes in cultured neurons use neurons at 6-7 DIV, which are still developing, growing processes and most importantly, are only partially synaptically connected.

These neurons cannot respond fully to synaptic stimulation since they have not yet formed mature spines; thus most neuronal ChIPseq studies have looked at transcription after 2 to 6 hours of KCl depolarization (often preceded by silencing with tetrodotoxin over night, Kim 2010, Malik 2014). In contrast, our approach uses mature DIV 21 neurons, stimulated with BIC for 15 minutes to drive CRTC1 rapidly into the nucleus and to assay immediate effects on transcription.

Creating viral tools to study CRTC1's role in neurons

A recurring problem in studying CRTC1's function is that none of the commercially available antibodies for CRTC1 are efficient for immunoprecipitation. The Martin lab has tested several CRTC1 antibodies over the years, but most of our published work uses the rabbit polyclonal CRTC1 antibody from Bethyl Labs. This antibody yields consistent results for both immunoblotting and immunofluorescence experiments, but is inadequate for immunoprecipitation assays. In order to circumvent this problem, we designed an adeno-associated virus to express a triple FLAG-tagged full-length CRTC1 (CRTC1-3xFLAG). We used a CaMKIIα promoter to ensure that CRTC1-3xFLAG would only be expressed in excitatory neurons since we observed that CRTC1 does not translocate to the nucleus of cultured inhibitory neurons. This AAV was produced at the Penn Vector Core and each batch of AAV CaMKIIα-CRTC1-3xFLAG was titered so that the protein would be expressed at near-endogenous levels by immunofluorescence in 75% of neurons, 7 days after viral transduction (data not shown). Protein levels were also assayed by immunoblotting to ensure that FLAG-tagged CRTC1 undergoes similar activity-dependent dephosphorylation as observed with the endogenous protein.

We observed that CRTC1-3xFLAG was cytoplasmic in most un-stimulated neurons by immunofluorescence (Fig 3.1 A). In order to ensure that CRTC1 translocation was not affected by viral over-expression or by the addition of a FLAG-tag, we compared AAV-transduced neurons that were either silenced with one hour of tetrodotoxin (TTX) to enrich for cytoplasmic CRTC1 or stimulated for 15min with bicuculline (BIC) to drive CRTC1 into the nucleus. We observed that CRTC1-3xFLAG mirrored endogenous CRTC1 as both forms of the protein were dephosphorylated and translocated to the nucleus in transduced neurons (Fig 4.1 B). Furthermore, we detected a range of expression levels, and noted that in cells that were highly over-expressing CRTC1, the protein was both nuclear and cytoplasmic, irrespective of stimulation. This is a crucial observation since, even in TTX-silenced samples,

some highly overexpressing cells still have nuclear CRTC1. Nevertheless, this virally expressed CRTC1-3xFLAG is a powerful tool for studying CRTC1's role in transcription as well as its regulation by activity.

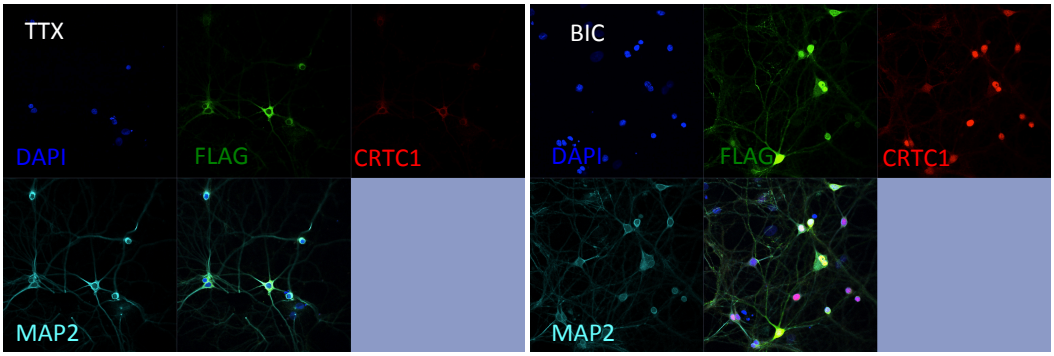

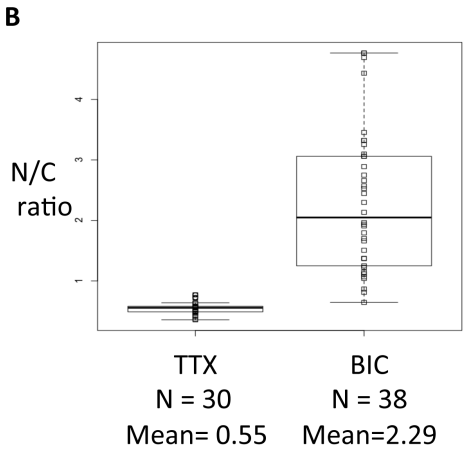

Figure 3.1: Expression of CaMKIIα-CRTC1-3xFLAG AAV in cortical primary cultures

(A) Flag-tagged CRTC1 is cytoplasmic at rest (not shown) and when neurons are silenced with TTX for one hour (left panel). Stimulation with 15 min BIC drives CRTC1-3xFLAG into the nucleus (right panel), recapitulating previously reported CRTC1 activity-dependent nuclear translocation (Toh H. Ch'ng et al. 2012).

(B) Quantification of CRTC1-3xFLAG nuclear to cytoplasmic ratios (calculated using intensity values from FLAG immunofluorescence signal).

Neuronal stimulation and experimental set up

We used rat cortical cultures that were grown in 10cm dishes for 14 days before adding the CaMKIIα-CRTC1-3xFLAG AAV. The cultures were incubated with virus overnight before replacing the virus-containing media with conditioned neuronal media. We waited an additional 7 days for the cells to express the viral construct and then either silenced or stimulated the neurons before crosslinking for ChIP-Seq (Fig 3.2 A).

We chose to use bicuculline to stimulate neuronal cell cultures because it drives synaptic activity in a physiological manner. By inhibiting $GABA_A$ receptors, bicuculline causes increases glutametergic excitatory synaptic transmission and allows for recurrent action potential bursting (Wiegert et al. 2009). We used 15 minutes of BIC stimulation since we previously observed that BIC treatment drives CRTC1 nuclear accumulation within minutes. As a control, we silenced the neurons using tetrodotoxin, which blocks voltage-gated sodium channels to prevent action potentials. This allows CRTC1 to shuttle out of the nucleus and effectively enriches for cytoplasmic CRTC1. Additionally, we used non-virally transduced, non-treated neurons as a baseline control to assess any potential effects of viral expression on neuronal health and development while also acting as a negative control for the FLAG immunoprecipitation for ChIP-Seq.

A

B

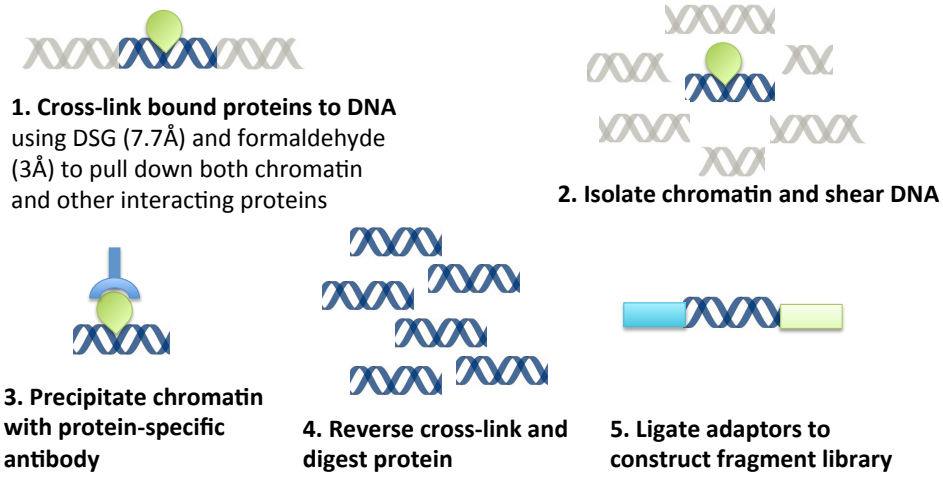

Figure 3.2: Schematic of experimental set up and ChIP-Seq protocol

(A) Cultured rat cortical neurons were grown for 14 days, AAV was added to express CaMKIIα-driven CRTC1-3xFLAG. Virus was allowed to express for 7 days before pharmacological treatments. Stimulated samples were treated with 15 minutes BIC and silenced samples were treated with 1 hour TTX prior to crosslinking for ChIP-Seq.

(B) Illustration of ChIP-Seq protocol. In order to capture both direct DNA interactions as well as secondary interactions (such as CRTC1 binding to CREB), we cross-linked using both formaldehyde (3 A linker) and DSG (7.7 A). We isolated chromatin from these cross-linked cells and sheared the DNA. We immunoprecipitated chromatin bound by specific proteins using antibodies against FLAG, CREB, and JUN. Reverse cross-linking releases the chromatin from any interacting proteins, which are subsequently digested to purify the chromatin. Sequencing adaptors are ligated to the chromatin fragments in order to prepare a sequencing library.

Results:

CREB is pre-bound to target genes

Several labs have used ChIP-Seq to study CREB's role in synaptic plasticity (Kim et al. 2010; Lesiak et al. 2013). We therefore used CREB ChIP-Seq in our preparation as a positive control. As previously reported, our data shows that CREB is pre-bound to DNA, poised to rapidly initiate transcription in response to specific cellular signals.

In order to validate that CREB binds at previously reported sites, we analyzed several immediate early genes (IEGs) that are known to be up-regulated in response to activity in a CREB-dependent manner. The example traces below show that CREB is pre-bound to the transcription start site (TSS) and distal regulatory regions of the Activity Regulated Cytoskeleton-associated (Arc) gene. I used the Arc gene and surrounding 21Kb of DNA as an example of a CREB-regulated IEGs. In this gene, the transcription start site (TSS) is on the right side of the gene, so that transcription starts from right to left, as indicated by the black arrow (Fig 3.3 A). Of note, CREB was bound in the same areas, irrespective of stimulation, although we detected a modest increase in CREB binding at these sites following stimulation (Fig 3.3 D).

We looked at several other immediate early genes, including Egr4, Nr4a1, Npas4, cFos, Zif268, and Cyr61, all of which showed similar ChIP-seq patterns to the Arc example.

CRTC1 co-localizes with pre-bound CREB following stimulation

We detected a dramatic increase in CRTC1-3xFLAG ChIP-seq signal after BIC stimulation compared to TTX silenced neurons (Fig 3.3 C). This is expected given that CRTC1 translocates in an activity-dependent manner, so very little CRTC1 should be in the nucleus when the neurons are silenced. We found that 96% of CRTC1 binding events after stimulation overlap with sites where CREB is pre-bound (Fig 3.3 B).

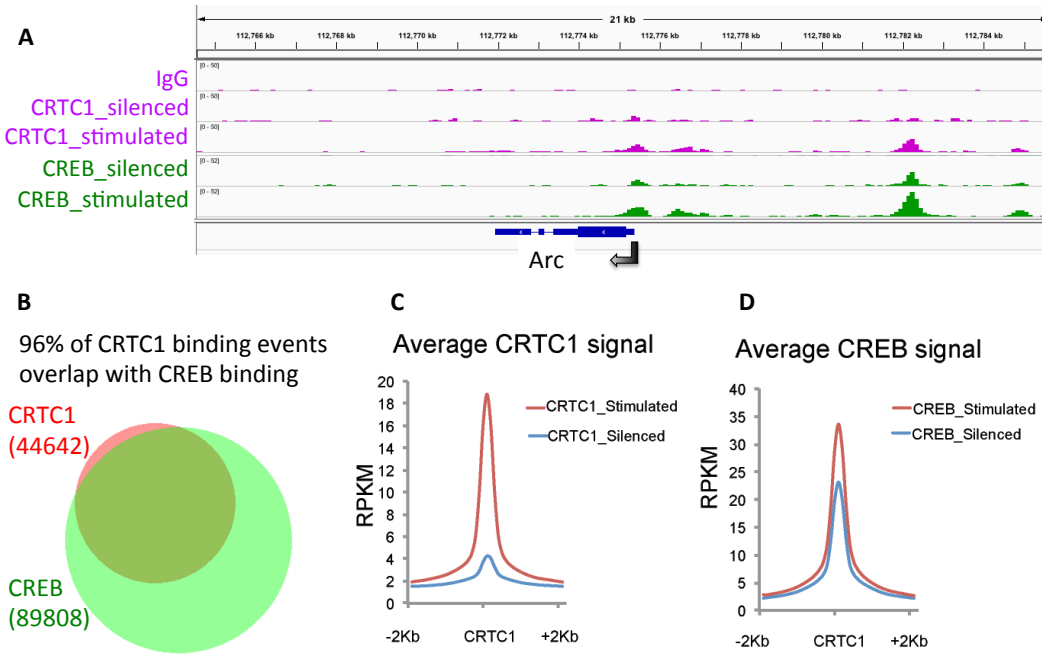

Figure 3.3: CRTC1 co-localizes with pre-bound CREB following stimulation

(A) Genome browser tracks representing ChIP-Seq data for the Arc gene locus and surrounding 21kB. CRTC1-3xFLAG traces are shown in purple, CREB traces are in green. For each set of traces, the tallest peak in the viewer is used to set the maximum data range for that gene locus. Each group includes two samples: neurons that were either silenced for 1 hour with TTX or stimulated with BIC for 15 minutes. IgG negative control shows minimal non-specific background signal.

(B) Venn diagram representing the overlap of CRTC1 with CREB-bound targets in stimulated neurons.

(C) Profiles of normalized read density for CRTC1-3xFLAG from silenced or stimulated neurons at CRTC1 peaks and surrounding 2kB.

(D) Profiles of normalized read density for CREB signal at CRTC1 peaks and surrounding 2Kb.

CRTC1 mainly occupies distal regulatory regions following activity-dependent nuclear translocation.

To better understand CRTC1's transcriptional role in neurons, we analyzed the genomic distribution of CRTC1 following stimulation. We observed that, among the 44,642 identified CRTC1 peaks, 31,919 (71.5%) were located in distal regions while only 12,723 (28.5%) were located within 2Kb of a transcription start site (TSS, Fig 3.4 B). This suggests that CRTC1 plays a role in coordinating responses from intragenic regulatory locations.

We further analyzed the DNA binding motifs enriched in areas where we detected CRTC1 ChIP-seq signal following neuronal stimulation. We used HOMER, a motif discovery algorithm that scores DNA binding sequences at genomic sites surrounding transcription factor binding events. To identify motifs that were highly enriched under CRTC1-bound targets, we compared the discovered motifs against random genomic sequences of equal length and GC content. Since CRTC1 does not bind DNA directly, but rather is known to bind CREB, which in turn binds DNA, we expected to see CREB binding motifs. In addition to CREB we also identified a number of other motifs to several other transcription factors (Fig 3.4 A). This suggests that CRTC1 may interact or associate with other transcription factors in addition to CREB.

A

de novo motif	log_{10}P-value	Best Match TF	
	-6.07e+03	Jun (AP-1 motif)	15% (3.66%)
	-4.475e+03	Egr2	37.5% (20.36%)
	-3.864e+03	Mef2c	26.1% (12.5%)
	-3.738e+03	NeuroD1	12 % (3.6%)
	-3.425e+03	Rfx1	7.5% (1.5%)
	-3.069e+03	CREB	32 % (18.4%)
	-2.296e+03	NF1	46.9% (33.2%)
	-1.792e+03	Prrx2	43.5% (31.6%)

B

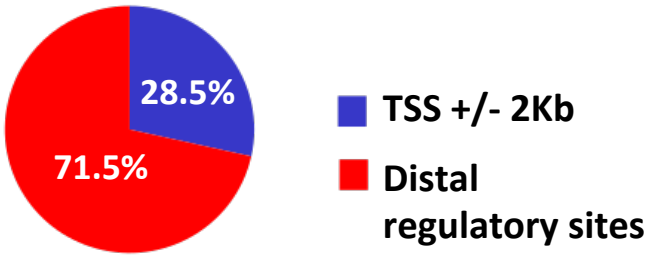

Figure 3.4: Characterization of CRTC1 occupancy following BIC stimulation

(A) Logos corresponding to enriched sequence elements identified by de novo motif analysis of CRTC1 binding after 15 minutes bicuculline stimulation. Significance (log_{10} P-value), percent of peaks containing at least one instance of the motif within 100 bp of the peak center, and, in parentheses, the expected motif frequency in a randomly selected sample of equal size are given.

(B) Percentage of CRTC1 binding events in promoter-proximal transcription start site (TSS +/- 2Kb) and distal genomic locations after bicuculline stimulation. CRTC1 binding is more pronounced in distal regions.

Potential CRTC1 interactors

Many of the transcription factors identified by our motif analysis are known to play important roles in synaptic plasticity. We reviewed published work about these factors to look for known interactions with CRTC1 or CREB during this process. Below are brief summaries of these factors and their roles in learning and memory.

JUN, like CREB, is a bZIP transcription factor that plays a crucial role in long term potentiation (LTP). Previous studies have shown that, in certain contexts, JUN can heterodimerize with CREB and thus alter the dimer's binding specificity (Hai and Currant 1991). Recent studies have shown that N-terminal phosphorylation of c-JUN is essential for hippocampal synaptic plasticity and long-term potentiation (Seo et al. 2012). Additionally, work in Hela cells showed that CRTC1 is recruited to AP-1 target gene promoters and associates with c-JUN and c-Fos to activate transcription and promote cell proliferation (Canettieri et al. 2009).

Early Growth Response factor 2, Egr2 (also known as Krox20) is a zinc finger transcription factor. Egr2 is crucial for hindbrain development and constitutive knock out of the protein is lethal. Surprisingly, conditional forebrain-specific knock out of Egr2 produces behaviorally normal mice that have superior implicit motor skill-learning abilities and enhanced long-term object recognition memory (Poirier et al. 2007). Unlike Egr1, which is required for consolidation of long-term memories, Egr2 may act as an inhibitory constraint for certain cognitive functions. Studies in awake rats show that Egr1 and Egr2 mRNAs are transcribed during LTP. Two hours after LTP induction, these mRNAs are no longer present, but Egr1 proteins persist for 8 hours and Egr2 proteins are still present over 30 hours post induction (Demmer et al. 1993).

Mef2C is a transcription factor that is critical for neuronal development, differentiation and survival. Deletion of Mef2C impairs hippocampal-dependent learning and memory by increasing the number of excitatory synapses and the potentiation of basal and evoked synaptic transmission.

Conversely, super-activation of Mef2C causes a reduction in excitatory post-synaptic sites without affecting performance on learning and memory tasks (Barbosa et al. 2008). Separate studies have shown that increasing Mef2C-mediated transcription decreases the number of dendritic spines and excitatory synapses in cultures hippocampal neurons. Parallel *in vivo* studies that locally and acutely increase Mef2 function in different areas of the brain cause learning and memory disruptions (Cole et al. 2012).

The basic helix-loop-helix transcription factor NeuroD1 associates with the p300/CBP transcription co-activator complex to regulate transcription of several cell differentiation pathways, including adult neurogenesis (Kuwabara et al. 2009). Regulatory Factor X1, Rfx1, is a helix-turn-helix transcription factor that is expressed in the brain. Knock out of Rfx1 leads to early embryonic lethality (Feng, Li, and Zuo 2011). Rfx1 may regulate gene expression in neurons as knock down of Rfx1 by siRNA decreases expression of glutamate transporters in cultured rat cortical neurons (Ma, Zheng, and Zuo 2006).

CRTC1 binding overlaps with CREB and JUN binding.

Since CRTC1 has been reported to interact with JUN in Hela cells (Canettieri et al. 2009), we chose to analyze JUN binding in relation to CREB and CRTC1. We used antibodies against JUN to perform ChIP-Seq on the same preparations of silenced and stimulated neurons that are described above (Fig 3.2 A).

ChIP-Seq analysis showed a high degree of overlap between CRTC1 and both CREB and JUN binding in stimulated neurons (Fig 3.5). Our data reveals that, in silenced neurons, JUN co-localized with pre-bound CREB. Stimulation led to increases in JUN ChIP-Seq signal in these pre-bound regions as well as in other genomic locations that were not bound by CREB or CRTC1. This suggests that, like CRTC1, JUN is recruited to transcription sites in an activity-dependent manner, but, like CREB, it is already pre-bound at many of these regions (Fig 3.5 C).

This data suggests that CRTC1 can co-bind both JUN and CREB following neuronal stimulation, yet these factors undergo different activity-dependent binding patterns. If we compare individual sites where CRTC1 binds during stimulation, we see that CREB is pre-bound and the ChIP-Seq signal at these sites changes minimally between silenced and stimulated neurons. JUN on the other hand, shows some binding in silenced neurons, but undergoes a dramatic increase in binding at CRTC1-bound sites following stimulation (Fig 3.5 E).

Our motif analysis suggests that there are probably other transcription factors binding at these sites along with CREB and JUN. Future experiments should examine these transcription factors to understand if they also play a role in transcription following neuronal stimulation.

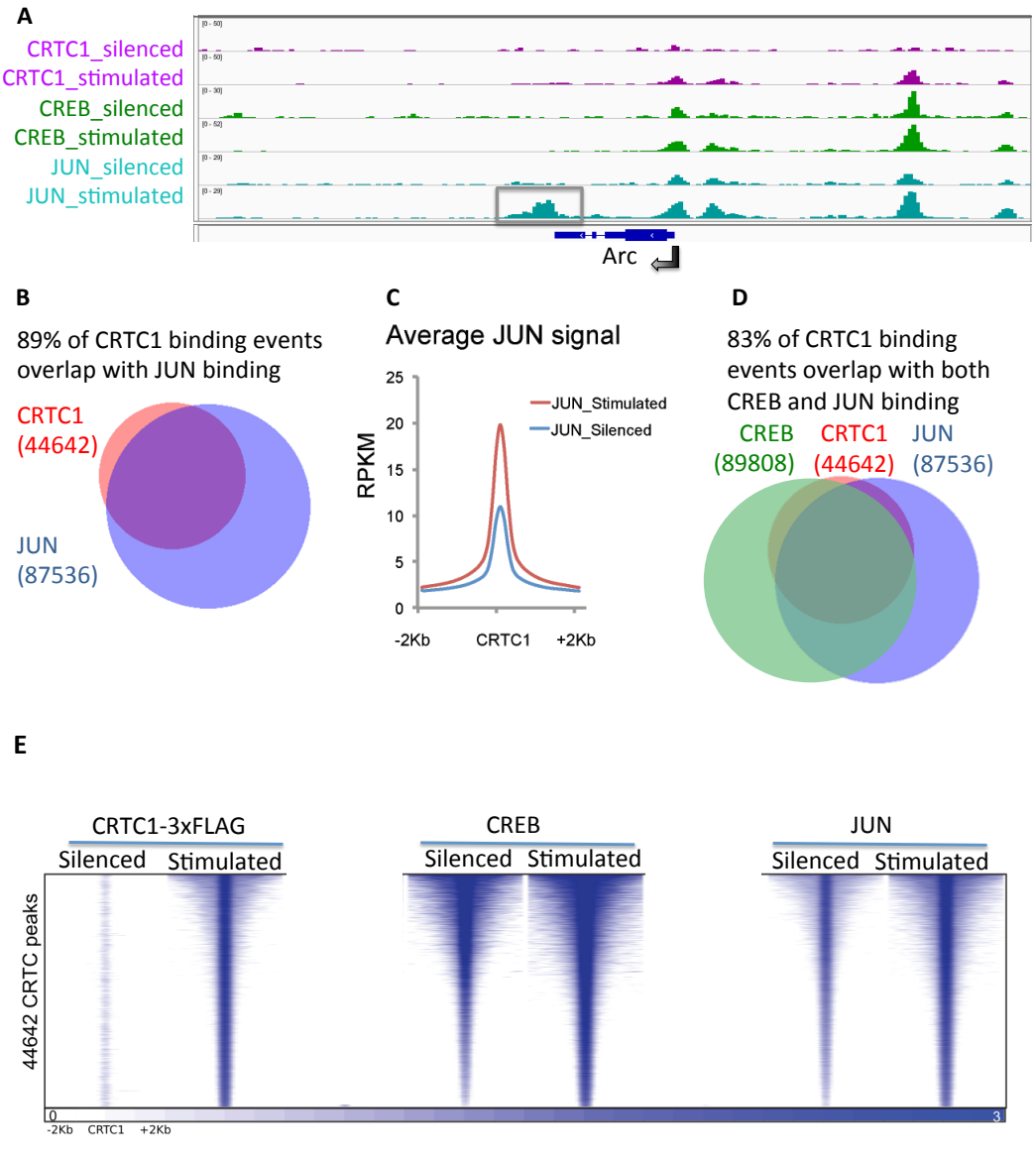

Figure 3.5: CRTC1 binding overlaps with CREB and JUN binding

(A) Genome browser tracks representing ChIP-Seq data for the Arc gene locus and surrounding 21kB. CRTC1-3xFLAG traces are shown in purple, CREB traces are in green and JUN traces are in cyan. For each set of traces, the tallest peak in the viewer is used to set the maximum data range for that gene locus. Each group includes two samples: neurons that were either silenced for 1 hour with TTX or stimulated

with BIC for 15 minutes. Grey box highlights area of increased JUN binding after stimulation without CREB or CRTC1 co-binding.

(B) Venn diagram representing the overlap of CRTC1 and JUN in neurons after 15 min BIC stimulation.

(C) Profiles of normalized read density for JUN signal around CRTC1 peaks.

(D) Venn diagram representing the overlap of CRTC1 binding events with CREB and JUN in neurons after 15 min BIC stimulation.

(E) Binding events were binarized (0 = unbound, white; 1 = bound, blue) for CRTC1-3xFLAG, CREB and JUN datasets. Genomic locations were grouped based on ATACseq signal for chromatin state after BIC treatment and rank ordered by ATAC signal intensity from stimulated neurons. Heat maps are centered on CRTC1 ChIP signal and represent 2Kb regions up/down stream from the center of each peak.

Changes in chromatin structure following neuronal stimulation

Since CRTC1 may interact with several factors, we wanted to take a broader view to analyze overall chromatin changes occurring at CRTC1-bound sites with neuronal stimulation. ATAC-Seq is a method that measures local chromatin accessibility. This method identifies open chromatin by using a Tn5 transposase to insert sequencing adaptors into open chromatin regions. These adaptors can then be used to amplify the tagged regions and to prepare libraries for sequencing (Fig 3.6 A). Only regions that are accessible to the transposase will be tagged and sequenced. ATAC-Seq has been used by other groups to identify differences between neuronal cell types (Mo et al. 2015), but because of difficulties in isolating intact neuronal nuclei, it had not been used to look at activity-dependent changes in neurons. In our application, this method allowed us to look at global activity-dependent changes in chromatin structure following neuronal stimulation.

When we stimulated neurons with 15 minutes BIC, we detected large increases in ATAC-Seq signal in the gene body of Arc (Fig 3.6 B). Other immediate early genes that are known to be up-regulated during synaptic plasticity showed a similar increase in ATAC signal specifically throughout the gene bodies. This increase is suggestive of very high transcriptional activity; RNA-Seq data will help validate whether this prediction is correct.

A

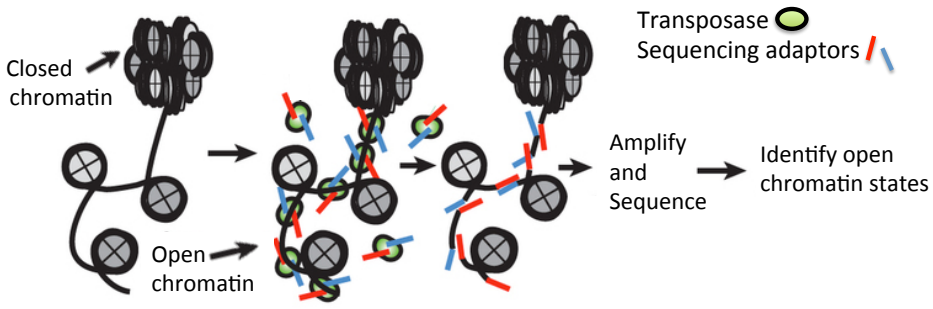

B

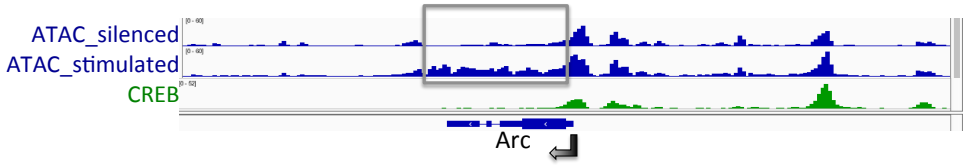

Figure 3.6: ATAC sequencing set up and preliminary results

(A) ATAC sequencing schematic adapted from Buenrostro et al. 2013.

(B) ATAC-Seq signal (blue) for the 21Kb surrounding the Arc gene. Peaks are aligned with CREB ChIP-Seq signal (green) to mark regions that are pre-bound by CREB, irrespective of activity. Grey box highlights increase in ATAC-Seq signal in the gene body of the Arc gene in stimulated neurons.

Are CRTC1-bound genes actively regulated?

This part of my project is still in progress. We decided to look at changes in gene expression by RNA-seq. We prepared samples at 15 min, 30 min, 1 hr and 2 hrs after BIC stimulation to assess increases in transcription in immediate early genes compared to later waves of transcription. We will assess if increases in transcription of different genes are transient or sustained. Additionally, we will be able to correlate this data with our ChIP-Seq data for CRTC1 in order to understand which genes are regulated by CRTC1. We will also be able to compare this data to our ATAC-Seq to better understand the relationship between chromatin state and gene expression in neurons.

What cellular processes are encoded by CRTC1 bound regions?

While waiting for our RNA-Seq data, we decided to analyze what types of genes are bound by CRTC1 after stimulation in our ChIP-Seq data set. Gene ontology (GO) analysis for genes that show CRTC1-3xFLAG activity-dependent binding highlights several biological processes and cellular components (Fig 3.7 A and B) that are crucial for synaptic plasticity. Changes in proteins at the post-synaptic density are the basis for spine enlargement and stabilization that is observed during long-term potentiation. “Site of polarized growth” and “growth cone” categories contain genes that are likely involved in the complex actin-mediated restructuring that needs to occur for spine growth and stabilization during plasticity. Additionally, many of the biological processes listed are relevant to synaptic plasticity and are necessary for the long-lasting changes in synaptic structure that underlie memory formation.

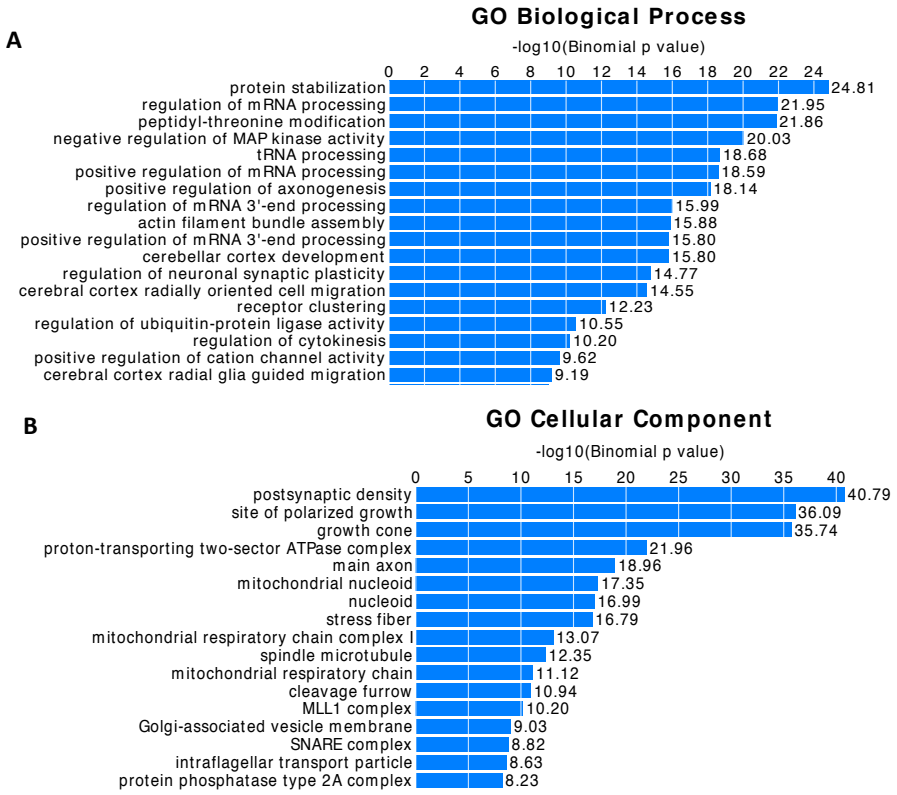

Figure 3.7: Gene ontology analysis for enriched cellular components (A) and biological processes (B) for genes that bound by CRTC1-3xFLAG after 15 min stimulation with bicuculline.

Conclusions and future directions:

The experiments summarized in this chapter led to several key findings that have expanded our current knowledge of CRTC1's role in neuronal transcription in response to stimulation. We show that CRTC1 binding correlates not only with CREB binding, but also with JUN binding. Additionally, we observed that both CRTC1 and JUN are recruited to CREB binding locations in an activity dependent manner. Finally, we show that stimulation increases chromatin accessibility, specifically throughout the gene bodies of immediate early genes. These newly opened chromatin regions are indicative of high transcriptional activity. RNA-Seq data (which is currently being analyzed) will allow us to validate whether the changes we observe by ChIP-Seq and ATAC-Seq result in differential gene expression at CRTC1-bound targets.

In the future, we hope to understand whether different stimuli can lead to differentially phosphorylated forms of CRTC1, which in turn could encode for specific transcriptional profiles once CRTC1 translocates into the nucleus. We have recently developed a conditional CRTC1 knock out mouse that, once fully characterized, will be an invaluable tool to study these pathways. The knock out mouse will allow us to assess the transcriptional effects of removing CRTC1 from this process. Additionally, without endogenous CRTC1, it will be much easier to test the role of phosphorylation by expressing forms of CRTC1 with different point mutations. These mutants may help us decode whether specific phosphorylation states are necessary to trigger different transcriptional profiles.

Methods:

Primary neuronal cultures. All experiments were performed using approaches approved by the UCLA Institutional Animal Care and Use Committee. All experiments use mature cortical neurons (DIV 21) dissected from newborn (P0-P1) rats and plated on poly-DL-lysine (0.5mg/ml) coated cover slips (Carolina Biologicals) or tissue culture dishes (6 well or 10cm). We plated one rat cortex per 10 cm dish to maximize cell density. Neuronal culture media is prepared using Neurobasal A media (Invitrogen) supplemented with β-mercaptoethanol (Sigma), monosodium glutamate (Sigma), B27 (Invitrogen) and GlutaMAX (Invitrogen). Neurons were grown in a 37°C, 5% CO_2 incubator. Neurons were incubated with various pharmacological agents in conditioned neuronal media in a 37°C, 5% CO_2 incubator for the indicated amount of time before cells were either fixed for immunocytochemistry or lysates were prepared for immunoblots.

Viral transduction and pharmacological treatments. Cortical cultures were transduced at DIV 14 with lentivirus expressing CRTC-3xFLAG driven by a CaMKIIα promoter and 7 days post-transduction, DIV 21 neurons were silenced with 1μM tetrodotoxin (TTX, Tocris) for 1 hr or stimulated with 40μM bicuculline (BIC, Sigma) for 15 min in conditioned media. Control samples (basal) were DIV 21 cortical cultures that received no virus and no pharmacological treatments to capture endogenous, un-stimulated CRTC1 levels.

Antibodies. Primary antibodies include mouse monoclonal antibodies against FLAG (Sigma, F1804), rabbit polyclonal against CRTC1 (Bethyl, A300-769A), polyclonal chicken antibody against MAP2 (Abcam, Ab5392), JUN (Abcam, Ab31419), CREB (Millipore, 06-863). All secondary antibodies are conjugated to Alexa dyes (488, 555, 633; Invitrogen).

Immunocytochemistry. Cells were fixed at room temperature for 10 min with 4% parafomalydehyde, permeabilized with 0.1% Triton-X 100 (Calbiochem) for 5 min and blocked in 10% goat-serum for 30 min. Neurons were then incubated in primary antibodies either for 4 hrs at room temperature or overnight at 4°C. Secondary antibodies and Hoechst nuclear dye (Invitrogen) were incubated at room temperature at 1:1000 dilution for 2 hrs. All antibodies were diluted in 10% goat serum and coverslips were mounted with Aqua Polymount (Polysciences).

Cross-linked ChIP-Seq (X-ChIP). Using 10 cm dishes of cultured cortical neurons, CRTC1-3xFLAG transduced neurons were prepared for TTX, BIC and basal conditions as described above on DIV 21. All samples were crosslinked prior to ChIP to assay transcription factor occupancy. To stabilize CRTC1 and its interactors on chromatin, cells were treated with 2 mM disuccinimidyl glutarate (DSG) for 25 minutes at room temperature prior to formaldehyde crosslinking (1% final concentration) for 10 minutes at room temperature. Crosslinking was quenched with 0.125 M final concentration glycine. Cross-linked cells were re-suspended in sonication buffer (50mM Hepes-KOH pH 7.5, 140mM NaCl, 1mM EDTA, 1% TritonX-100, 0.1% Na-deoxycholate, 0.1% SDS) and sonicated using a Diagenode Bioruptor for three 10-minute rounds using pulsing settings (30 sec ON; 1 min OFF). 10 ug of sonicated chromatin was then incubated overnight at 4^{o}C with 5 ug of antibodies-conjugated to magnetic beads (Active Motif, 53033). The antibodies used were: FLAG M2 (Sigma, F1804), CREB (Millipore, 06-863), c-JUN (Abcam, ab31419). Following the IP the beads were washed twice with RIPA buffer (50mM Tris-HCl pH8, 150 mM NaCl, 2mM EDTA, 1% NP-40, 0.1% Na-deocycholate, 0.1% SDS), low salt buffer (20mM Tris pH 8.1, 150mM NaCl, 2mM EDTA, 1% Triton X-100, 0.1% SDS), high salt buffer (20mM Tris pH 8.1, 500mM NaCl, 2mM EDTA, 1% Triton X-100, 0.1% SDS), LiCl buffer (10mM Tris pH 8.1, 250mM LiCl, 1mM EDTA, 1% Na-deoxycholate, 1% NP-40), and 1xTE. DNA was extracted by reverse crosslinking at 60^{o}C overnight with proteinase K (20ug/ul) and 1% SDS followed by phenol:chloroform:iso-amylacohol purification.

Illumina/Solexa sequencing library preparation, sequencing, and quality control were performed as recommended by Illumina protocols, except that PCR amplification step was limited to 10 cycles. Libraries were sequenced using single-end 50 bp sequencing reactions.

ATAC-seq library construction and sequencing. ATAC-seq was prepared as previously described in Buenrostro et al., 2013. Approximately 50,000 virally transduced neurons were prepared for TTX, BIC and basal conditions as described above. Cells were re-suspended in 50µl lysis buffer (10 mM Tris pH 7.4, 10 mM NaCl, 3 mM $MgCl_2$, 0.1% NP40, and 1 × Complete Protease inhibitor (Roche)) and spun at 500*g* for 10 min at 4 °C to collect nuclei. Nuclei were washed twice in 1x PBS and subsequently re-suspended in 50 µl Transposase reaction (25 µl 2 × Tagmentation buffer, 22.5 µl water, 2.5 µl Tn5 Transposase enzyme, following instructions by Illumina). Reactions were incubated for 30 min at 37 °C and DNA purified using Qiagen MinElute columns (Qiagen). The transposed DNA was subsequently amplified with custom primers as described (Buenrostro et al., 2013) for 7-9 cycles and libraries were visualized on a 2% TBE gel prior to sequencing with a single-end-sequencing length of 50 nucleotides.

RNA-Seq. We obtained RNA from independent biological replicates of cortical neurons transduced with CRTC1-3xFLAG AAV and either silenced with TTX or stimulated with BIC. Control samples received no virus and no pharmacological treatments (basal). RNA was extracted with TRIzol (Invitrogen), column purified with RNeasy kit (Qiagen, Valencia, CA), and treated on column with 0.5 kunitz units of DNAse prior to elution according to the manufacturer's instructions. Messenger RNA was captured using oligodT Dynabeads (Life Technologies). Strand-specific RNA-Seq libraries were constructed as described in (Parkhomchuk et al., 2009).

Quantification and Statistical Analysis

Data Analysis and Visualization: ChIP-Seq reads were mapped to the rat genome (rn4) using Bowtie software (Langmead et al. 2009)and only reads aligned to a unique position with no more than two sequence mismatches were retained for further analysis. Multiple reads mapping to the same location and strand in the genome were collapsed to a single read to account for clonal amplification effects. For ChIP-Seq of TFs and ATAC-Seq, peaks were called using MACS2 software (Zhang et al. 2008) using a bandwidth parameter of 150bp. Peaks with q-val cut-off < 0.005 and fold >= 4-fold were retained.

Genome signal tracks of features (transcription factors and ATAC-seq) were calculated by partitioning the genome into non-overlapping bins of 100b. RPKM values were calculated for each bin using the number of sequencing reads that overlap with the corresponding bin. Tracks were visualized in the IGV genome browser (Thorvaldsdottir et al. 2013).

To produce the heatmaps, in Figure 3.5, we aligned CRTC1 peaks at their summit and tiled the flanking up- and downstream regions within +/-2kb in 100bp bins. For each location, we calculated RPKM values over all 100bp bins by using the number of sequencing reads that overlap each bin after extension by 200bp in the direction of the alignment. To control for input, we computed at each bin a $\log_2$ input-normalized RPKM value as $\log_2(RPKM_{FOREGROUND})$ - $\log_2(RPKM_{Input})$, where $RPKM_{FOREGROUND}$ denotes the RPKM of the corresponding TF data set and $RPKM_{Input}$ denotes the RPKM value of the corresponding whole genome 'Input'. For visualization in figures, each 100 bp bin was displayed with JavaTreeview (Eisen et al. 1998). Metaplots were produced by computing the average input-normalized RPKM value for each 100bp bin across all locations in the given set.

Ontology Annotation: To associate transcription factor peaks with the closest gene for Ontology analysis (Fig 3.7) we used the GREAT tool (McLean et al. 2010) with default parameters.

Assigning peaks to TSS (+/-2Kb) regions: We computed the proportion of transcription factor binding summits of CRTC1 that are located within 2 kb of annotated transcription start sites (rn4 RefSeq TSS) and the rest (distal)

Motif analyses: We calculated motif instances within 200 bp around ChIP-Seq summits by using the findMotifsGenome.pl procedure from HOMER (Heinz et al. 2010) with the following command line arguments: findMotifsGenome.pl {peak.bed} rn4 {peaks.out} -size 200 -mask -cache 1000

References:

Alberini, Cristina M. 1999. “Genes to Remember.” *Journal of Experimental Biology* 202: 2887–91.

Barbosa, Ana C, Mi-Sung Kim, Mert Ertunc, Megumi Adachi, Erika D Nelson, John McAnally, James A Richardson, et al. 2008. “MEF2C, a Transcription Factor That Facilitates Learning and Memory by Negative Regulation of Synapse Numbers and Function.” *Proceedings of the National Academy of Sciences of the United States of America* 105 (27): 9391–96. doi:10.1073/pnas.0802679105.

Bourtchuladze, Roussoudan, Bruno Frenguelli, Julie Blendy, Diana Cioffi, Gunther Schutz, and Alcino J. Silva. 1994. “Deficient Long-Term Memory in Mice with a Targeted Mutation of the cAMP-Responsive Element-Binding Protein.” *Cell* 79 (1). Cell Press: 59–68. doi:10.1016/0092-8674(94)90400-6.

Buenrostro, Jason D, Paul G Giresi, Lisa C Zaba, Howard Y Chang, and William J Greenleaf. 2013. “Transposition of Native Chromatin for Fast and Sensitive Epigenomic Profiling of Open Chromatin, DNA-Binding Proteins and Nucleosome Position.” *Nature Methods* 10 (12): 1213–18. doi:10.1038/nmeth.2688.

Canettieri, Gianluca, Sonia Coni, Michele Della Guardia, Valentina Nocerino, Laura Antonucci, Laura Di Magno, Robert Screaton, Isabella Screpanti, Giuseppe Giannini, and Alberto Gulino. 2009. “The Coactivator CRTC1 Promotes Cell Proliferation and Transformation via AP-1.” *Proceedings of the National Academy of Sciences of the United States of America* 106 (5): 1445–50. doi:10.1073/pnas.0808749106.

Ch’ng, Toh H., Besim Uzgil, Peter Lin, Nuraly K. Avliyakulov, Thomas J. O’Dell, and Kelsey C. Martin. 2012. “Activity-Dependent Transport of the Transcriptional Coactivator CRTC1 from Synapse to Nucleus.” *Cell* 150 (1). Elsevier Inc.: 207–21. doi:10.1016/j.cell.2012.05.027.

Ch’ng, Toh Hean, Martina DeSalvo, Peter Lin, Ajay Vashisht, James A Wohlschlegel, and Kelsey C Martin. 2015. “Cell Biological Mechanisms of Activity-Dependent Synapse to Nucleus Translocation of

CRTC1 in Neurons." *Frontiers in Molecular Neuroscience* 8. Frontiers Media SA: 48. doi:10.3389/fnmol.2015.00048.

Cole, Christina J, Valentina Mercaldo, Leonardo Restivo, Adelaide P Yiu, Melanie J Sekeres, Jin-Hee Han, Gisella Vetere, et al. 2012. "MEF2 Negatively Regulates Learning-Induced Structural Plasticity and Memory Formation." *Nature Neuroscience* 15 (9). doi:10.1038/nn.3189.

Conkright, Michael D, Gianluca Canettieri, Robert Screaton, Ernesto Guzman, Loren Miraglia, John B Hogenesch, Marc Montminy, and La Jolla. 2003. "TORCs : Transducers of Regulated CREB Activity The Salk Institute for Biological Studies." *Molecular Cell* 12: 413–23.

Conkright, Michael D, Ernesto Guzma, Lawrence Flechner, Andrew I Su, John B Hogenesch, and Marc Montminy. 2003. "Genome-Wide Analysis of CREB Target Genes Reveals A Core Promoter Requirement for cAMP Responsiveness Salk Institute for Biological Studies." *Molecular Cell* 11 (1): 1101–8.

Demmer, Jerome, Michael Dragunow, Patricia A. Lawlor, Sara E. Mason, John D. Leah, Wickliffe C. Abraham, and Warren P. Tate. 1993. "Differential Expression of Immediate Early Genes after Hippocampal Long-Term Potentiation in Awake Rats." *Molecular Brain Research* 17 (3): 279–86. doi:10.1016/0169-328X(93)90012-E.

Dwarki, V J, M Montminy, and I M Verma. 1990. "Both the Basic Region and the 'Leucine Zipper' Domain of the Cyclic AMP Response Element Binding (CREB) Protein Are Essential for Transcriptional Activation." *The EMBO Journal* 9 (1). European Molecular Biology Organization: 225–32. http://www.ncbi.nlm.nih.gov/pubmed/2136830.

Eisen, M B, P T Spellman, P O Brown, and D Botstein. 1998. "Cluster Analysis and Display of Genome-Wide Expression Patterns." *Proceedings of the National Academy of Sciences of the United States of America* 95 (25): 14863–68. http://www.ncbi.nlm.nih.gov/pubmed/9843981.

Feng, Chenzhuo, Jiejie Li, and Zhiyi Zuo. 2011. "Expression of the Transcription Factor Regulatory Factor

X1 in the Mouse Brain." *Folia Histochemica et Cytobiologica* 490047 (2): 344–51. doi:10.5603/FHC.2011.0047.

Hai, Tsonwin, and Tom Currant. 1991. "Cross-Family Dimerization of Transcription Factors Fos/Jun and ATF/CREB Alters DNA Binding Specificity." *Biochemistry* 88: 3720–24.

Heinz, Sven, Christopher Benner, Nathanael Spann, Eric Bertolino, Yin C. Lin, Peter Laslo, Jason X. Cheng, Cornelis Murre, Harinder Singh, and Christopher K. Glass. 2010. "Simple Combinations of Lineage-Determining Transcription Factors Prime Cis-Regulatory Elements Required for Macrophage and B Cell Identities." *Molecular Cell* 38 (4): 576–89. doi:10.1016/j.molcel.2010.05.004.

Kim, Tae-Kyung, Martin Hemberg, Jesse M Gray, Allen M Costa, Daniel M Bear, Jing Wu, David A Harmin, et al. 2010. "Widespread Transcription at Neuronal Activity-Regulated Enhancers." *Nature* 465. doi:10.1038/nature09033.

Kovács, Krisztián a, Pascal Steullet, Myriam Steinmann, Kim Q Do, Pierre J Magistretti, Olivier Halfon, and Jean-René Cardinaux. 2007. "TORC1 Is a Calcium- and cAMP-Sensitive Coincidence Detector Involved in Hippocampal Long-Term Synaptic Plasticity." *Proceedings of the National Academy of Sciences of the United States of America* 104 (11): 4700–4705. doi:10.1073/pnas.0607524104.

Kuwabara, Tomoko, Jenny Hsieh, Alysson Muotri, Gene Yeo, Masaki Warashina, Dieter Chichung Lie, Lynne Moore, Kinichi Nakashima, Makoto Asashima, and Fred H Gage. 2009. "Wnt-Mediated Activation of NeuroD1 and Retro-Elements during Adult Neurogenesis." *Nature Publishing Group* 12. doi:10.1038/nn.2360.

Langmead, Ben, Cole Trapnell, Mihai Pop, and Steven L Salzberg. 2009. "Ultrafast and Memory-Efficient Alignment of Short DNA Sequences to the Human Genome." *Genome Biology* 10. doi:10.1186/gb-2009-10-3-r25.

Lesiak, Adam, Carl Pelz, Hideaki Ando, Mingyan Zhu, Monika Davare, Talley J Lambert, Katelin F Hansen, et al. 2013. "A Genome-Wide Screen of CREB Occupancy Identifies the RhoA Inhibitors Par6C and

Rnd3 as Regulators of BDNF-Induced Synaptogenesis." *PloS One* 8 (6). Public Library of Science: e64658. doi:10.1371/journal.pone.0064658.

Ma, Kaiwen, Shuqiu Zheng, and Zhiyi Zuo. 2006. "The Transcription Factor Regulatory Factor X1 Increases the Expression of Neuronal Glutamate Transporter Type 3." *The Journal of Biological Chemistry* 281 (30). American Society for Biochemistry and Molecular Biology: 21250–55. doi:10.1074/jbc.M600521200.

Mayr, Bernhard, and Marc Montminy. 2001. "Transcriptional Regulation by the Phosphorylation-Dependent Factor CREB." *Nature Reviews Molecular Cell Biology* 2 (8). Nature Publishing Group: 599–609. doi:10.1038/35085068.

McLean, Cory Y, Dave Bristor, Michael Hiller, Shoa L Clarke, Bruce T Schaar, Craig B Lowe, Aaron M Wenger, and Gill Bejerano. 2010. "GREAT Improves Functional Interpretation of Cis-Regulatory Regions." *Nature Biotechnology* 28 (5): 495–501. doi:10.1038/nbt.1630.

Millhouse, Scott, Joseph J. Kenny, Patrick G. Quinn, Vivien Lee, and Brian Wigdahl. 1998. "ATF/CREB Elements in the Herpes Simplex Virus Type 1 Latency-Associated Transcript Promoter Interact with Members of the ATF/CREB and AP-1 Transcription Factor Families." *Journal of Biomedical Science* 5 (6). Kluwer Academic Publishers: 451–64. doi:10.1007/BF02255935.

Mo, Alisa, Eran A. Mukamel, Fred P. Davis, Chongyuan Luo, Gilbert L. Henry, Serge Picard, Mark A. Urich, et al. 2015. "Epigenomic Signatures of Neuronal Diversity in the Mammalian Brain." *Neuron* 86 (6): 1369–84. doi:10.1016/j.neuron.2015.05.018.

Poirier, Roseline, Hélène Cheval, Caroline Mailhes, Patrick Charnay, Sabrina Davis, and Serge Laroche. 2007. "Paradoxical Role of an Egr Transcription Factor Family Member, Egr2/Krox20, in Learning and Memory." *Frontiers in Behavioral Neuroscience* 1. Frontiers: 6. doi:10.3389/neuro.08.006.2007.

Rutberg, Se, Tl Adams, M Olive, N Alexander, C Vinson, and Sh Yuspa. 1999. "CRE DNA Binding Proteins

Bind to the AP-1 Target Sequence and Suppress AP-1 Transcriptional Activity in Mouse Keratinocytes." *Oncogene* 18: 1569–79.

Seo, Jinsoo, Jinpyo Hong, Sung Joong Lee, and Se Young Choi. 2012. "C-Jun N-Terminal Phosphorylation Is Essential for Hippocampal Synaptic Plasticity." *Neuroscience Letters* 531 (1). Elsevier Ireland Ltd: 14–19. doi:10.1016/j.neulet.2012.09.048.

Thorvaldsdottir, H., J. T. Robinson, and J. P. Mesirov. 2013. "Integrative Genomics Viewer (IGV): High-Performance Genomics Data Visualization and Exploration." *Briefings in Bioinformatics* 14 (2): 178–92. doi:10.1093/bib/bbs017.

Vo, N, and R H Goodman. 2001. "CREB-Binding Protein and p300 in Transcriptional Regulation." *The Journal of Biological Chemistry* 276 (17). American Society for Biochemistry and Molecular Biology: 13505–8. doi:10.1074/jbc.R000025200.

Wiegert, J Simon, Frank Hofmann, Hilmar Bading, and C Peter Bengtson. 2009. "A Transcription-Dependent Increase in Miniature EPSC Frequency Accompanies Late-Phase Plasticity in Cultured Hippocampal Neurons." *BMC Neuroscience* 10. doi:10.1186/1471-2202-10-124.

Zhang, Yong, Tao Liu, Clifford A Meyer, Jérôme Eeckhoute, David S Johnson, Bradley E Bernstein, Chad Nussbaum, et al. 2008. "Model-Based Analysis of ChIP-Seq (MACS)." *Genome Biology* 9 (9). BioMed Central: R137. doi:10.1186/gb-2008-9-9-r137.

Zhou, Yang, Hao Wu, Shuai Li, Qian Chen, Xue-Wen Cheng, Jing Zheng, Hiroshi Takemori, and Zhi-Qi Xiong. 2006. "Requirement of TORC1 for Late-Phase Long-Term Potentiation in the Hippocampus." *PloS One* 1 (1): e16. doi:10.1371/journal.pone.0000016.

Chapter 4

Characterization of CRTC1 phosphorylation in neurons

This chapter summarizes the experiments and tools that were used to characterize CRTC1's phosphorylation sites and their potential role in its activity-dependent regulation. Our interest in the phosphorylation of CRTC1 led us to examine several potential interacting partners, including kinases and phosphatases that could regulate CRTC1's phosphorylation state.

Identifying CRTC1 phoshorylation sites.

Neuronal stimulation with bicuculline (BIC) or forskolin (FSK) triggers dramatic dephosphorylation of CRTC1, detected as a large decrease in molecular weight by immunoblot (Fig 4.1 B). Dephosphorylated CRTC1 is no longer bound to 14-3-3 proteins that anchor it at the synapse and is thus free to translocate into the nucleus to activate CREB-dependent gene transcription (Fig 4.1 A). This translocation and the associated change in molecular weight are blocked by the calcineurin inhibitor cyclosporinA (CsA). Immunoblot and 2-dimentional (2D) gel electrophoresis analysis of CRTC1 from either tetrodotoxin-silenced (TTX) or stimulated (BIC, FSK) neurons, illustrate the robust changes in the molecular weight and isoelectric point (pI) of CRTC1 following neuronal activation (Fig 4.1 C). These changes are consistent with distinct phosphorylation states since they collapse to much lower molecular weights after incubation of the lysate with calf intestinal phosphatase (CIP, Fig 4.1 B, C). Additionally, our immunoblot and 2D gel data indicate that different types of activity lead to different CRTC1 dephosphorylation states, as seen in differences in immunoblot bands in Fig 4.1B and different CRTC1 spots in Fig 4.1C, which could represent distinct, differentially phosphorylated forms of the protein (Ch'ng et al., 2012).

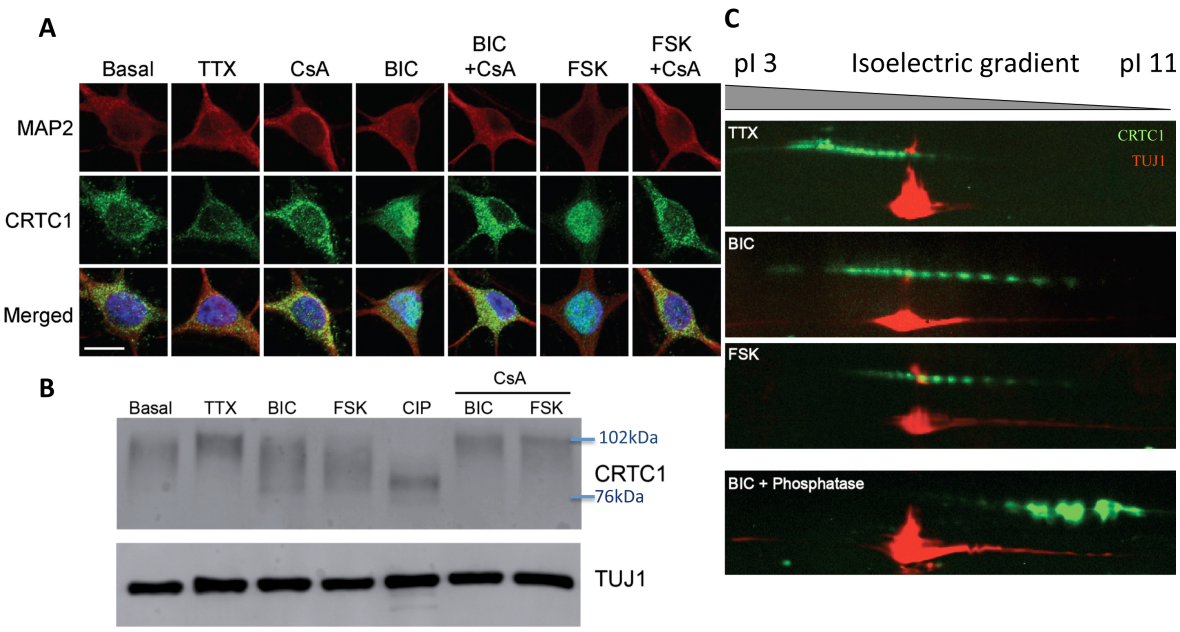

Figure 4.1: Stimulation drives nuclear translocation of CRTC1 in a calcineurin-dependent process and triggers complex changes in CRTC1 phosphorylation**.** Adapted from Ch'ng et al., 2012.

(A) Hippocampal cultures were pretreated with Cylclosporin A (CsA; 5 mM) for 4 hr prior to a 1 hr stimulation with bicuculline (BIC; 40 mM) or with forskolin (FSK; 25 mM). Neurons were fixed and immunostained with antibodies against MAP2 (red), CRTC1 (green), and Hoechst nuclear dye (blue, merged).

(B) Cultured hippocampal neurons were incubated with tetrodotoxin (TTX; 1 mM), BIC, or FSK in the presence or absence of CsA. After 10 min, neuronal cultures were lysed, CIP samples were dephosphorylated with Calf Intestinal Phosphatase. Samples were separated by SDS-PAGE and immunoblotted with antibodies against TUJ1 (55kDa) or CRTC1 (~75-100kDa).

(C) Cultured hippocampal neurons were stimulated as described in (B), and lysates were subjected to 2D gel electrophoresis and immunoblotted with antibodies against CRTC1 (green) and TUJ1 (red).

We were interested in investigating the possibility that the pattern of phosphorylation of CRTC1 serves as a code that directs not only CRTC1 translocation, but also its transcriptional activity in the nucleus. We hypothesized that CRTC1 undergoes differential dephosphorylation depending on the type of stimulation received by the cell. These distinct phosphorylation patterns could, in turn, inform CRTC1's impact on gene transcription once in the nucleus. We approached this hypothesis by asking a series of questions, specifically:

1. What CRTC1 sites are phosphorylated at rest?
2. What CRTC1 sites are dephosphorylated with neuronal activity?
3. Which CRTC1 sites orchestrate its nuclear translocation?
4. Which CRTC1 sites are important for CRTC1's transcriptional activity?
5. Do other types of post translational modifications (PTMs) affect function of CRTC1 in neurons?

In order to answer these questions, we first decided to identify which sites are phosphorylated on CRTC1. We used a mouse neuroblastoma cell line, Neuro2A (N2A), in order to identify phosphorylated residues on CRTC1. We transiently transfected N2A cells with full-length HA-tagged CRTC1, immunoprecipated CRTC1 using HA-conjugated beads, ran the samples on an SDS-PAGE gel, and cut out CRTC1 bands for mass spectrometry analysis. Using this protocol, we identified 50 different phosphorylation sites (Fig 4.2 A, B) that are highly conserved across 10 different species. We repeated this experiment twice, using different mass spectrometry machines, which could explain the low overlap between the two samples (Fig 4.2 C).

CRTC1 has an unusually high number of phosphorylatable sites (Serine/Threonines/Tyrosines), including almost twice the expected number of Serines, based on reported amino acid frequency in mammalian non-membrane proteins (Gaur, 2014).

Amino acid (AA)	Reported AA Occurrence	CRTC1 AA Occurrence
Serine (S)	8.15%	13.1 % (83 S)
Threonine (T)	5.16%	7.8% (50 T)
Tyrosine (Y)	2.6%	2% (13 Y)
Total (S/T/Y)	15.91%	23% (146 S/T/Y)

We next compared the sites that we identified by mass spectrometry across 10 different species in order to identify sites conserved through evolution that might be critically important for CRTC1's role and regulation. We noted that sites in the first half of the protein were more highly conserved, especially those present in amino acids 130 to 160, where seven out of the eight sites identified are 100% conserved (Fig 4.2 A).

A

1 MATSNNPRKF SEKIALHNQK QAEETAAFEE VMKDLSLTRA ARLQLQKSQY

51 LQLGPSRGQY YGGSLPNVNQ IGSSSVDLAF QTPFQSSGLD TSRTTRHHGL

101 VDRVYRERGR LGSPHRRPLS VDKHGRQADS CPYGTVYLSP PADTSWRRTN

151 SDSALHQSTM TPSQAESFTG GSQDAHQKRV LLLTVPGMED TGAETDKTLS

201 KQSWDSKKAG SRPKSCEVPG INIFPSADQE NTTALIPATH NTGGSLPDLT

251 NIHFPSPLPT PLDPEEPPFP ALTSSSSTGS LAHLGVGGAG QGMNTPSSSP

301 QHRPAVVSPL SLSTEARRQQ AQQVSPTLSP LSPITQAVAM DALSLEQQLP

351 YAFFTQTGSQ QPPPQPQPPP PPPPVSQQQP PPPQVSVGLP QGGPLLPSAS

401 LTRGPQLPPL SVTVPSTLPQ SPTENPGQSP MGIDATSAPA LQYRTSAGSP

451 ATQSPTSPVS NQGFSPGSSP QHTSTLGSVF GDAYYEQQMT ARQANALSRQ

501 LEQFNMMENA ISSSSLYNPG STLNYSQAAM MGLSGSHGGL QDPQQLGYTG

551 HGGIPNIILT VTGESPPSLS KELSSTLAGV SDVSFDSDHQ FPLDELKIDP

601 LTLDGLHMLN DPDMVLADPA TEDTFRMDRL

Color code for percent of sites conserved among 10 species:
zebrafish, puffer fish, xenopus, chicken, opossum, dog, horse,
rat, mouse and human
100%, 90%, 80%, 70%, 60%, <50%

B

1 MATSNNPRKF SEKIALHNQK QAEETAAFEE VMKDLSLTRA ARLQLQKSQY

51 LQLGPSRGQY YGGSLPNVNQ IGSSSVDLAF QTPFQSSGLD TSRTTRHHGL

101 VDRVYRERGR LGSPHRRPLS VDKHGRQADS CPYGTVYLSP PADTSWRRTN

151 SDSALHQSTM TPSQAESFTG GSQDAHQKRV LLLTVPGMED TGAETDKTLS

201 KQSWDSKKAG SRPKSCEVPG INIFPSADQE NTTALIPATH NTGGSLPDLT

251 NIHFPSPLPT PLDPEEPPFP ALTSSSSTGS LAHLGVGGAG QGMNTPSSSP

301 QHRPAVVSPL SLSTEARRQQ AQQVSPTLSP LSPITQAVAM DALSLEQQLP

351 YAFFTQTGSQ QPPPQPQPPP PPPPVSQQQP PPPQVSVGLP QGGPLLPSAS

401 LTRGPQLPPL SVTVPSTLPQ SPTENPGQSP MGIDATSAPA LQYRTSAGSP

451 ATQSPTSPVS NQGFSPGSSP QHTSTLGSVF GDAYYEQQMT ARQANALSRQ

501 LEQFNMMENA ISSSSLYNPG STLNYSQAAM MGLSGSHGGL QDPQQLGYTG

551 HGGIPNIILT VTGESPPSLS KELSSTLAGV SDVSFDSDHQ FPLDELKIDP

601 LTLDGLHMLN DPDMVLADPA TEDTFRMDRL

RED= first N2A mass spec (31 sites tot)
BLUE= second N2A mass spec (38 sites tot)
GREEN= overlap (19 sites)
non-overlap (not GREEN): 31 sites
Tot number of phosphorylated sites (combined): 50
only included sites id'ed with >80% confidence

Figure 4.2: Conservation and reproducibility of CRTC1 phosphorylation sites

(A) Conservation of CRTC1 phosphorylation sites identified through mass spectrometry analysis of over-expressed HA-tagged CRTC1 in N2A neuroblastoma cells. Adapted from Ch'ng et al., 2015 to include serine/threonine amino acid substitutions.

(B) Comparison of phosphorylation sites identified in two biological replicates. Samples were run on two different mass spectrometry machines, which could explain low reproducibility.

Having identified the sites that are phosphorylated at rest, our next goal was to use mass spectrometry analysis to identify sites that are dephosphorylated with activity. Mass spectrometry requires large amounts of starting material and since we do not have antibodies that immunoprecipitate CRTC1 efficiently, we decided to try using non-neuronal cell lines in which we could easily express tagged-versions of CRTC1 by plasmid-based transfections. We attempted to stimulate N2A cells in order to trigger CRTC1 dephosphorylation and nuclear translocation, as observed in neurons. Unfortunately, we observed that CRTC1 in N2A cells does not respond to the same types of stimulation as in neurons. We tested a variety of different stimulation paradigms (bicuculline, forskolin, KCl depolarization, ionomycin, constitutively active calcineurin) that drive CRTC1 to the nucleus in neurons, as well as ways to prevent CRTC1 from being exported out of the nucleus (Leptomycin B, Fig 3.3 B), but we did not observe robust nuclear accumulation of CRTC1. Ionomycin, which promoted dephosphorylation of CRTC1, was not well tolerated and caused most of the cells to detach from the cover slips during the immunofluorescence protocol. Lower concentrations of ionomycin may resolve this issue, but the dephosphorylation observed may also be related to the health of the cells.

Additionally, we differentiated N2A cells into neurons using retinoic acid treatment or serum starvation, but we did not observe CRTC1 dephosphorylation and nuclear translocation even in differentiated cells. We tested several other cell lines (including the human neuroblastoma cell line SY5Y, NIH 3T3, HEK, HELA and CHO cells), but were unable to consistently elicit CRTC1 dephosphorylation (by immunoblot) correlating with nuclear translocation (by immunofluorescence) in non-neuronal cells. In some cases, we observed nuclear accumulation without detectable changes by immunoblot while other treatments showed dephosphorylation by immunobot but no changes in CRTC1 sub-cellular localization. We tested both expression of HA-CRTC1 and HA-CRTC1$^{1-270}$ with similar results.

Of note, others in the lab have repeated versions of these experiments with mixed results. Chris Yi observed weak translocation in N2A cells using constitutively active calcineurin and, more recently,

Shivan Bonanno observed dephosphorylation and some nuclear accumulation (or potentially overall increase) of CRTC1 in HEK cells after 4 hours of incubation with combined forskolin and calcium ionophore A23187. Since this stimulation is so long, this change could be due to translocation or to new protein synthesis. Additionally, the changes in molecular weight that accompany this nuclear accumulation in HEK cells look different than the immunoblot banding pattern we see in neurons, suggesting cell-specific differential regulation of the phosphorylation state of CRTC1. Our current understanding is that CRTC has distinct functions in a variety of cell types, which could explain this observed difference.

It is possible that CRTC1 is regulated by different stimuli in non-neuronal cell types and that, unlike in neurons, only a few sites are dephosphorylated with translocation. Since our goal was to understand the dephosphorylation changes that accompany nuclear translocation in neurons, none of these cell lines and stimulations seemed appropriate for this application. In light of these observations, we decided to return to primary neuronal cultures, transduced with a custom made adeno associated virus (AAV) for CRTC1-3xFLAG driven by a CaMKIIα promoter, in order to express tagged-CRTC1 and immunoprecipitate it using the FLAG tag. These neurons could then be either silenced or stimulated to enrich for dephosphorylated or phosphorylated CRTC1, respectively (Fig 4.4).

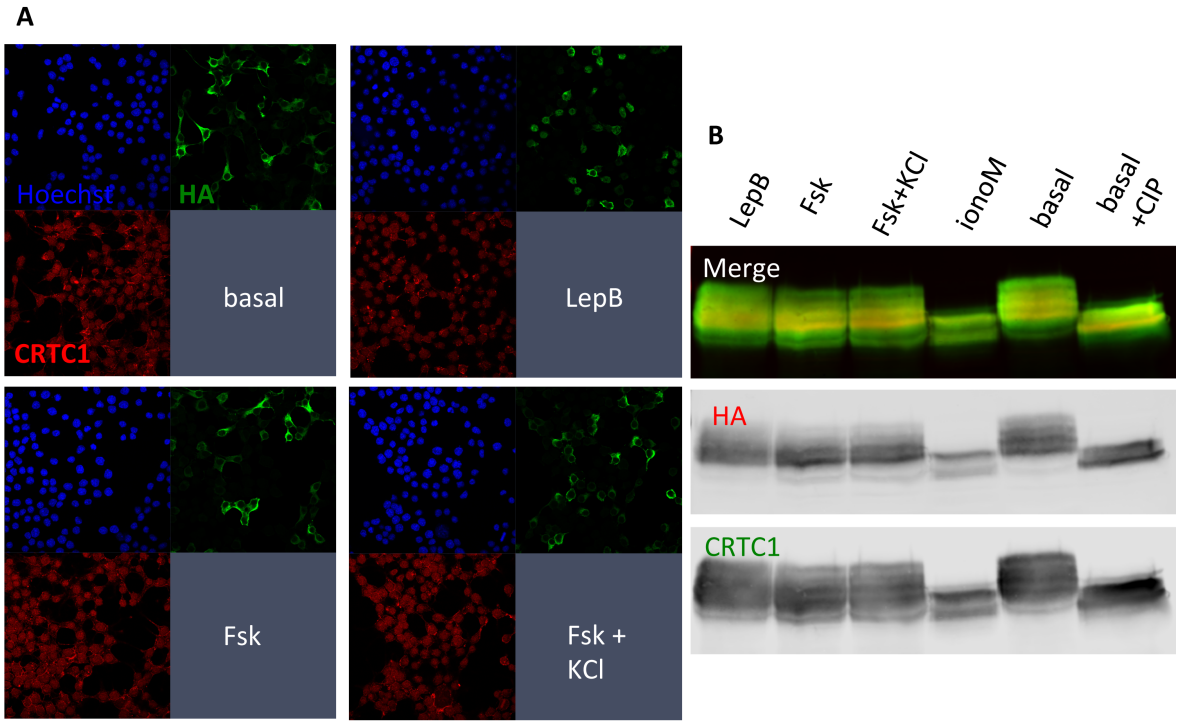

Figure 4.3: Nuclear accumulation and dephosphorylation of CRTC1 in N2A cells

(A) CRTC1 does not accumulate in the nucleus of N2A cells following stimulation. N2A cells were either left untreated (basal) or incubated with forskolin (FSK; 25 uM for 30 min), FSK + KCl (25 uM FSK for 30 min + 40 mM KCl for 10 min), or nuclear export inhibitor Leptomycin B (LepB, 10 nM for 30 min). Cells were fixed and immunostained with antibodies against HA (green), CRTC1 (red), and Hoechst nuclear dye (blue).

(B) Activity does not trigger changes in CRTC1 phosphorylation in N2A cells as previously show in neurons. N2A cells were either left untreated (basal) or incubated with FSK, FSK + KCl, LepB or ionomycin (ionoM; 1 uM for 30 min), which increases intracellular Ca^{2+} levels. Cells were lysed and dephosphorylated with Calf Intestinal Phosphatase (basal +CIP) as a control. Samples were separated by SDS-PAGE and immunoblotted with antibodies against the HA tag (red in merged image) or CRTC1 (~75-100kDa, green in merged image). Individual staining for HA and CRTC1 are shown below the merged image to compare banding patterns. Ionomycin undergoes similar dephosphorylation as the CIP

control, suggesting that this type of stimulation could lead to nuclear accumulation, however, it also seems to be toxic to the cells since they do not adhere to the coverslips after ionomycin treatment, making it impossible to assess nuclear accumulation by immunofluorescence.

See laboratory notes from 11/26/2013 for additional details.

Figure 4.4: Diagram of experimental set up for mass spectrometry analysis

Cultured rat cortical neurons were grown for 14 days before adding AAV to express CaMKIIα-driven CRTC1-3xFLAG. Virus was allowed to express for 7 days before treatments. Samples were stimulated with 15 minutes BIC or silenced with 1 hour TTX prior to lysis and immunoprecipitation using anti-FLAG antibodies.

We used mass spectrometry to identify sites that are dephosphorylated with neuronal activity. Mass spectrometry analysis to identify differentially phosphorylated sites relies on thorough coverage of all potential peptide fragments and thus requires large amounts of starting material (Fig 4.5). In order to isolate enough starting material for mass spectrometry analysis, we used ten 10cm dishes of rat primary neuronal cultures (DIV 21, 7 days post transduction) per treatment. Cultures were transduced with AAV at 14 DIV and allowed to express CRTC1-3xFLAG for 7 days. At DIV 21, neurons were either silenced for 1 hour with tetrodotoxin (TTX) or stimulated for 15 minutes with bicuculline (BIC). CRTC1-3xFLAG was immunoprecipitated using FLAG-conjugated beads in order to isolate the phosphorylated and de-phosphorylated states of CRTC1 (Fig 4.4). Unfortunately, our large-scale, virally transduced primary neuronal culture preparations still provided insufficient starting material for this type of analysis. The data seemed to indicate that there were more phosphorylated sites in the BIC sample, which we would expect to be de-phosphorylated compared to the TTX sample. It is important to take into consideration that most of the sites identified were “low confidence” meaning that the data was insufficient in pinning down the exact location of the phosphorylated reside. Only one “high confidence” site, S587, that was present in TTX samples but not in BIC samples.

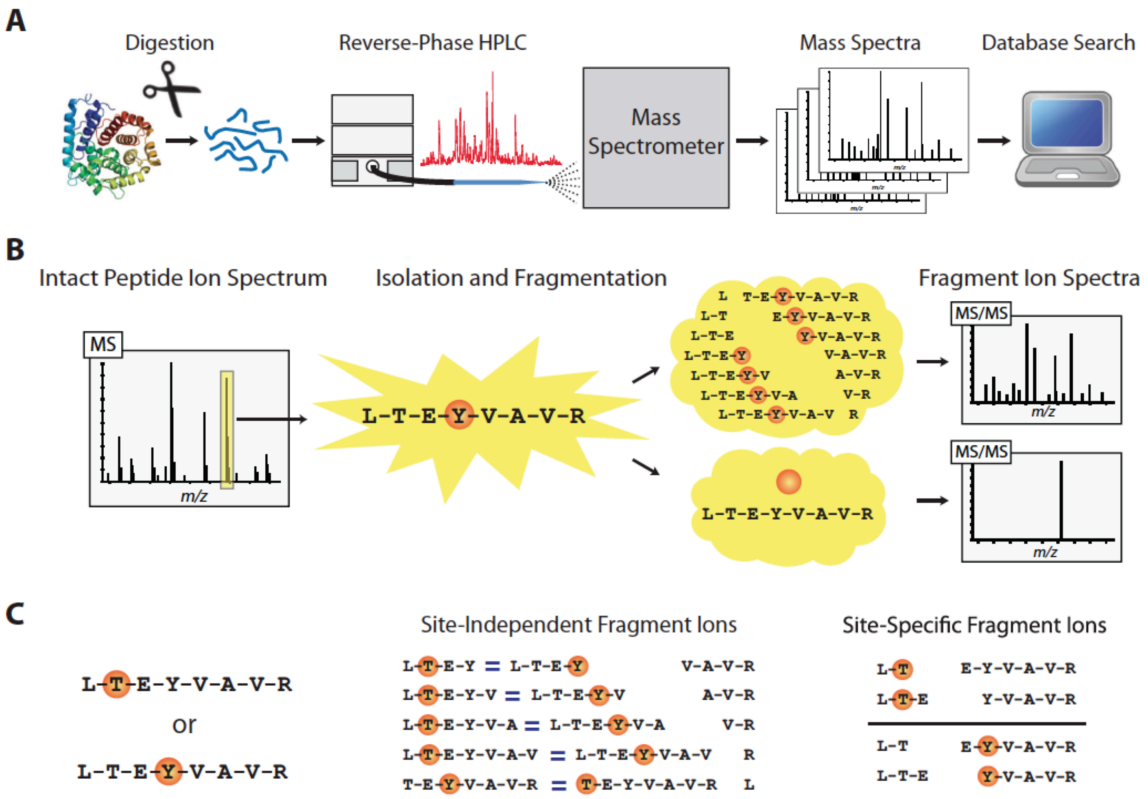

Figure 4.5: Tandem mass spectrometry (MS/MS) analysis of protein phosphorylation (Dephoure et al., 2013).

(A) Samples are digested using proteolytic enzymes to create peptide fragments. These peptides are separated by reverse-phase high-performance liquid chromatography. Algorithms that use spectral data and sequence information are used for peptide matching.

(B) The mass spectrometer generates the mass of intact peptides. Each of these peptides can then be isolated individually and further fragmented by collision with an inert gas. The resulting fragments are then detected in an MS/MS (MS2) scan and can be used to identify phosphorylated residues (orange circles) with sufficient coverage (top path). In many cases, fragmentation can de-phosphorylate the peptide (bottom path), thus losing information about the position of the phosphorylated residue.

(C) In order to identify phosphorylated sites in peptides with more than one S/T/Y, site-specific fragment ions must have different mass in order to determine which residue is modified. In this example, site-

independent fragment ions cannot distinguish between a phosphorylated threonine or tyrosine. Site-specific fragment ions have a different mass depending on whether the threonine or tyrosine is phosphorylated and thus can be used to identify which site is modified.

Another issue we encountered during mass spectrometry analysis is that digestion of CRTC1 results in suboptimal peptide fragments for phosphate-modification analysis. Two common enzymes used for enzymatic digestion for mass spectrometry are trypsin and chymotrypsin. CRTC1 only has a few trypsin cut sites, which creates peptide fragments that are too large to be useful in identifying phosphorylated residues (Fig 4.5 B, C). Chymotrypsin creates more peptide fragments, but many of these have multiple phosphorylatable sites, making it difficult to identify which sites are actually modified. To address these issues, we may need to test different enzymes to optimize digestion of CRTC1.

In parallel, we decided to use Stable Isotope Labeling of Amino Acids in Cell Culture (SILAC) heavy-labeled N2A cells as a spike-in standard for our neuronal samples to quantitatively identify differentially phosphorylated residues (Fig 4.6). We used N2A cells as our SILAC standard since cells need to be actively dividing in order to incorporate the heavy isotopes used for labeling and cultured neurons are post-mitotic. We prepared virally-transduced neuronal cultures as described above, and either TTX-silenced or BIC-stimulated the cells in order to prepare phosphorylated and de-phosphorylated CRTC1 samples respectively. We planned to spike-in equal amounts of heavy-labeled N2A standard to each of the samples. This SILAC standard should act as a reference and internal control since the sample and standard are digested and analyzed together. This method should allow us to quantify and compare the number and location of phosphorylated residues in the two samples. All of the necessary samples for this experiment were prepared and gel slices containing immunoprecipitated CRTC1 from both neurons and N2As are ready for analysis by mass spectrometry.

Alternatively, there are a variety of other approaches that could be used to study CRTC1 phoshorylation and other post-translational modifications. As mentioned above, different enzymes could be used in order to digest CRTC1 into smaller fragment sizes to create more overlapping peptides for analysis of phosphorylated residues. Recent improvements for in-gel digest techniques could help

increase starting material and advances in mass spectrometry technology should progressively increase sensitivity. This would make it easier to work with smaller amounts of starting material, which has been one of the main limitations of working with neurons. Additionally, using Electron-Transfer Dissociation (ETD) to further fragment peptides while maintaining post-translational modification intact should greatly improve the quality of this type of analysis (Mikesh et al., 2006).

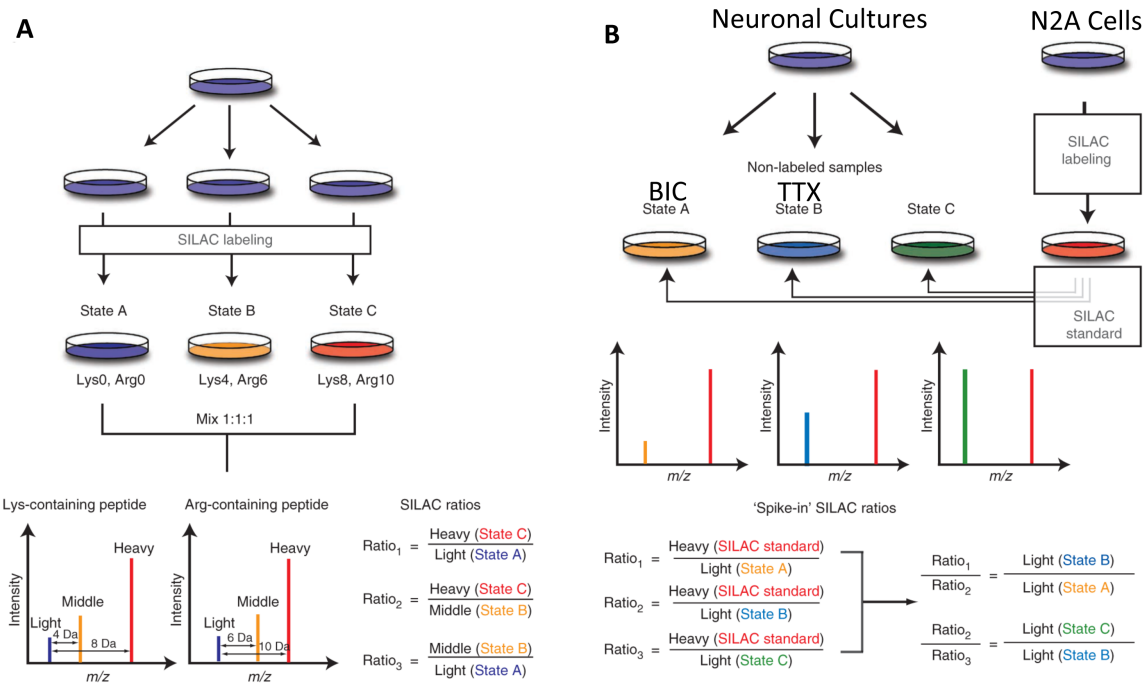

Figure 4.6: Spike-in SILAC (Stable Isotope Labeling of Amino Acids in Cell Culture) Standard. Adapted from Geiger et al., 2011.

(A) Classical SILAC protocol, using two or three differentially heavy-labeled cell populations that are combined and analyzed together by LC-MS/MS. Each peptide appears as a doublet or triplet with distinct mass differences in the MS spectra. Ratios between these samples are calculated by comparing peak intensities.

(B) In our Spike-in SILAC protocol, we separate the labeling from the experiment. We prepared neuronal cultures that were transduced with AAV-CaMKIIα-CRTC1-3xFLAG and then either silenced (1hr TTX) or stimulated (15min BIC). In parallel, we prepared heavy labeled N2A cells, to be combined with each neuronal sample before LC-MS/MS analysis. The difference between experimental samples is then calculated as a ratio or ratios by comparing the ratio of one sample to the standard divided by the ratio of the other sample to the same standard.

Designing phospho-specific antibodies to study CRTC1 function

In a parallel approach, we custom designed 4 antibodies against CRTC1 (Fig4.7 A). We created one polyclonal antibody that recognizes CRTC1's arginine rich Nuclear Localization Sequence (NLS). Additionally, we created three polyclonal phospho-specific affinity-purified antibodies for S64, S151 and S245, the sites identified in chapter 1 that are responsible for regulation of CRTC1's nuclear translocation. Phospho-specific antibodies are created by immunizing an animal with a phosphorylated protein peptide and then selecting for antibodies that recognize only the phosphorylated form.

The animal's immune system then creates a mix of pan antibodies that recognized both the phospho- and de-phoshporylated forms of the peptide and phospho-specific antibodies that only recognize the modified peptide (Fig 4.7 B). Sequential column purification steps are used to separate the antibodies that are not specific for the modified peptide from those that recognize the phosphorylated peptide. This process produces two batches of antibodies, one phospho-specific (pS64, pS151, pS245) and one pan antibody (S64 NP, S151 NP, S245 NP) that recognizes the non-phosphorylated version of the peptide. Our custom antibody production yields varied significantly. They are summarized in Fig 4.7 C.

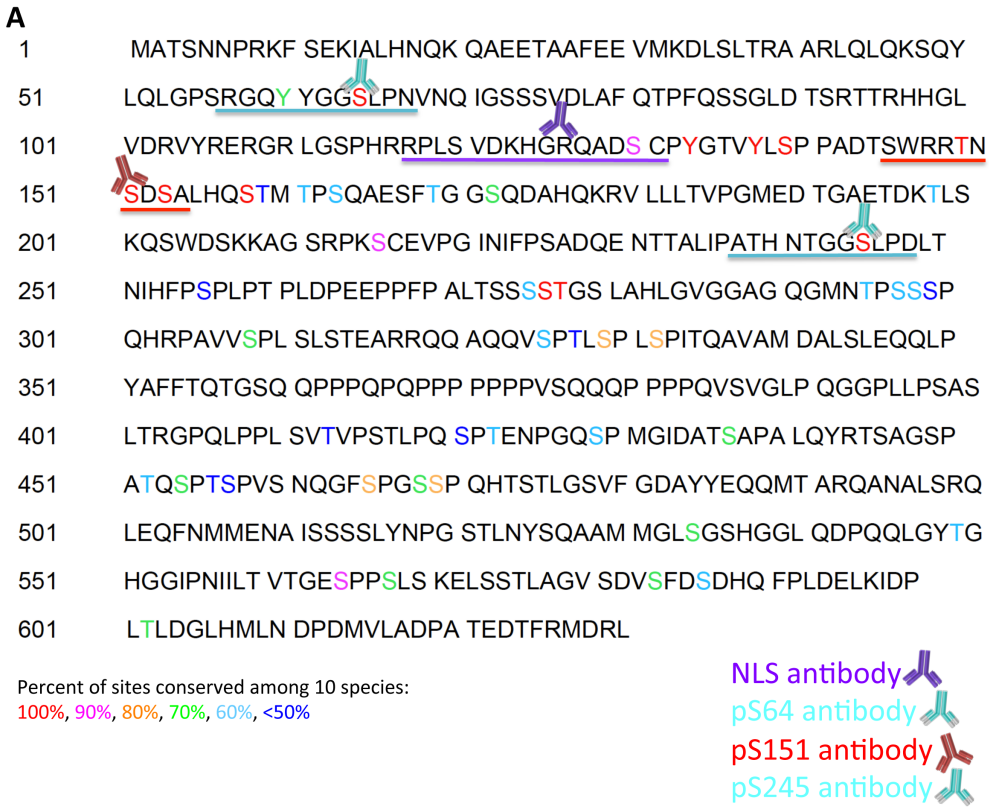

Antibody	Concentration (mg/ml)
CRTC1 (Bethyl)	0.2
pS64	1.569
S64 NP	0.617
pS151	0.491
S151 NP	0.905
pS245	2.529
S245 NP	2.025
NLS	0.955

Figure 4.7: Design and purification of custom antibodies for CRTC1.

(A) The NLS antibody recognizes the arginine rich region that we previously identified as CRTC1's nuclear localization sequence (NLS). The other three antibodies are phospho-specific antibodies that recognize

phosphorylated S64, S151 and S245. Note that the amino acids flanking S64 and S245 have very high homology, which could help explain cross-reactivity between these two antibodies. Color-coded amino acids denote conservation across 10 species.

(B) Schematic of phospho-specific antibody purification protocol. Immunization with a phospho-specific peptide will yield a mixture of antibodies recognizing both the phospho and non-phosho forms of the peptide. Antibodies that recognize the non-phosphorylated (NP) peptide are first depleted using non-phosphorylated peptide bound to a column. The flow through is applied to a column with bound phosphorylated peptide to remove any non-binding antibodies and further purify for the desired phosho-specific antibody. The antibody against the NP peptide can be eluted off of the first column and used as a control to test the specificity of the phosphorylated antibody.

(C) Table summarizing production yield for both the phospho-specific and non-phospho specific antibodies produced, in comparison to commercial Bethyl Labs CRTC1 antibody.

We used serine-to-alanine mutants of the three phospho sites (S64A, S151A, S245A) to confirm the specificity of these antibodies. We expressed a variety of constructs in HEK cells (summarized in Fig 4.8 A) in order to validate the specificity of these antibodies.

We tested these antibodies in HEK cells overexpressing CRTC1$^{1\text{-}270}$-Dendra2 and saw modest specificity by immunoblot. The NLS antibody seems to be specific for CRTC1 (no bands in CRTC2), and it recognizes two bands in CRTC1^{270} which could be phosphorylated and non-phosphorylated forms of CRTC1 since we see them collapse to a lower molecular weight after CIP treatment. The band in the CIP treated sample curls at the edges which may be due to large amounts of CIP at 50kDa that could displace the CRTC1 band (Fig 4.8 B). One way to get around this technical problem would be to use lambda phosphatase in the future.

The pS151 antibody does not recognize pS151 by immunoblot (Fig 4.8 D). We detect some antibody binding in the CRTC1^{270}-Den and S245 CRTC1^{270}-Den, but we do not see binding to full length CRTC1. This likely means that the antibody is not specific, but it could also indicate that S151 is not phosphorylated in HEK cells. Phospho-specific antibody tests for serine 64 and 245 indicate that the pS64 antibody cross-reacts with both pS64 and pS245 while the antibody for pS245 is specific for pS245 (Fig 4.8 F, I).

These immunoblots indicate that the pS64 antibody recognizes both S64 and S245 phosphorylation and cannot distinguish between the two. Interestingly, pS245 antibody does seem to be specific for pS245 and does not recognize phosphorylation at S64 (Fig 4.8 H, K). The antibodies against non-phosphorylated peptide for S151 and S245 (Fig 4.8 E, J) do not give any signal, while the antibody again non-phosphorylated S64 recognizes the same bands as the phospho-specific one (Fig 4.8 G).

A

WB lane	Constructs for custom antibody validation
1	Dendra
2	CRTC2-Den
3	CRTC1-Den
4	CRTC1-Den + CIP
5	CRTC1^{270}-Den
6	CRTC1^{270}-Den + CIP
7	S64A CRTC1^{270}-Den
8	S151A CRTC1^{270}-Den
9	S245A CRTC1^{270}-Den
10	Mock
11	S64A/S245A CRTC1^{270}-Den

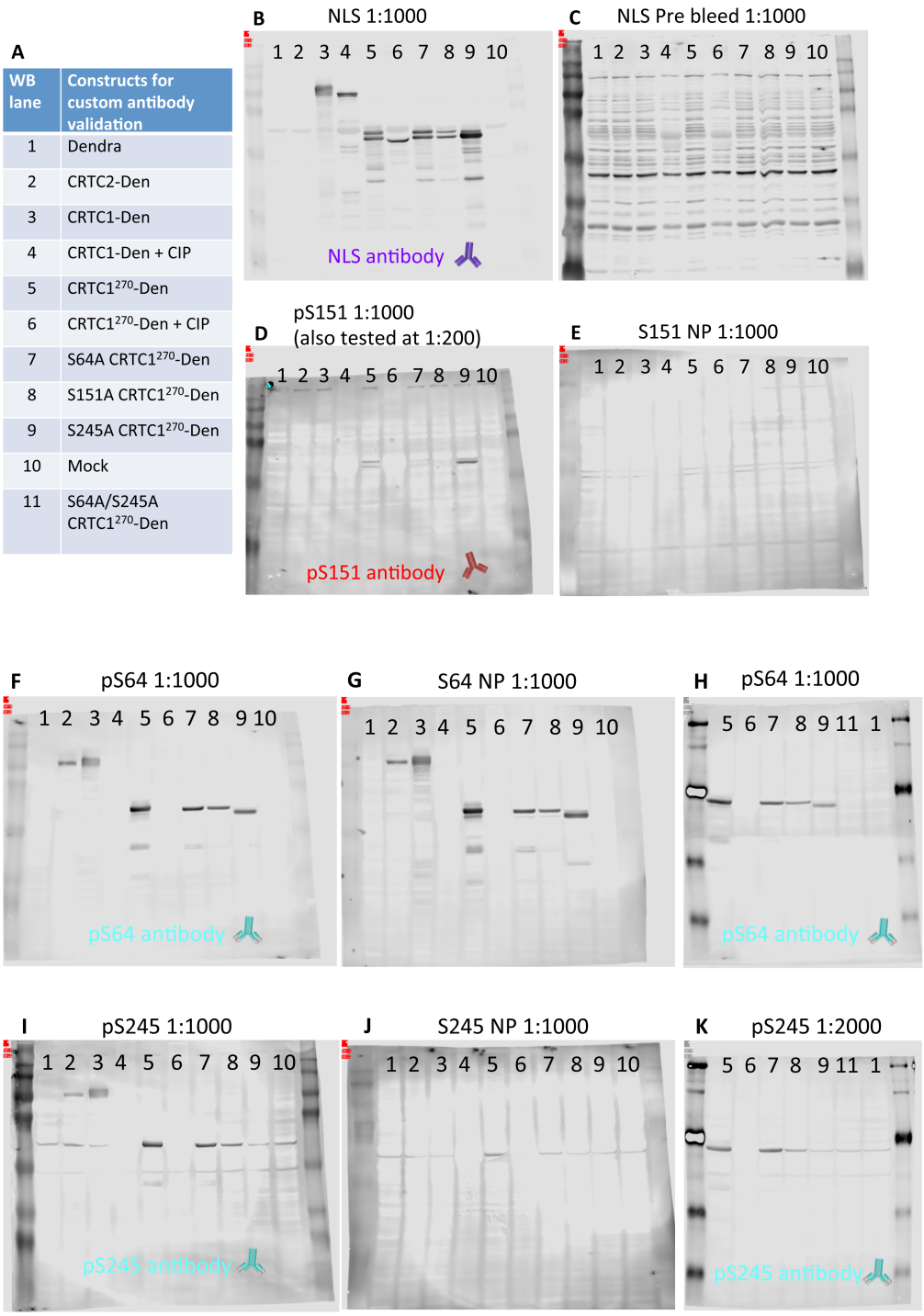

Figure 4.8: Custom antibody immunoblot validation using samples from HEK cells

(A) Table summarizing the constructs used for validation of custom NLS and phospho-specific antibodies. Each construct was transiently transfected into HEK cells and allowed to express for 16 hours. Cells were lysed in RIPA buffer. Each lane was loaded with 15ug of the indicated sample.

To test for specificity, immunoblots were incubated with the indicated dilutions of

(B) NLS antibody, (C) NLS pre-bleed, (D) pS151 antibody, (E) non-phosphorylated S151 antibody (S151 NP), (F) pS64 antibody, (G) non-phosphorylated S64 (S64 NP), (I) pS245, and (J) non-phosphorylated S245 (S245 NP) antibody. (H/K) Since the peptides used to create the pS64 and pS245 antibodies have very similar amino acid composition, we wanted to make sure that they did not cross-react. To test this, we used a S64A/S245A CRTC1^{270}-Dendra double mutant and then incubated with either pS64 (H) or pS245 (K) antibodies. All unlabeled lanes are molecular weight markers.

In order to assess whether our custom-made NSL and phospho-specific antibodies are suitable for immunofluorescence, we again expressed several constructs in HEK cells. As expected based on the immunoblotting results, none of the antibodies were exceptionally good, but we did detect specific labeling for the NLS, pS64 and pS151 antibodies (Fig 4.9 A, B, C). Most of the antibody staining (red) overlapped with areas of very high overexpression (as assessed by Dendra-2 staining, green) of our test constructs. It is important to note that the intensity of the Dendra2 fluorescence does not correlate with the staining from custom antibodies for CRTC1. This suggests that the antibodies may only be recognizing only a small fraction of the protein present.

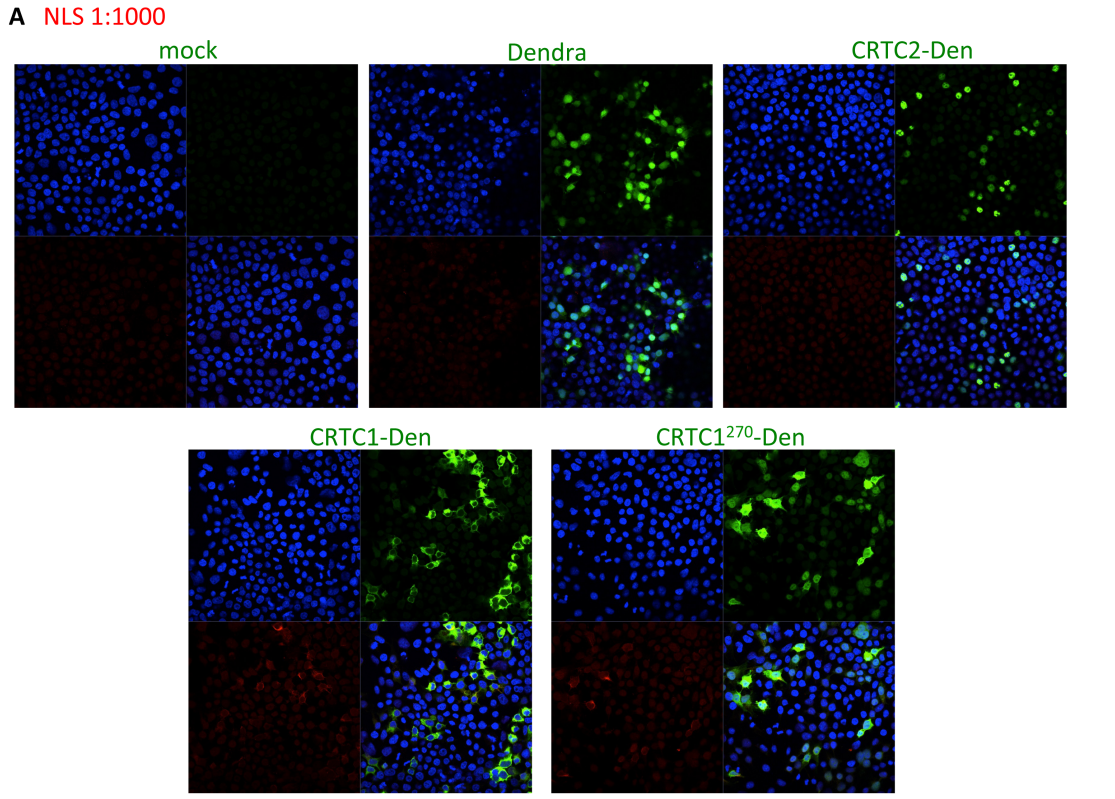
A NLS 1:1000
mock
Dendra
CRTC2-Den
CRTC1-Den
CRTC1270-Den

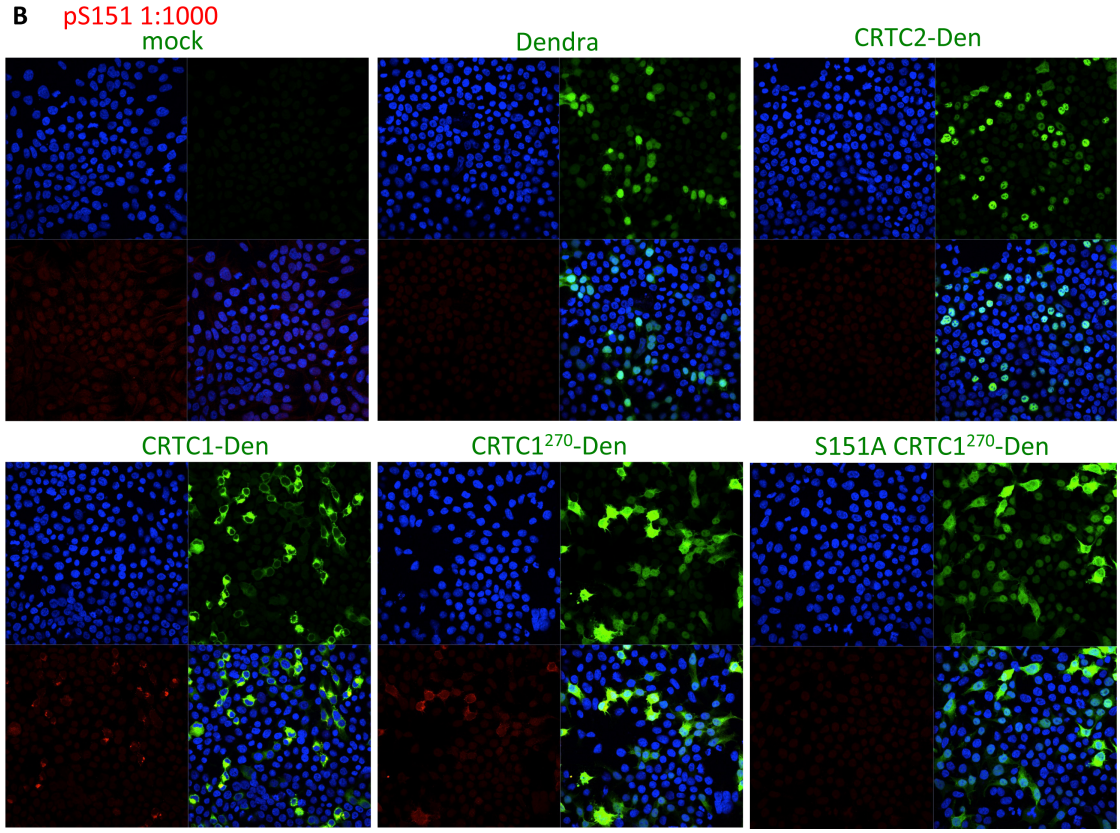
B pS151 1:1000
mock
Dendra
CRTC2-Den
CRTC1-Den
CRTC1270-Den
S151A CRTC1270-Den

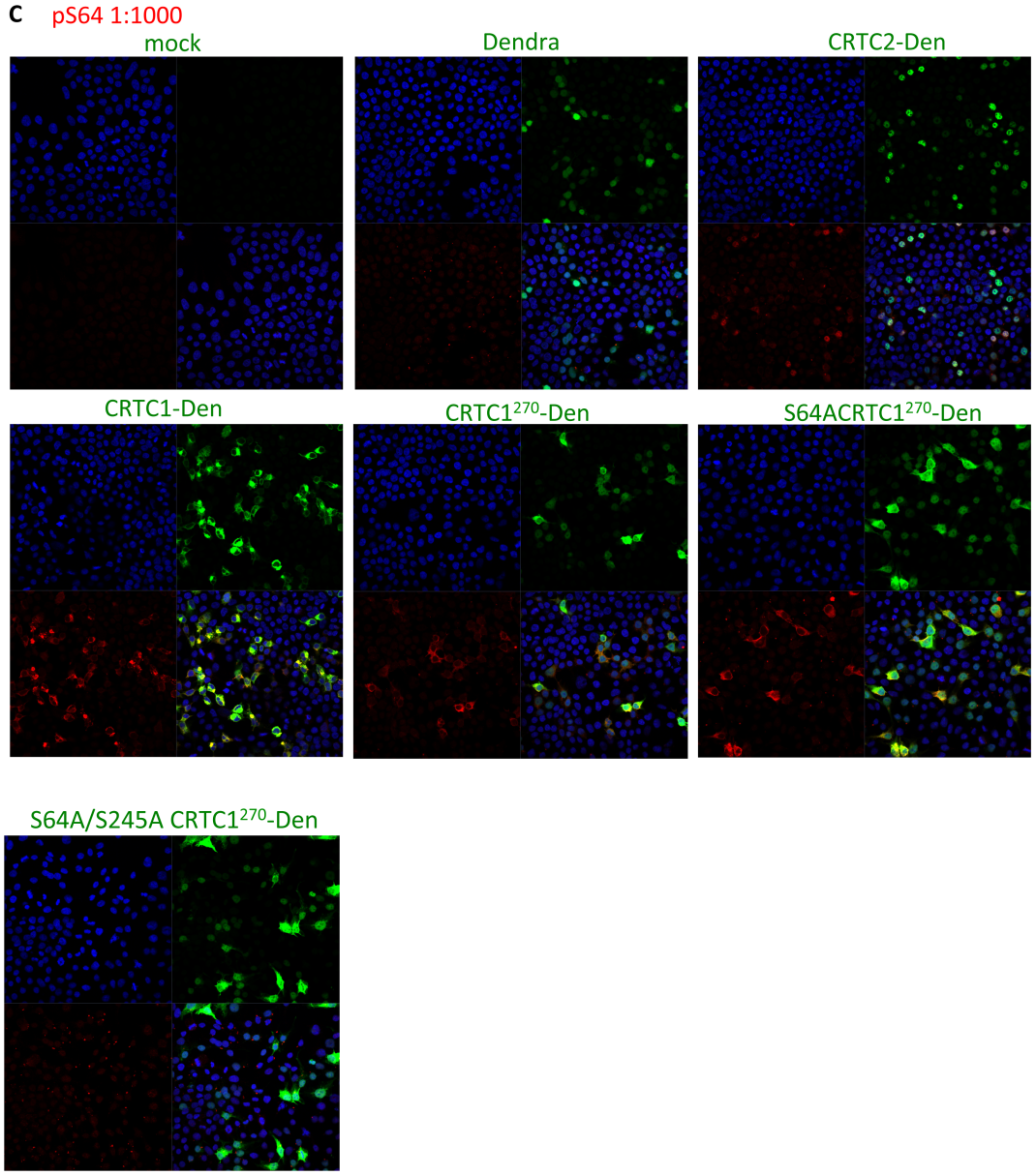
C
pS64 1:1000
mock
Dendra
CRTC2-Den
CRTC1-Den
CRTC1270-Den
S64ACRTC1270-Den
S64A/S245A CRTC1270-Den

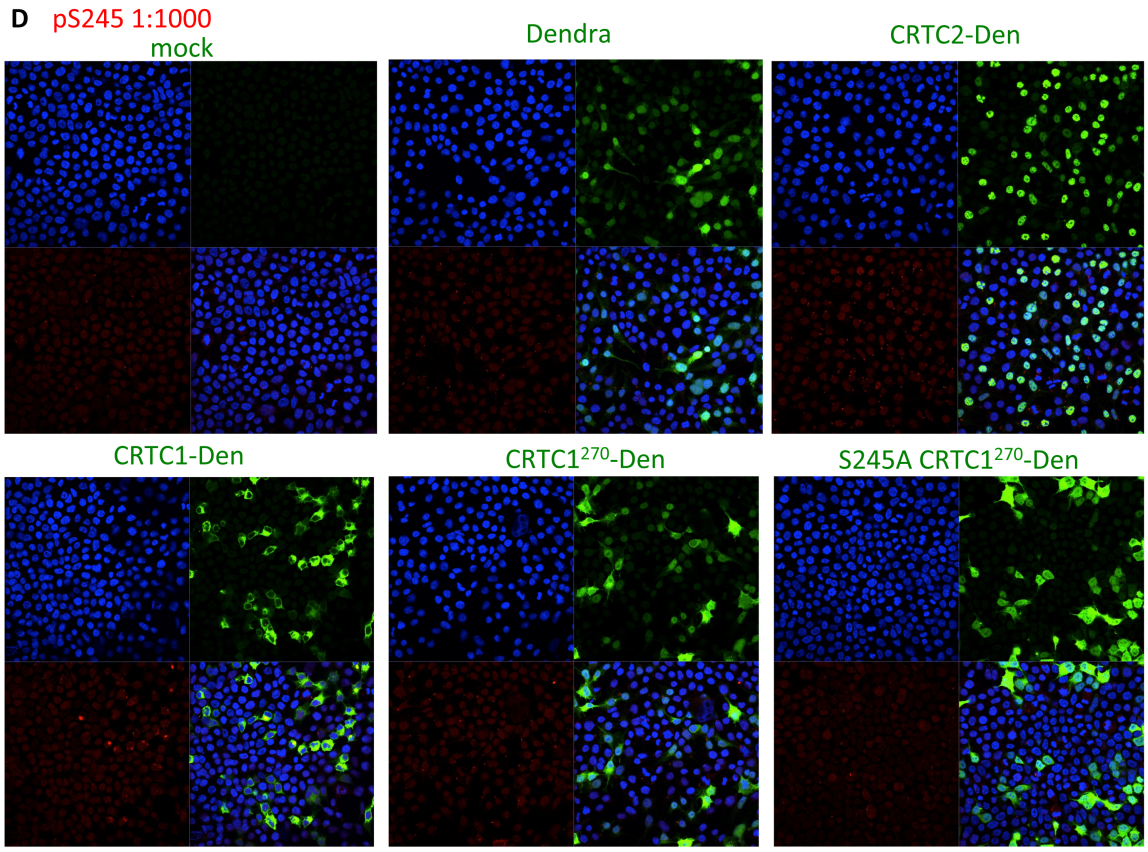

Figure 4.9: Custom antibody immunofluorescence validation using HEK cells

HEK cells were transiently transfected with the constructs labeled in green on top of each panel. Cells were fixed and immunostained with antibodies against Dendra2 (green), DAPI nuclear dye (blue) and the indicated custom antibody below (also labeled in red for each set of images):

(A) NLS antibody

(B) pS151

(C) pS64

(D) pS245

Unfortunately, when tested in neurons with endogenous CRTC1 and in neurons expressing CRTC1-3xFLAG, as well as immunoprecipitated samples of CRTC1-3xFLAG, we were not able to detect any immunoreactivity with these antibodies (data not shown; experiments by Shivan Bonanno). This tells us that the phospho-specific antibodies are not sensitive enough to detect the small amounts of CRTC1 in neurons. Unfortunately, we cannot increase expression in neurons, since high levels of over expression affect the translocation of the protein.

One of the main reasons for creating the NLS antibody was that, while the commercially available Bethyl CRTC1 antibody works well for immunoblots and immunofluorescence, we have never been able to use it efficiently for immunoprecipitations. Creating a CRTC1 antibody that immunoprecipiates the protein efficiently would be a great addition to our lab's molecular toolbox and would greatly expand the types of experiments we are able to perform with endogenous CRTC1.

To test the efficiency of the NLS antibody, we first compared it to the non-specific NLS pre-bleed after immunoprecipitation from 2-week old rat brain lysates. The NLS antibody does immunoprecipitate some endogenous CRTC1 (Fig 4.10 B), but 5ug of the custom made NLS antibody binds less CRTC1 than 1ug of the commercial Bethyl CRTC1 antibody (Fig 4.10 C). This suggests that the custom NLS antibody is actually worse than the commercial available Bethyl CRTC1 antibody and thus should not be used for future immunoprecipitation experiments. See laboratory notes from 10/31/2014 for additional details.

Table 4.1 summarizes the results of these antibody tests.

A

WB lane	Sample
1	NLS pre-bleed IP
2	NLS IP (5ug)
3	NLS IP (1ug)
4	Bethyl CRTC1 IP (1 ug)

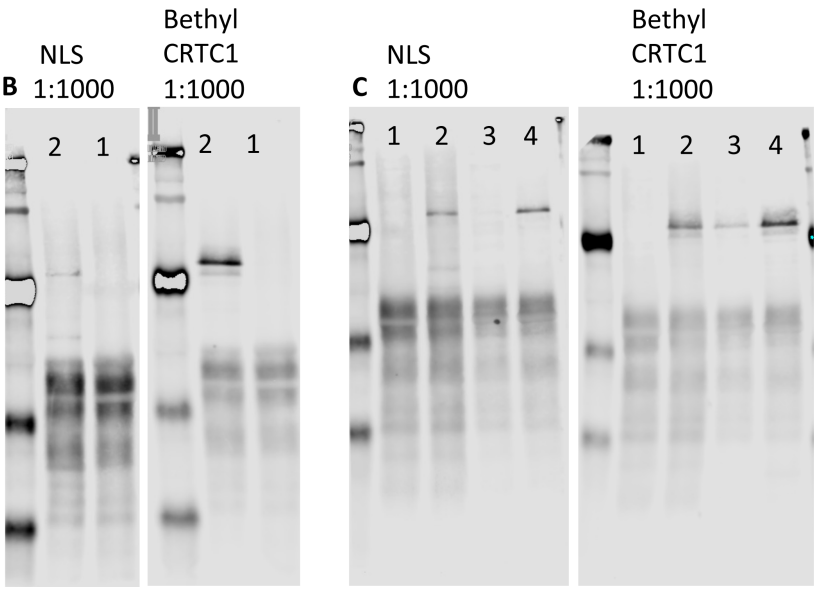

Figure 4.10: NLS antibody validation for immunoprecipitation

(A) Table summarizing samples loaded into each lane. All unlabeled lanes are molecular weight markers, for size reference.

(B/C) Using the antibodies and concentrations summarized in (A), CRTC1 was immunoprecipitated from 2-week old rat brain lysates and immunoblotted using either the NLS antibody (left) or the Bethyl CRTC1 antibody (right) at the indicated dilution.

See laboratory notes from 10/6/2014 and 10/11/2014 for additional details.

Antibody	Specific?	WB	IF	IP
NLS	Yes (not CRTC2)	Yes 1:1000	Yes 1:1000	Yes (worse than Bethyl Ab)
pS64	Yes (pS64/pS245)	Yes 1:1000	Yes 1:1000	N/A
pS151	Maybe?	Weak 1:200	Yes 1:1000	N/A
pS245	Yes (pS245)	Yes 1:2000	No	N/A

Table 4.1: Summary of antibody tests

See laboratory notes from 9/26/2014 for additional details.

The Martin lab uses both mice and rats for our experiments, depending on the application. We noticed that the immunoblot banding pattern for CRTC1 varies between the two species and decided to compare samples side by side. We started by running brain lysates from an adult mouse and a 3-week old rat, with or without phosphatase (CIP) treatment. We tested both the commercial Bethyl CRTC1 antibody as well as our custom-made NLS antibody. Immunoblotting with both antibodies indicates that CRTC1 from 3-week old rat brain lysates is more heavily phosphorylated than CRTC1 from adult mouse brain lysate (Fig 4.11 B).

Since we tested for species differences, but did not control for age differences, we repeated this experiment comparing protein immunoprecipitated using our custom-made NLS antibody (10ug) from age-matched juvenile mice and rats (2 weeks old) as well as adults from both species. The goal of this experiment was to assess the NLS antibody for immunoprecipitaiton and testing for species/age differences was a secondary endpoint. Immunoprecipitation with the NLS antibody seems to select for lower-molecular weight forms of CRTC1. Differences in banding pattern from proteins of different ages/species are still detectable in this preparation, but the differences observed by blotting with Bethyl CRTC1 versus the custom NLS antibody are not as obvious as in Fig 4.11 (data not shown, see lab notebook 11/7/2014).

Nevertheless, we noticed differences in CRTC1 phosphorylation that correlate with both age and species, so it may be useful to repeat this experiment by running the lysates directly without immunoprecipitation. Taken together, these data suggest that CRTC1 is differentially modified depending on both species and developmental stage, thus confounding comparisons that do not control for these factors. It would be very informative to look at CRTC1 expression across development in different species to map out the post-translational modification changes in CRTC1.

A

WB lane	Sample
1	Mouse brain lysate (adult)
2	Mouse brain lysate + CIP
3	Rat brain lysate (3 wk old)
4	Rat brain lysate + CIP

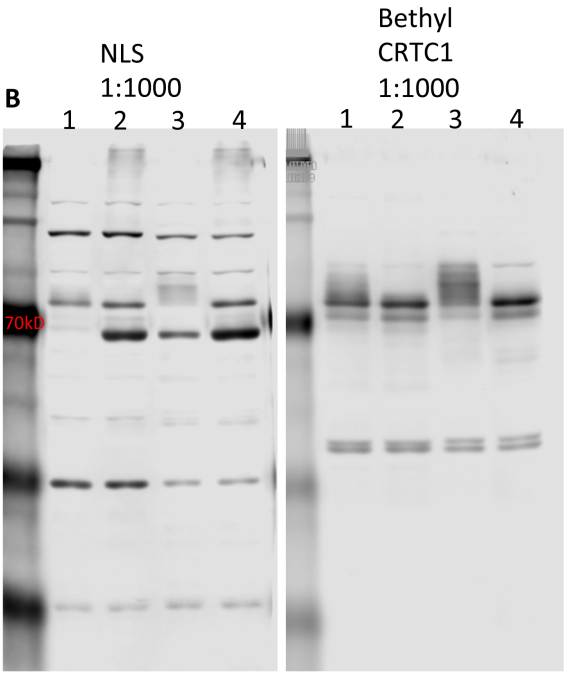

Figure 4.11: Comparing differences in CRTC1 staining for rat vs mouse samples

(A) Table summarizing samples loaded into each lane. Calf Intestinal Phosphatase (CIP) treatment dephosphorylates CRTC1 to highlight differences between the phosphorylated and dephosphorylated forms of CRTC1. All unlabeled lanes are molecular weight markers, for size reference.

(B) Using the samples summarized in (A), CRTC1 was immunoblotted using either the NLS antibody (left) or the Bethyl CRTC1 antibody (right) at the indicated dilution.

Identifying CRTC1 regulators

One of the first projects I worked on during my PhD hoped to identify factors that are crucial for the nuclear translocation of CRTC1 in response to activity. Since proteins larger than ~50 kDa require active transport into the nucleus, we hypothesized that other proteins such as importins might be involved in shuttling CRTC1 into the nucleus. In order to identify CRTC1 interacting proteins, we expressed a CRTC1-GST fusion protein (since we had not created the FLAG-tagged CRTC1 virus yet). Expression of the full length CRTC1-GST protein proved to be difficult as we repeatedly detected degradation products by immunoblotting instead of the full length protein. After extensive trouble-shooting, we decided to express the first half of CRTC1, termed CRTC1$^{1-270}$, fused to GST which drastically reduced the protein degradation. We had shown that CRTC1$^{1-270}$ is both necessary and sufficient for activity dependent CRTC1 nuclear translocation in neurons and were confident that this portion of the protein would be involved in the nucleo-cytoplasmic shuttling of CRTC1. It is important to remember that GST fusion proteins are produced in bacteria and therefore lack post-translational modifications, such as phosphorylation. In retrospect, this is a major drawback in this experiment since we later showed that phosphorylation sites are critically important for encoding CRTC1's subcellular localization. Using a non-phosphorylated version of the protein means that any binding we detected in this experiment should be to the un-modified, de-phosphorylated form of the protein.

While we did not identify any candidates for nuclear import, our mass spectrometry results indicated a wide array of potential protein interactors, including a number of kinases and phosphatases summarized in Table 4.2.

	Phosphatases
ID	**Gene Name**
PP1 *	Serine/threonine-protein phosphatase PP1-gamma
PP2B *	Serine/threonine-protein phosphatase 2B (calcineurin)
ACP1 *	Low molecular weight phosphotyrosine protein phosphatase
PP2A *	Serine/threonine-protein phosphatase 2A
PPP3C	Protein phosphatase 3, gamma isoform

	Kinases
ID	**Gene Name**
PTK2	PTK2 protein tyrosine kinase 2
CNKSR2	Connector enhancer of kinase suppressor of Ras 2
CKMT2	Creatine kinase, mitochondrial 2
DDR2	Discoidin domain receptor family, member 2
KALRN *	Kalirin, RhoGEF kinase
MAST1	Microtubule associated serine/threonine kinase 1
MAST3 *	Microtubule associated serine/threonine kinase 3
MAPK10 *	Mitogen-activated protein kinase 10
MAPK3	Mitogen-activated protein kinase 3
PRKCC *	Protein kinase C, gamma
TTN	Titin
MARK2 *	Serine/threonine-protein kinase MARK2

Table 4.2: List of phosphatases and kinases identified by GST pull-down of CRTC1$^{1-270}$. Asterisks (*) denote proteins that were validated to interact with CRTC1$^{1-270}$ by immunoblot after GST pull-down.

We decided to follow up on a subset of these potential interacting proteins to understand if they play a role in the regulation of CRTC1 in neurons. I validated these interactions by confirming that these proteins are binding to GST-CRTC1$^{1-270}$ via immunoblot. To further verify these interactions, I performed reverse immunoprecipitations, using antibodies against the different interactors followed by immunoblotting for CRTC1. Based on these GST pulldowns and reverse immunoprecipitations, CRTC1 interacts with several proteins including Acid Phosphatase 1 (ACP1), Protein Phosphatase 2a (PP2a), Microtube-associated serine/threonine-protein kinase 3 (Mast3) and Serine/threonine-protein kinase 2 (Mark2).

We tested the function of ACP1 and PP2a using pharmacological inhibitors specific for each phosphatase. We stimulated neurons in the presence of NSC87877 (abbreviated NSC) or Cantharidin (abbreviated Canth) to block ACP1 and PP2a function, respectively. Cortical rat cultures were pre-incubated for one hour with TTX, CsA, NSC and Canth or 30 minutes with Okadaic acid (OK). BIC samples were incubated with BIC for 15 minutes in order to stimulate nuclear translocation. Cells were either scraped directly in sample buffer for immunoblot samples or fixed and processed for immunocytochemistry. We found that both NSC and Cantharidin led to significantly lower nuclear accumulation of CRTC1 following BIC stimulation compared to silenced (TTX) controls. This suggests that both ACP1 and PP2a may play a role in the regulation of CRTC1's subcellular localization.

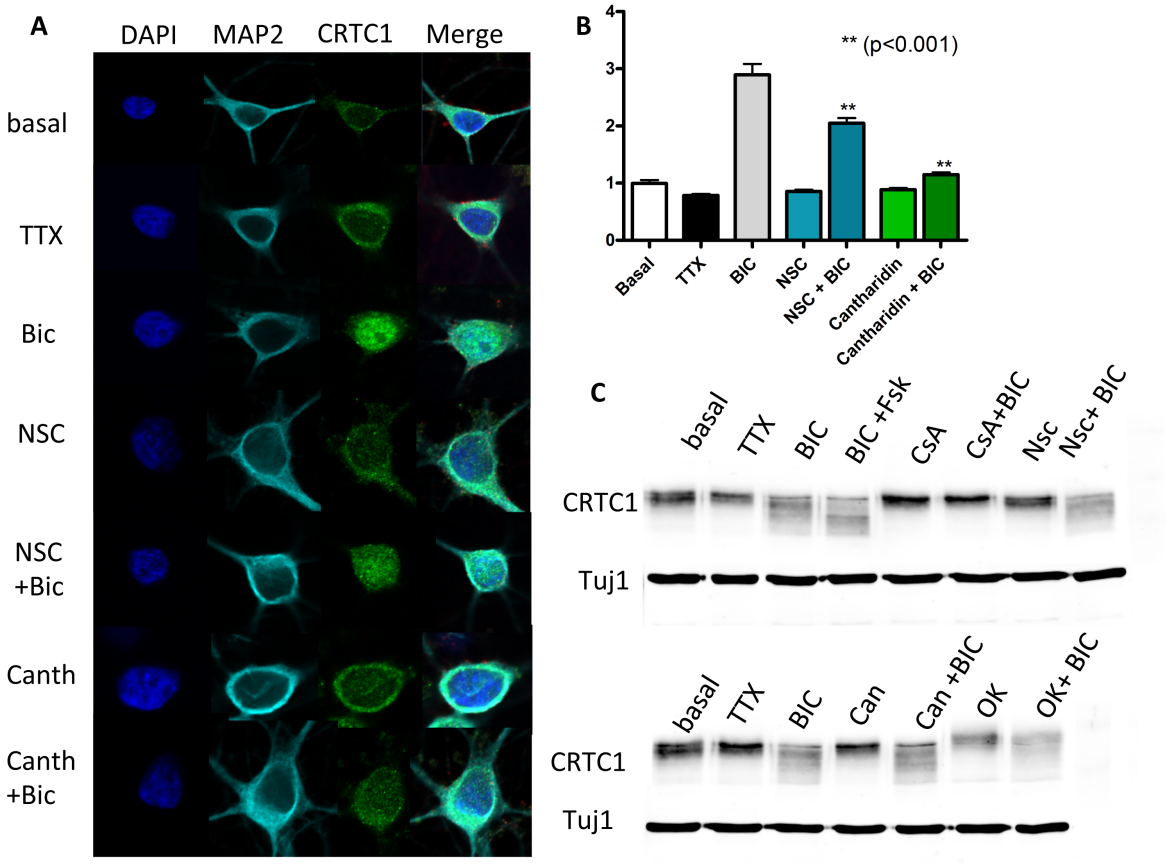

Figure 4.12: Effects of ACP1 and PP2A inhibitors on CRTC1 translocation in neurons

(A) Hippocampal cultures were pre-treated with ACP1 blocker, NSC87877 (NSC; 1 hr, 10uM), PP2a blocker, Cantharidin (Canth; 1 hr, 10uM), or calcineurin inhibitor, Cyclosporine A (CsA, 1 hr, 5uM) with or without bicuculline stimulation (BIC; 10 min, 40 uM). These neurons were compared to basal, tetrodotoxin (TTX, 1 hour, 1mM) silenced and BIC stimulated neurons. Neurons were fixed and immunostained with antibodies against MAP2 (cyan), CRTC1 (green), and DAPI nuclear dye (blue).

(B) Nuclear to cytoplasmic ratios of CRTC1, calculated using CRTC1 intensity values, quantify changes in nuclear CRTC1 represented in (A).

(C) The same samples were lysed in sample buffer after the described treatments in order to assess changes in the molecular weight of CRTC1. Another PP2a inhibitor, Okadaic Acid (OK, 30 min, 5nM) was also tested. We also tested for Tuj1 staining as a loading control.

ACP1 and phosphorylation changes on CRTC1

PP2a is a ubiquitous serine/threonine phosphatase with broad substrate specificity that could have effects on a variety of cellular functions. Additionally, based on our mass spectrometry data, there are dozens of serine/threonine sites that PP2a could act on (since consensus sequences on PP2a substrates have not been identified). On the other hand, ACP1, also known as Low Molecular Weight Phosphotyrosine Protein Phosphatase, is highly expressed in the brain (Magherini et al., 1998) and enriched at synaptic terminals (Tanino et al., 1999), making it a strong candidate as an activity-dependent regulator of CRTC1. Since ACP1 is highly specific for phosphotyrosines, we identified potential targets using our mass spectrometry data. We found three phosphorylated tyrosine sites from our data, at Y60, Y133 and Y137. A literature search for phosphorylated CRTC1 residues reveled that in non-neuronal cells, Y50 has also been identified after enrichment using a phospho-tyrosine specific antibody. Since Y61 is immediately adjacent to Y60 and since it is highly conserved, we decided to include it as a possible site of ACP1 activity. These five sites, Y50, Y60, Y61, Y133 and Y137, are potential candidate sites for ACP1-dependent CRTC1 dephosphorylation.

Pharmacological inhibition of ACP1 suggested that ACP1 may play a role in the subcellular localization of CRTC1 (Fig 4.12). Thus we began by examining the effect of these phospho-incompetent tyrosine mutants on CRTC1 translocation. We further hypothesized that various phosphorylation states of CRTC1 encode not only for subcellular localization, but also for its downstream interactions with transcription factors in the nucleus. I planned to assess the role of ACP1-dependent dephopshorylation of CRTC1 on gene transcription by comparing changes in transcription of specific CRTC1-dependent CREB genes following either overexpression or siRNA-mediated knockdown of ACP1.

I used Accell siRNA for ACP1 to knock down endogenous ACP1 in neurons (Fig 4.13 A). I tested several different lengths of siRNA incubation and observed highest percent of knock down after 5 days (Fig 4.13 B). Since CRTC1 translocates with activity, we wanted to assess whether ACP1 underwent

activity dependent translocation along with its proposed substrate. We analyzed ACP1 subcellular localization with either silenced (TTX) or stimulated (TTX withdrawal) neurons and observed no effects on ACP1 subcellular localization or expression levels (Fig 4.13 C, D). See laboratory notes from 10/23/2014 and 12/09/2014 for additional details on immunoblots and 1/14/2015 for immunofluorescence.

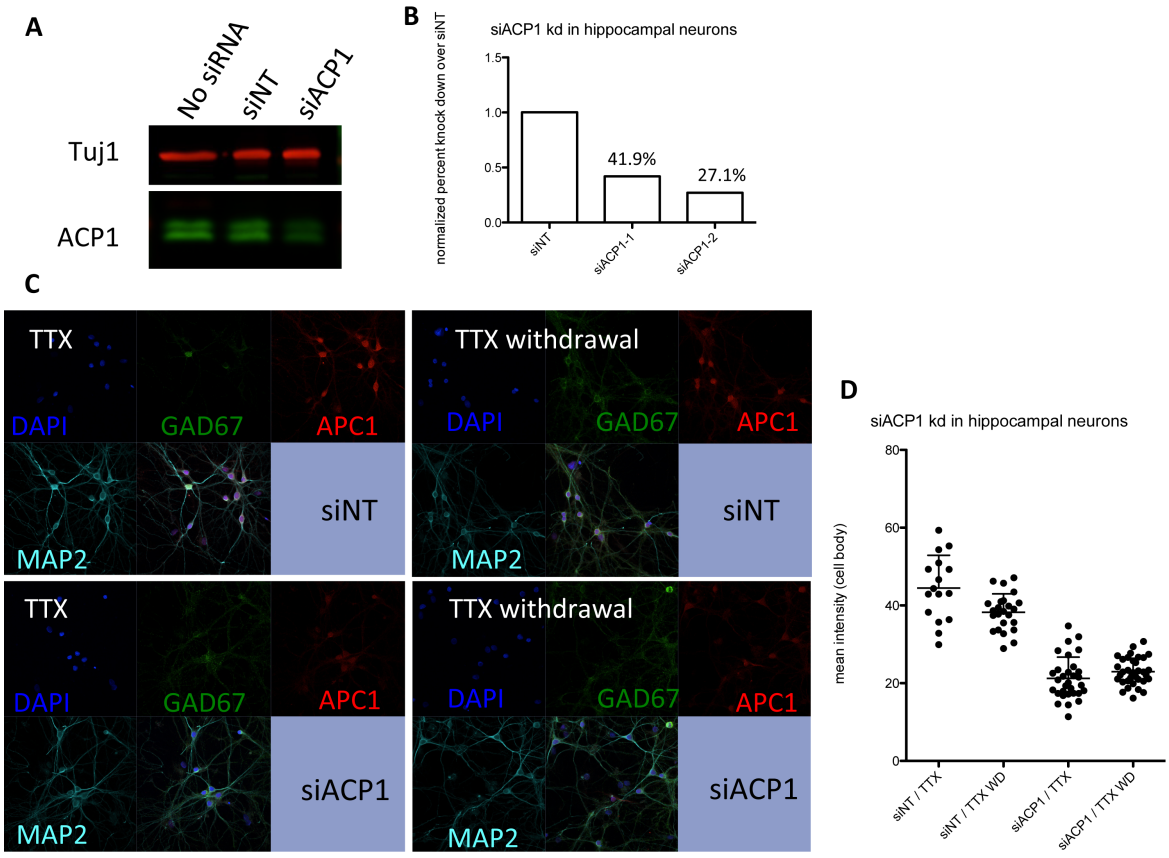

Figure 4.13: Effects of ACP1 knockdown in hippocampal neurons

(A) Hippocampal neuronal cultures (14 DIV) were either left untreated (no siRNA), treated with non-targeted control siRNA (siNT) or with ACP1 siRNA (siACP1) for 5 days to assess extent of siRNA-mediated knockdown of ACP1. Cells were lysed in sample buffer and separated by SDS-PAGE. ACP1 protein (green) is reduced after siACP1 treatment, compared to Tuj1 control (red)

(B) siRNA-mediated knockdown of ACP1 was quantified by immunoblot as a percent of knock down compared to non-target control (siNT) in hippocampal neuronal cultures in two independent experiments (siACP1-1 and siACP1-2)

(C) Hippocampal neuronal cultures were treated with siRNA (as described in A) followed by either silencing with TTX or stimulation by TTX withdrawal (Saha et al, 2011). Neurons were fixed and

immunostained with antibodies against MAP2 (cyan), GAD67 (green), ACP1 (red) and DAPI nuclear dye (blue) to ensure that the silencing and stimulation paradigms have no effects on ACP1 subcellular localization or expression levels.

(D) siRNA-mediated knockdown of ACP1 was quantified by calculating mean intensity values of ACP1 in the cell body of neurons. ACP1 subcellular localization and expression do not change significantly after silencing or stimulating the neurons.

Next, I tested the effects of ACP1 knock down on CRTC1 translocation since our pharmacological inhibition of ACP1 decreases CRTC1 nuclear accumulation following stimulation (Fig 4.12) and since de-phosphorylation is crucial for CRTC1 release from 14-3-3 proteins. We did not observe any significant changes in activity-dependent CRTC1 nuclear accumulation following siRNA-mediated knockdown of ACP1. This could be due to incomplete knockdown of ACP1, but could also suggest that ACP1 does not play a role in regulating synapto-nuclear translocation of CRTC1.

In parallel, I designed single, double and quintuple phospho-incompetent phenylalanine (Y to F) mutants and phospho-mimetic glutamate (Y to E) mutants for the five tyrosine sites in order to look at the effects of their phosphorylation on CRTC1 function. I created lentiviruses expressing:

- CaMKIIα-CRTC1-3xFLAG (control)
- CaMKIIα-Y5F-CRTC1-3xFLAG (5 mutations: Y50F, Y60F, Y61F, Y133F, Y137F)
- CaMKIIα-Y60F/Y61F-CRTC1-3xFLAG
- CaMKIIα-Y133F/Y137F-CRTC1-3xFLAG

See laboratory notes from 12/7/2014 for additional details on viral production.

These mutants could be useful to study the effects of tyrosine phosphorylation on CRTC1 translocation, interacting partners or its role in transcription. Unfortunately, viral titers were too low for most biochemical applications and we did not observe any obvious effects on CRTC1 translocation by immunofluorescence. This suggests that dephosphorylation at these tyrosines alone is not sufficient to trigger CRTC1 nuclear translocation. It is possible that the phosphorylation state of these tyrosines could play a more important role in regulating CRTC1-dependent transcription in the nucleus. To test whether these mutations affect CRTC1 function would require a deeper understanding of CRTC1's transcriptional role in neurons. The data covered in Chapter 3 attempts to address this issue by elucidating CRTC1's transcriptional role in neurons. Based on this data, these tyrosine mutants could be revisited to test whether expression of candidate genes is affected by dephosphorylation of specific residues. Overall,

the information encoded in CRTC1's post translational modifications in response to different stimuli could elicit differential transcriptional responses once CRTC1 translocates to the nucleus.

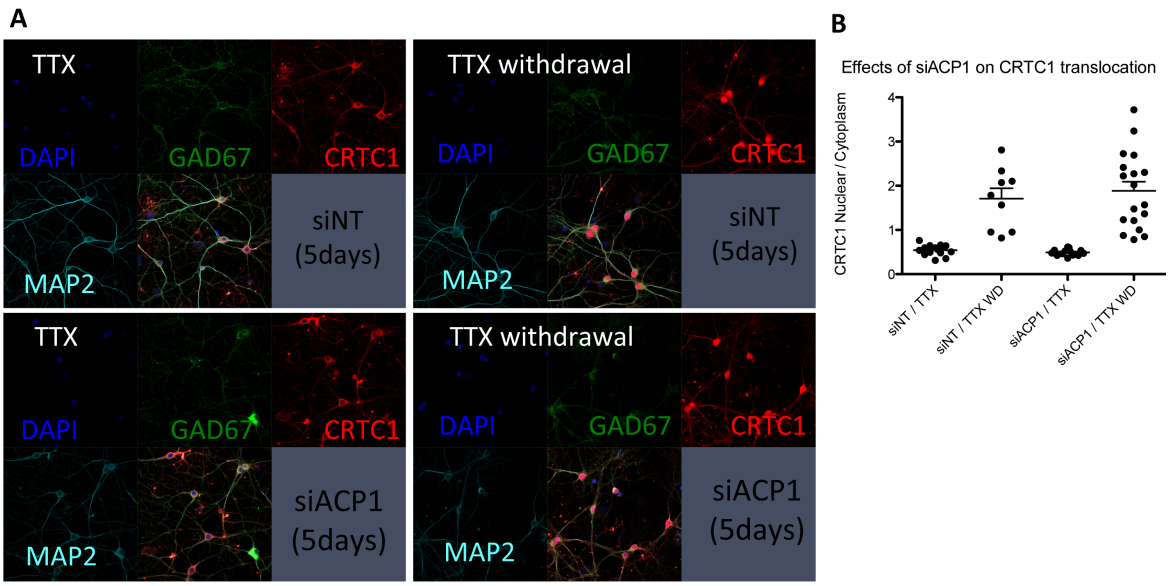

Figure 4.14: Effects of siACP1 on CRTC1 translocation

(A) Hippocampal neuronal cultures (14 DIV) were either treated with non-targeted control siRNA (siNT) or with ACP1 siRNA (siACP1) for 5 days and either silenced with TTX or stimulated by TTX withdrawal. Neurons were fixed and immunostained with antibodies against MAP2 (cyan), GAD67 (green), CRTC1 (red) and DAPI nuclear dye (blue).

(B) Nuclear to cytoplasmic ratios of CRTC1, calculated using CRTC1 intensity values, quantify changes in nuclear CRTC1 represented in (A).

Identifying CRTC1 interacting proteins using CRTC1-3xFLAG in neurons

Since the GST-CRTC1$^{1-270}$ pull-downs have a variety of drawbacks described above, we decided to use the AAV construct to overexpress CRTC1-3xFLAG in neurons and isolate interacting proteins when CRTC1 is either in its phosphorylated (synaptic) or dephosphorylated (nuclear) states. We used the same approach described in Figure 4.4, except using the immunoprecipitated sample to identify binding partners rather than to look for post-translational modification by mass spectrometry. This approach proved to have its own drawbacks.

Our goal was to differentiate between proteins binding CRTC1 at the synapse and proteins binding to it in the nucleus. We compared these samples to FLAG immunoprecipitations from non-virally transduced, unstimulated neurons. The mass spectrometry analysis showed very high background binding, with over half of the proteins being identified in all three samples. Since the non-virally transduced samples do not have any FLAG tag present, this suggests that the FLAG antibody is binding non-specifically to these proteins. These observations were consistent across biological replicates.

We noted that many of the proteins we identified in these samples contain low complexity domains. This non-specific binding may arise from the disruption of molecular interactions that normally guide these proteins' binding partners and structure. As we lyse the cells for immunoprecipitation, breaking down subcellular compartments creates an environment in which these low complexity domains may bind promiscuously to other abundant proteins containing low complexity domains, such as RNA binding proteins. Additionally, tight regulation of local concentrations is very important for the role of intrinsically disordered proteins. Lysing the cell means that these proteins are no longer in their specific microenvironments and may therefore bind other proteins that they would not encounter because of compartmentalization within the cell.

Another issue to consider is that the lysis protocol used for immunoprecipitation will open the cell membrane faster than the nuclear membrane. This could enrich for the cytoplasmic

(phosphorylated) form of CRTC1 over the nuclear (dephosphorylated) form. We addressed this by preparing nuclear and cytoplasmic fractions to enrich for the dephosphorylated and phosphorylated forms of the protein, but it is very difficult to prepare pure nuclear and cytoplasmic fractions from DIV 21 cultured neurons. Additionally, while we include phosphatase and protease inhibitors in the lysis buffer, it is possible that the lysis conditions cause disruptions in specific protein interactions. For instance, since we are lysing the nucleus, we need to DNAse treat the lysate to reduce viscosity before immunoprecipitation. Losing its interaction with DNA could cause CREB to change conformation (since CREB also has intrinsically disordered domains) that would, in turn, prevent it from interacting with CRTC1. One avenue that we explored to bypass this constraint was to crosslink proteins before immunoprecipitation. This technique has been used to purify stable structures in stress granules, but needs to be further adapted for application in neurons.

Conclusions

Phosphorylation of CRTC1 serves as a regulatory code to direct its activity-dependent translocation from synapse to nucleus. We hypothesized that additional changes in CRTC1's phosphorylation state may encode for different stimuli that need to be relayed to the nucleus to elicit appropriate transcriptional responses. The experiments described above attempt to determine what additional sites are dephosphorylated with activity. Current technological advances in mass spectrometry may provide greater phospho-peptide detection sensitivity and make these experiments more feasible.

We also observed that CRTC1 in different cell types does not recapitulate the post-translational modification changes that we see in neurons. Additionally, we noted differences between neuronal CRTC1 from rats and mice, and between young (2 weeks) pups and adults. It will be very interesting to follow up on these preliminary observations and describe CRTC1's role in development as well as mature neurons.

To better understand CRTC1's role in neurons, we created several tools, such as an AAV expressing FLAG-tagged, CaMKIIα-driven CRTC1. Using this virus to express FLAG-tagged CRTC1, we noticed that high levels of overexpression affected FLAG-CRTC1's subcellular localization at rest and prevented its activity-dependent translocation following stimulation. In some cases where overexpression occurred, we noted that endogenous CRTC1 still translocated in an activity-dependent manner, but FLAG-tagged CRTC1 did not respond to stimulation. This suggests that, like many intrinsically disordered proteins, CRTC1 is susceptible to changes in stoichiometry and should, whenever possible, be studied at endogenous cellular concentrations. Moreover, CRTC1 is very sensitive to activity and we have observed that even accidentally bumping the dish of cultured neurons can lead to activity that drives CRTC1 into the nucleus. For these reasons, it is imperative to check the neurons by

immunofluorescence to assess both the level of CRTC1 expression and the extent of nuclear translocation for each experiment.

We encountered several challenges in identifying CRTC1's binding partners. First, we attempted to isolate CRTC1 from whole cell lysates. At any given time, CRTC1 may be enriched in the cytoplasmic or nuclear compartments, but both forms are still present. Since we don't see a clear difference in CRTC1 immunoprecipitated from stimulated and silenced neurons, it is possible that the FLAG antibodies preferentially bind certain conformations of CRTC1. Another issue is that whole cell lysis opens up the cell membrane more easily than the nuclear membrane, thus biasing the lysate to represent more cytoplasmic CRTC1.

To address this, we tried to isolate nuclear and cytoplasmic fractions to look at CRTC1's binding partners in its phosphorylated and dephosphorylated states in different subcellular compartments. While we have greatly improved our protocols for nuclear and cytoplasmic fractions from cultured cortical neurons, we still are unable to prepare pure subcellular fractions. This is likely because we use neurons at DIV 21 that have created extensive processes and synaptic connections with each other. We observed that making pure fractions becomes increasingly harder as the neurons get older and their arborizations become more complex and interconnected.

Nevertheless, we have identified several potential CRTC1 interacting proteins, including ACP1, which may play a role in regulating CRTC1's phosphorylation code. Understanding CRTC1's role in activity-dependent transcription in neurons will guide future experiments to elucidate the role of these proteins in orchestrating complex changes in CRTC1's post translational modifications.

Materials and Methods

Plasmids and antibodies. Commercial plasmids include Dendra2 (Evrogen) and CRTC1 (Open Biosystems, Huntsville, AL). All Dendra-fusion CRTC, CRTC1$^{1-270}$, and phosho-mutant constructs were created by Toh Hean Ch'ng. All AAV and Lentiviral CRTC-3xFLAG and phosho-mutant constructs were created by Martina DeSalvo. Antibodies used in all these experiments include: rabbit polyclonal antibodies against CRTC1 (Bethyl, Montgomery, TX), Dendra2 (Evrogen, Moscow, Russia), Mark2 (Proteintech), Mast3 (Proteintech) , ACP1 (Abgent), mouse monoclonal antibodies against TUJ1 (Covance, Princeton, NJ), HA-epitope (Sigma, St. Louis, MO), FLAG-epitope (Sigma), GAPDH (Fitzgerald, Acton, MA), GAD67 (Millipore, Billerica, MA), rabbit monoclonal antibodies again PP2a (Cell Signaling Technologies) and polyclonal chicken antibody against MAP2 (Phosphosolutions, Aurora, CO). Custom antibodies were designed in house and produced commercially by New England Peptides (Gardner, MA). They are described and characterized in the main text. All secondary antibodies are conjugated to Alexa dyes (488, 546, 555, 568 and 633; Invitrogen, Carlsbad, CA).

Viruses and expression constructs. Adeno-associated viruses were designed in house and produced by the Penn Vector Core (Philadelphia, PA). Viral transduction of neurons was carried out in a reduced volume (250 µl / 1 ml) for 16 h before replacement with conditioned neuronal medium. The integrated constructs were allowed to express for at 6-7 days prior to experiments. Since viral titer differs between different production rounds, each batch was titrated so that approximately 75% of neurons were expressing the FLAG tag and expression levels of CRTC1-3xFLAG were close to endogenous CRTC1 levels.

Dissociated neuronal culture protocols and pharmacological treatments. All experiments in this chapter uses mature cortical neurons (DIV 21) dissected from newborn (P0-1) rats and plated on poly-

DL-lysine (0.5 mg/ml) coated cover slips (Carolina Biologicals, Burlington, NC) or culture dishes. Neurons were cultured in Neurobasal A media (Invitrogen, Carlsbad, CA) supplemented with β-mercaptoethanol (Sigma), monosodium glutamate (Sigma), B27 (Invitrogen) and GlutaMAX (Invitrogen). Neurons were incubated with various pharmacological agents in conditioned neuronal media in a 37°C, 5% CO_2 incubator for the appropriate amount of time before cells were either fixed for immunocytochemistry or lysates were collected for immunoblots. The following pharmacological agents were used: bicuculline (BIC, 40 μM; Sigma), forskolin (FSK, 25 μM; Calbiochem, San Diego, CA), tetrodotoxin (TTX, 1 μM; Tocris, Ellisville, MO), cyclosporin A (CsA, 5 μM; Sigma), NSC87877 (NSC, 10uM; Tocris), Cantharidin (Canth, 1uM; Tocris), Okadaic Acid (OK, 5-50nM; Tocris), ionomycin (ionoM, 1uM; Sigma) and leptomyocinB (lepB, 10mM; Sigma).

Immunocytochemistry. All cells were fixed at room temperature with parafomalydehyde (4%) for 10 min, permeabilized with 0.1% Triton-X 100 (Calbiochem) for 5 min and blocked in 10% goat-serum for 30 min. Neurons were then incubated in primary antibodies either for 4 hrs at room temperature or overnight at 4°C. Secondary antibodies and Hoechst nuclear dye (Invitrogen) were incubated at room temperature at 1:1000 dilution for 2 hrs. All antibodies were diluted in 10% goat serum and coverslips were mounted with aqua/polymount (Polysciences, Warrington, PA).

Cell cultures and transfections. HEK293T and N2A cell lines were grown in Dulbecco's Modified Eagle Media (DMEM; Invitrogen) supplemented with 10% fetal bovine serum (HyClone, Logan, UT). Transfection of plasmids in cell lines was carried out with Lipofectamine 2000 (Invitrogen) using protocols recommended by the manufacturer.

siRNA treatment. For siRNA treatment of ACP1 in neurons, we purchased custom designed siGENOME SMARTpool Accell siRNA from Dharmacon (Lafeyette, CO) and scambled, non-targeted control (siNT). The Accell siRNA (1 μM) was delivered into neurons directly and allowed to incubate for 5 days. After the incubation period, cells were subjected to treatments as described in the text and either fixed for immunocytochemistry or harvested in lysis buffer for analysis via immunoblots. See laboratory notes from 5/20/2014 and 10/23/2014 for additional details.

Image analysis and synapse quantification. All nuclear to cytoplasmic quantification was performed with imageJ. All data sets are presented as mean ± SE either as bar graphs or scatter plots.

Mass Spectrometry. Protocol for phosphopeptide identification in N2A cells is described in Chapter 2. See laboratory notes from 4/27/2015 and 5/25/2015 for additional details. For identification of phosphorylation sites from neuronal samples, neurons expressing CRTC1-3xFLAG were either silenced with 1 hr TTX or stimulated with 15 min BIC before immunoprecipitation using FLAG antibody (Sigma). Samples were separated by SDS-PAGE and bands corresponding to CRTC1 were excised and submitted for mass spectrometry analysis through the Wohlschlegel lab.

Stable isotope labeling of cells in culture (SILAC). Using DMEM media for SILAC (Cat # 89985, DMEM minus L-Lysine and L-Arginine) supplemented with 10% Dialyzed FBS (ThermoFisher Scientific Cat # 88440), dissolve $^{13}C_6$ L-Lysine-2HCl (Cambridge Isotope Lab. Inc, CLM-2247-H) and $^{13}C_6$ L-Arginine-HCl (Cambridge Isotope Lab. Inc, CLM-2265-H) to a final concentration of 0.46mM and 0.47mM respectively, for double heavy labeling of lysines and arginines. Filter media using a 0.22μm filter and store at 4°C, protected from light. Passage N2A cells in double heavy-labeled media for 8 cell doublings, by splitting cells every 2 days. Maintain density so that cells are actively growing in log phase (between 30-90%

confluency). After 8 cell doublings, incorporation of heavy L-lysine and L-arginine should be > 95%. Harvest cells from one 10cm dish using native lysis buffer and perform TCA precipitation for analysis by Wohlshelgel lab to determine incorporation efficiency. Prepared frozen stock of heavy-labeled N2A cells. See laboratory notes from 1/8/2016 for additional details.

GST pulldowns. Mouse brain lysates were subjected to pulldowns using purified GST-CRTC1$^{1-270}$ bound on glutathione sepharose beads (GE Healthcare, Piscataway, NJ). After two hours incubation at 4°C, the GST pulldowns were washed, eluted and subjected to immunoblot analysis using antibodies specific for CRTC1, GST, ACP1, PP2a, Mast3 or Mark2.

References:

Ch'ng, T. H., DeSalvo, M., Lin, P., Vashisht, A., Wohlschlegel, J. A., & Martin, K. C. (2015). Cell biological mechanisms of activity-dependent synapse to nucleus translocation of CRTC1 in neurons. *Frontiers in Molecular Neuroscience*, *8*, 48. http://doi.org/10.3389/fnmol.2015.00048

Ch'ng, T. H., Uzgil, B., Lin, P., Avliyakulov, N. K., O'Dell, T. J., & Martin, K. C. (2012). Activity-dependent transport of the transcriptional coactivator CRTC1 from synapse to nucleus. *Cell*, *150*(1), 207–221. http://doi.org/10.1016/j.cell.2012.05.027

Dephoure, N., Gould, K. L., Gygi, S. P., & Kellogg, D. R. (2013). Mapping and analysis of phosphorylation sites : a quick guide for cell biologists. *Molecular Biology of the Cell*, *24*, 535–542. http://doi.org/10.1091/mbc.E12-09-0677

Gaur, R. K. (2014). Amino acid frequency distribution among eukaryotic proteins. *IIOAB Journal*, *5*(2), 6–11.

Geiger, T., Wisniewski, J. R., Cox, J., Zanivan, S., Kruger, M., Ishihama, Y., & Mann, M. (2011). Use of stable isotope labeling by amino acids in cell culture as a spike-in standard in quantitative proteomics. *Nature Protocols*, *6*(2), 147–157. http://doi.org/10.1038/nprot.2010.192

Magherini, F., Giannoni, E., Raugei, G., Cirri, P., Paoli, P., Modesti, A., … Ramponi, G. (1998). Cloning of murine low molecular weight phosphotyrosine protein phosphatase cDNA: identification of a new isoform. *FEBS Letters*, *437*(3), 263–266. http://doi.org/10.1016/S0014-5793(98)01241-1

Mikesh, L. M., Ueberheide, B., Chi, A., Coon, J. J., Syka, J. E. P., Shabanowitz, J., & Hunt, D. F.

(2006). The utility of ETD mass spectrometry in proteomic analysis. *Biochimica et Biophysica Acta*, *1764*(12), 1811–22. http://doi.org/10.1016/j.bbapap.2006.10.003

Tanino, H., Yoshida, J., Yamamoto, R., Kobayashi, Y., Shimohama, S., & Fujimoto, S. (1999). Abundance of Low Molecular Weight Phosphotyrosine Protein Phosphatase in the Nerve-Ending Fraction in the Brain. *Biological Pharmacy Bulletin*, *22*(8), 794–798. http://doi.org/10.1248/cpb.37.3229

Chapter 5

Discussion and Concluding Remarks

The transcription factor cAMP Response Element Binding Protein (CREB) is required for this process (Alberini 2009). Initial studies in flies and *Aplysia califonica* began to delineate the role for cAMP signaling and CREB during learning and memory. Studies in mammals confirmed that CREB played a key role in hippocampal long term potentiation (LTP), a key process underlying synaptic plasticity. The synaptic strengthening observed in LTP can be divided into two phases: transcription-independent early-LTP (E-LTP) and late-LTP (L-LTP) which requires new gene transcription (Kandel 2001). CREB knockout mice were used to demonstrate that this protein is required for transcription-dependent L-LTP, but not for the transcription-independent E-LTP (Bourtchuladze et al. 1994). Despite years of research in this area, it is still not clear how calcium and cAMP signaling cascades converge to activate CREB-dependent gene transcription. CREB is involved in a variety of cellular processes suggesting that the mechanism by which it is activated must be tightly regulated in order to specifically respond to a wide range of distinct stimuli (Johannessen et al. 2004).

More recently, screens to identify modulators of CREB-dependent transcription led to the characterization of Transducers of Regulated CREB (TORCs), which were later re-named CRTCs, for CREB-Regulated Transcriptional Coactivators (Conkright et al. 2003; Iourgenko et al. 2003). CRTCs respond to coincident elevations of cAMP and calcium by translocating into the nucleus where they potentiate CREB-mediated transcription (Altarejos and Montminy 2011). Through the data presented here, we expand our current knowledge of CRTC1 to better understand how synaptic activity orchestrates transcription of specific genes. This thesis explores the molecular mechanisms underlying this process by focusing on CRTC1's role and regulation in neurons.

We began by investigating CRTC1's regulation in neurons and the mechanisms involved in its synapse to nucleus translocation. CRTCs had been extensively studied in pancreatic β islet cells, which lack the extensive dendritic branching characteristic of neurons. Nevertheless, many of the mechanisms described in non-neuronal cells were conserved in neurons (Ch'ng et al. 2012). In Chapter 2, we decipher

how CRTC1 rapidly moves from distal synapses to the soma through dynein-mediated transport along microtubules (Ch'ng et al. 2015). We also identify an arginine-rich nuclear localization signal that is required for nuclear import and we use phospho-incompetent mutations to show that three highly conserved serines need to be dephosphorylated in order to trigger CRTC1 translocation. Additionally, we explore the types of stimuli necessary to trigger CRTC1 translocation in neurons. We observe that local influxes of calcium through synaptic NMDA and AMPA glutamate receptors as well as L-type Voltage Gated Calcium Channels lead to CRTC1's translocation (Ch'ng et al. 2015). These findings are crucial to understanding the complex role of CRTC1 in neurons.

Chapter 3 summarizes several key findings about CRTC1's role in transcription in response to neuronal stimulation. Our data suggests that CRTC1 may co-bind with JUN along with CREB. Neuronal stimulation leads to recruitment of both CRTC1 and JUN to CREB binding locations. Additionally, we used ATAC-seq to look at changes in chromatin state during neuronal stimulation. We observed increased chromatin accessibility in the gene bodies of immediate early genes following stimulation, which is suggestive of high transcriptional activity in these genomic areas. CRTC1's role will be further elucidated with RNA-Seq data that will demonstrate whether our observations by ChIP-Seq and ATAC-Seq result in differential gene expression at CRTC1-bound targets.

In Chapter 4, I summarize several projects that may be useful resources for the lab in planning future experiments. This data provides a partial picture of CRTC1's role in neurons and may serve as starting points to revisit these types of experiments as our molecular toolbox improves. We attempted to characterize the activity-dependent phosphorylation changes in CRTC1 occurring in neurons, but we faced several challenges, from low starting material to structural complications. CRTC1 has an unusually high number of phosphorylation sites. Phosphorylation prediction software DISPHOS predicts that 76% of its serines (64 our of 84 sites) should be phosphorylated. In our experiments, we identified 50 phosphorylated serines, threonines and tyrosines using N2A cells, but were unable to identify sites that

undergo activity-dependent changes in neurons. We hope that Electron Transfer Dissociation (ETD) mass spectrometry may improve our detection of these key sites. Furthermore, we attempted to characterize CRTC1's interacting partners, but were again challenged with several obstacles, including low amounts of starting material from neurons. More importantly, the intrinsically disordered nature of CRTC1's structure allows for low complexity regions to bind non-specifically to other abundant proteins that also contain low complexity domains such as RNA binding proteins and keratins. This issue could be resolved by briefly crosslinking proteins before cell lysis in order to preserve interactions that may be disrupted as the cells break open.

CRTC1 is much more complex than we originally anticipated. With 50 differentially phosphorylated sites, low complexity regions that allow for flexible binding to a variety of interactors and finely-tuned synapto-nuclear shuttling, CRTC1 continues to puzzle us as a biological enigma that still need to be fully deciphered. As an intrinsically disordered protein, it plays a role in signal sensing and transduction through synapse to nucleus translocation in response to activity. Once in the nucleus, it binds CREB as previously reported, but our data suggests that it may be interacting with other transcription factors as well. Additionally, CRTC1 could potentially use its low complexity domains to play a scaffolding role to bring together several key transcriptional proteins to orchestrate specific gene transcription.

In light of this knowledge, we need to re-examine our approach and potentially design new tools to address these challenges. For instance, based on the information we have gathered so far, it will be crucial to work with endogenous levels of the protein. We have unsuccessfully attempted to create a tagged-CRTC1 knock-in mouse, but this tool may be worth revisiting as it would be incredibly useful to study CRTC1 in its endogenous state/concentration. Additionally, we have learned that observations in non-neuronal cell lines do not extrapolate to neurons and that we see pronounced differences in CRTC1

modifications even when comparing mice and rats or animals of different ages. All of these concerns should be taken into account in crafting new hypotheses and designing new experiments.

References:

Alberini, Cristina M. 2009. “Transcription Factors in Long-Term Memory and Synaptic Plasticity.” *Physiological Reviews*, no. 80: 121–45. doi:10.1152/physrev.00017.2008.

Altarejos, Judith Y, and Marc Montminy. 2011. “CREB and the CRTC Co-Activators: Sensors for Hormonal and Metabolic Signals.” *Nature Reviews. Molecular Cell Biology* 12 (3). Nature Publishing Group: 141–51. doi:10.1038/nrm3072.

Bourtchuladze, Roussoudan, Bruno Frenguelli, Julie Blendy, Diana Cioffi, Gunther Schutz, and Alcino J. Silva. 1994. “Deficient Long-Term Memory in Mice with a Targeted Mutation of the cAMP-Responsive Element-Binding Protein.” *Cell* 79 (1). Cell Press: 59–68. doi:10.1016/0092-8674(94)90400-6.

Ch’ng, Toh H., Besim Uzgil, Peter Lin, Nuraly K. Avliyakulov, Thomas J. O’Dell, and Kelsey C. Martin. 2012. “Activity-Dependent Transport of the Transcriptional Coactivator CRTC1 from Synapse to Nucleus.” *Cell* 150 (1). Elsevier Inc.: 207–21. doi:10.1016/j.cell.2012.05.027.

Ch’ng, Toh Hean, Martina DeSalvo, Peter Lin, Ajay Vashisht, James A Wohlschlegel, and Kelsey C Martin. 2015. “Cell Biological Mechanisms of Activity-Dependent Synapse to Nucleus Translocation of CRTC1 in Neurons.” *Frontiers in Molecular Neuroscience* 8. Frontiers Media SA: 48. doi:10.3389/fnmol.2015.00048.

Conkright, Michael D, Gianluca Canettieri, Robert Screaton, Ernesto Guzman, Loren Miraglia, John B Hogenesch, Marc Montminy, and La Jolla. 2003. “TORCs : Transducers of Regulated CREB Activity The Salk Institute for Biological Studies.” *Molecular Cell* 12: 413–23.

Iourgenko, Vadim, Wenjun Zhang, Craig Mickanin, Ira Daly, Can Jiang, Jonathan M Hexham, Anthony P Orth, et al. 2003. “Identification of a Family of cAMP Response Element-Binding Protein Coactivators by Genome-Scale Functional Analysis in Mammalian Cells.” *Proceedings of the National Academy of Sciences of the United States of America* 100 (21): 12147–52.

doi:10.1073/pnas.1932773100.

Johannessen, Mona, Marit Pedersen Delghandi, and Ugo Moens. 2004. “What Turns CREB On?” *Cellular Signalling* 16 (11): 1211–27. doi:10.1016/j.cellsig.2004.05.001.

Kandel, E R. 2001. “The Molecular Biology of Memory Storage: A Dialogue between Genes and Synapses.” *Science (New York, N.Y.)* 294 (5544): 1030–38. doi:10.1126/science.1067020.